ASPECTS OF MOULD DESIGN IN ELECTROSLAG CASTING

by

JAYANT MORESHWAR SATHAYE

B.Tech., Indian Institute Of Technology, Madras, 1977

A THESIS SUBMITTED IN PARTIAL FULFILMENT OF

THE REQUIREMENTS FOR THE DEGREE OF

MASTER OF APPLIED SCIENCE

in

THE FACULTY OF GRADUATE STUDIES

Department Of Metallurgical Engineering

We accept this thesis as conforming

to the required standard

THE UNIVERSITY OF BRITISH COLUMBIA

February 1983

Department of Metallurgical Engineering

The University of British Columbia
2075 Wesbrook Place
Vancouver, Canada
V6T 1W5

Date: 9th February 1983

Abstract

Electroslag casting is a process technique used to produce castings using electroslag melting. It is likely that channel cooled Aluminium moulds will be employed. Thus, the criteria for the design of moulds to be used in this process were examined.

Temperatures in a mould section were measured and compared to those calculated from a model developed assuming 3-D quasi steady state heat flow and reasonable agreement was found. In the model the two major boundary conditions are the heat transfer coefficient to the coolant and the heat flux on the hot face. The former can be estimated from established correlations for heat transfer in tubes such as the Petukhov and the Sieder-Tate relations. The latter had to be measured and a heat flux sensor was developed for this.

Proposals were made to qualitatively explain the heat flux variation along the mould height, but it was not possible to estimate the heat flux for a casting of arbitrary shape in a simple manner. According to the slag crystallisation mechanism proposed the influence of mould on the surface quality of the casting was found to be negligible.

Table of Contents

List of Tables

List of Figures

Acknowledgement

I would like to thank Prof. Alec Mitchell for all the time he spared for me and especially for his style of guidance.

Gus Sidla's assistance was invaluable and is very much appreciated. Ed Barry and Rudy Cardeno were very helpful during the experimental stages.

The pleasant nature of the staff in the department and of fellow graduate students made my stay very enjoyable.

I also wish to express my gratitude to Consarc Corporation, Rancocas, New Jersey for their financial support.

I. INTRODUCTION

1.1 The Electroslag Process

The utilisation of the electroslag process began in the early 1940's with the Kellogg electric ingot process. The process was originally developed by R.K.Hopkins, but western industry did not involve itself seriously till the 1960's. Investigators in the Soviet Union, meanwhile, discovered that the weld metal in an electroslag weld was purer and had fewer inclusions than the base metal. They then developed the process with the prime aim of improving the quality of air-melted electric furnace steel. Since then, it has been used to produce castings too. Following this lead the process has been used in many other countries in the manufacture of ingots. A Japanese firm uses this process to manufacture reformer tubes but apart from this there are almost no significant engineering applications of electroslag cast metal, as is, in the western world.

The electroslag process involves the melting of a solid electrode through a liquid electrically conducting slag into a water cooled metallic mould. An electric potential is applied across the electrode and the mould. The slag forms the only significant resistance and almost all the heat is generated within it. The electrode is melted progressively and the ingot solidifies in similar fashion, i.e. progressively and to a

certain extent directionally. It reduces, significantly, the number of inclusions and can control the solidification rate thus eliminating shrinkage porosity and minimising segregation. The produced metal is considered more reliable. Attempts are being made to establish electroslag castings in engineering use.

The term 'casting' implies that complex shapes, relative to ingots, will be considered. This signifies that mould design will be an important aspect in deliberations about electroslag casting and fresh designs will be required for every new shape.

1.2 The Mould

The mould, in general, is a container for the liquid metal and serves to shape the casting. Additionally it should minimise the probability of such defects as hot tears. Basic principles of mould design utilised in conventional casting are applicable here. The extra feature is that the mould must be able to abstract the heat fluxes liable to occur in the electroslag process and should foster the formation of a smooth surface.

1.2.1 Heat Flow In And To The Mould

Most published work on heat transfer to the mould in the electroslag process has concentrated on the conditions occurring in ingot remelting. Nearly 35-50 percent of the heat generated in the slag passes directly to the mould and another 20-25

percent passes indirectly to the mould.[1,2,3,4] The heat flux has been found to reflect the pattern of heat generation with the peak heat flux being in the range of 1.6 MW/m^2.

Early work on the heat balance of the process was done by Soviet workers at Kiev, the essence of which is reviewed in the book edited by Medovar et al.[1] Depending on electrode configuration (bifilar, 3-phase, etc.), the slag depth and the metal slag interfacial area; between 46 to 65% of the power input goes directly to the slag. An empirical relation has been developed for this as shown in fig. 1. The heat flux too varies with the above. In addition, it varies with the height of the ingot casting, the power input and the mould shape.

Many measurements of heat flux are reported. In some cases two peaks appear, one at the air slag interface and the other at the slag metal interface and in other cases a peak does not occur, but there is a broad band of high heat flux from the liquid slag, as is shown in fig 2. The heat flux from the slag reduces with increasing liquid metal head, increasing distance from the electrode and decreasing power input. As the slag skin thickness increases, the mid slag region heat flux/ metal head flux ratio tends to come closer to 1.

Much of this has been confirmed by Holzgruber[3] and by Joshi.[5] Similar energy balances and heat flows can be deduced from the work described below.

Pocklington and Patrick[6] report on heat flow in 3 phase slab production. The moulds were jacketed and 1 D approximation was used to calculate heat fluxes from thermocouples inserted in
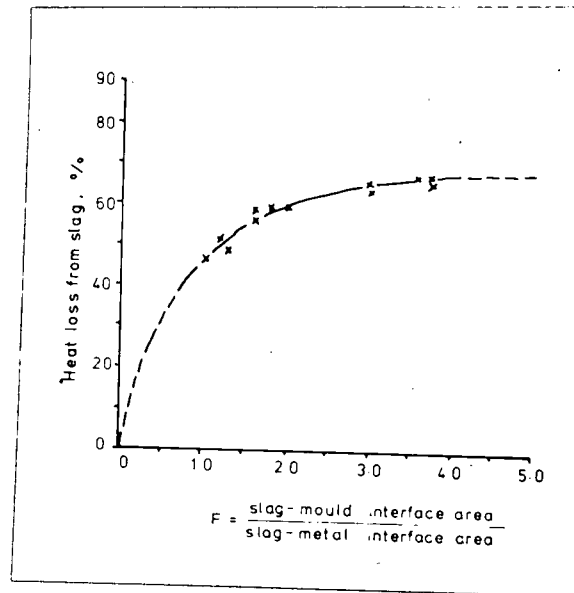
Figure 1 - Heat Loss vs. Parameter F
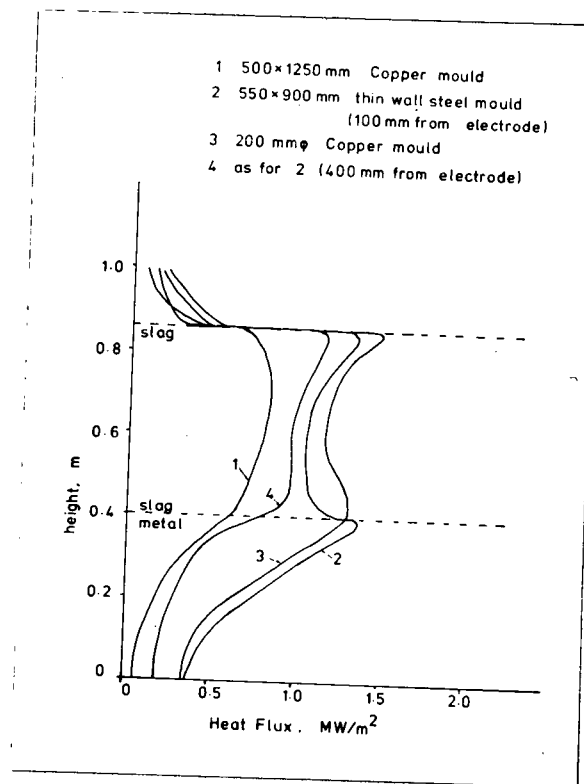
Figure 2 - Heat Flux Variation

the wall. Heat flux variations were found to depend on slag composition and the remelting conditions. Peaks of temperature were found in what they called 'Form' 4 curves, but this did not translate into peaks of heat flux. Maximum heat fluxes were of the order of 1 - 1.2MW/m² for most slags and about 1.8 MW/m² for 70:15:15 slag. Greater variation of heat flow around the periphery was found compared to conticast moulds. It was suggested that small heat flux differentials may minimise distortion of the mould.

Some experiments were carried out by the Albany Metallurgy Research Centre.[7] A 3 piece jacketed mould was used in a laboratory furnace. They observed 3 peaks in the heat flux curve with maximum flux of about 3 MW/m². The temperature differential of the cooling water between the inlet and the outlet was used to determine the heat flux and it is likely that very high precision measurements were required.

Kusamichi et al[8] conducted interesting experiments in which slag was frozen onto a water cooled copper pipe in a crucible of molten slag. Two thermocouples were kept very close to the pipe so that the slag solidified around them and the measured temperatures were used to estimate the effective thermal conductivities of slag skins, the thermal resistances, and the heat transfer coefficients. The resistance of the slag skin and that of the slag skin - mould interface were found to be of major importance and this is shown in Table I. Differences were noted for different slags, but it must be pointed out that crystallisation is different in the real process.

Table I - Thermal Resistance - from Kusamichi et al[8]

a. in Crucible

Slag			Thermal Resistance (s.deg./Cal)					
CaF_2	Al_2O_3	Cao	Total	Bath-Crust	Crust	Crust-Pipe	Cu Pipe	Pipe-water
0	50	50	35.4	4.6	28.5	0.7	0.01	2.2
50	25	25	30.3	3.6	14.3	10.9	0.01	1.7
100	0	0	21.7	2.9	5.4	12.0	0.01	1.3

b. in ESR

CaF_2	Al_2O_3	Cao	Total	Bath-Crust	Crust	Crust-Pipe	Cu Pipe	Pipe-water
0	50	50	0.81	0.19	0.48	0.09	0.007	0.04
50	25	25	0.43	0.09	0.21	0.10	0.007	0.02

In (b) read mould for pipe.

Kondo, Kodama et al,[9] measured heat fluxes of up to 0.8 - 1 MW/m² in 800 mm industrial moulds. A peak in the heat flux distribution was seen at the slag metal interface level for 70:15:15 slag and it was claimed that remelting of the slag skin of a 70:30 slag was observed.

The difference between Soviet investigators and the others is noteworthy. The Soviets developed a direct heat sensor which was thermally insulated from the rest of the mould, the signal being generated by a thermopile. The others merely inserted thermocouples into the mould wall and justified the technique by suggesting that 1-D approximation was acceptable.

1.2.2 Heat Transfer To The Mould In Mathematical Models

It is of interest to examine the boundary conditions at the slag mould interface employed by the various mathematical models around. Many models did not include the slag, but one may compare the conditions at the top of the ingot. Sun and Pridgeon[10] determined the conductance, h, by plunging Copper rods into molten slag and metal and measuring heating rates. Their value for "h" to the mould varied from .006 to .00745 cals./cm²sK. Carvajal and Geiger[11] used 0.4 cals./cm²sK and they did not model the slag. Elliott and Maulvault[12] used values from .01 to .02 cals./cm²sK as did Paton and co-workers.[13] Joshi[5] experimentally estimated it to be .0115 cals./cm²sK while Ballantyne[14] used .02.

More advanced models including fluid flow have been developed by Kreyenberg and Schwerdtfeger[15] and by Dilawari, Choudhary and Szekely.[17,18,19] These workers did not consider heat transfer coefficients but fixed the slag boundary to be at its liquidus temperature. In a recent paper Choudhary and Szekely[19] used wall functions to estimate the heat transfer coefficient to the slag skin boundary and predicted that the heat transfer coefficient will remain near constant. This situation is attributed to a nearly invariant temperature gradient close to the mould wall in the slag along the length of the mould face. In general, these modellers were interested in the pool shape and the local solidification time at the centre of the ingot.

1.2.3 Design Of Moulds

In the case of ingot remelting most moulds are jacketed and water cooled as a non-boiling system using principles as detailed by Mitchell and Smailer.[2] Channel-cooled moulds (moulds with holes drilled in the walls) have also been used especially in the moving-mould and ingot-withdrawal techniques. Early moulds were made of steel(with spray cooling) but practice soon switched to copper. Steel moulds had to be relatively thinner for good axial heat conduction and the danger of burn-through was heightened. Further, copper moulds were found to last much longer and so were cheaper in the long run. Larger moulds are made from slabs of thicker section since the stresses the mould must take are much higher.

Cremisio and Zak[20,21] have discussed the design of slab moulds in detail. Mould design starts with the minimum water velocity required to maintain non-boiling conditions. The mould wall thickness is generally selected from experience and the rest of the detailed design follows from this. They are of the view that flat surfaces in moulds face more demanding conditions than curved surfaces as in round moulds. The design should permit movement in the horizontal and vertical planes while maintaining restraint in the third plane. Creep resulting from thermal stresses is the chief problem in such moulds.

Channel cooled moulds have sufficient restraints built in as a result of their physical construction. However, they face higher temperatures on the hot face. Such a design may frequently not be used in full-length moulds since this may

entail inordinately high water pressures to ensure sufficiently high water-flow rates.

Soviet researchers were the early developers of the process and have done extensive work in the field. The gist of this work has been summarised in the book edited by Medovar et al.[1] Highly involved empirical design techniques have been developed and it appears that their work is the most detailed published so far.

Various methods of water cooling were investigated, e.g., jacket cooling, channel cooling and "rib" cooling. Schemes for cooling with liquid metals and organic liquids were formulated but it is not known if this was put into practice. Both evaporative and forced convection were considered with the latter being generally preferred.

The Soviet approach to design is from two directions; from the slag to the mould and from the coolant to the mould. Using the empirical methods mentioned in section I.2.1 the heat flux to mould wall is estimated. Taking a safety factor the water velocity is chosen depending on the mould type (i.e. the "efficiency") and from this the detailed hydraulic design is carried out.

The expected maximum mould temperature at the mould-coolant interface is estimated from the heat flux to the coolant, the coolant temperature and the heat transfer coefficient. The heat transfer coefficient is approximated using Borishansky's correlation[54] for nucleate boiling forced convection and modified by an efficiency factor to reflect the

geometry. The temperature distribution is then worked out in the vertical and horizontal sections using carbon conducting paper, i.e. a 2-D technique.

For the vertical section through the cooling channel, the heat flux estimate is used as the boundary condition, but this is raised 30% for the horizontal section arbitrarily. At the channel the boundary condition is a fixed temperature condition. The maximum temperatures calculated are then compared to the maximum temperature tolerable and the design accepted on this basis.

The design pays less attention to the influence of axial heat flow. The most important parameters are the heat flux and the heat transfer coefficient to the coolant. In a sample calculation the maximum mould face temperature reached 350°C. The tolerable temperature was given as 500°C. No material was mentioned but from the value of the thermal conductivity used it is assumed that the material was copper.

This represents very high mould temperatures when compared with western design. It must be pointed out, however, that most of this work was done more than 10-15 years ago with probably limited computing resources.

The approach to evaporative mould design is similar. In practice, mould thicknesses are lower (about 5mm) and the material employed is steel. Such moulds apparently are not used to-day.

1.2.4 Water Cooled Moulds Used Elsewhere

Water cooled moulds are also employed in other processes. Vacuum arc melting moulds are also designed using the same techniques. However, the heat fluxes are lower and the region of high heat flux is narrow which, practically, means that lower water flow velocities are used. There is creep deformation, but the number of heats obtained is sufficient to economically amortise the cost of repair and the cost of the mould.[21] The same remarks are probably applicable for electron beam melting moulds.

Moulds in continuous casting of steel are subject to similar heat fluxes and have been subjected to intensive study.[23,24] Earlier, the problem of mould distortion was attempted to be solved by lowering temperatures in the mould wall.[41] Attempts are now being made to reduce the possibility of intermittent boiling and to gauge the effect of thermal stresses[24]; and so design to reduce product rejection.

1.2.5 Probable Mould Type In ESC

In electroslag casting, the casting is not expected to be very tall. Further there will probably be frequent changes in section. One piece moulds, if employed, will have to be cast. Such moulds may have casting defects (e.g. blow-holes) and it will be difficult to either jacket them or to have the cooling channels integrally cast. Therefore, it is likely that the mould will be made of short sections joined together by

mechanical means. This system favors channel cooling of moulds since it is thought that water-jacketing of each section will be too expensive.

It is unlikely that electroslag casting production runs will be very large meaning that copper moulds would probably make this process noncompetitive. The only other material, commonly available, with a sufficiently high thermal conductivity is aluminium. This change will cause higher temperatures in the mould wall[25], but there is no report of any untoward effect on the process or the cast metal.

1.3 Surface Quality

Electroslag ingots have a good surface and this was passed off intuitively as being due to a thin slag skin. Mitchell and Etienne[26] suggested that, as in other solidification processes, this was due to the presence of a cylindrical liquid metal head. This is generally accepted with variations , primarily on the existence or non-existence of a liquid film between the slag skin and the solidifying metal. A bad surface can come about only as a result of meniscus solidification, leading to intermittent rippling.

1.3.1 Slag Skin Crystallisation

The use of water cooled moulds makes the formation of a solid slag layer, called the slag skin, on the mould surface inevitable. There has been little published information on the formation of slag skins by the solidification of different slags.

Sharapov et al,[60] examined the role of the slag skin. They divided slags into two major groups, those with two components, and those with many components. Both types of slag caused three layers to form in the slag skin with the two layers nearest the metal held to form on reheating of the original skin. The third layer closest to the metal was said to be liquid till the metal solidified. Multi-component slags were preferred in moving mould processes because they permitted a thicker third layer.

Kamensky et al,[27] considered the thermal stability of the slag and the structure of its boundary, the slag skin. The thickness was governed by heat transfer. On petrographic examination of a 70:30 slag skin they found five layers. The first layer had calcium aluminate crystals with the gaps filled with fluorite with the former as high as 70%. The second layer has columnar corundum crystals (upto 80%) and the third layer has fluorite (92%, rest glass) oriented in the direction of heat flow. Layer 4 is the same as layer 3 with a small quantity of needles of corundum. Layer 5 has extremely long and large corundum needles (12mm in length) oriented in the heat flow direction. These needles were much longer than those to be found in granulated slag. They observed that this structure

meant that the phenomenon of fractional crystallisation was ocurring. The higher alumina content of the skin (twice as high) was attributed to thermodiffusion of fluoride ions and enrichment by ions of the type $(Al_4O_7)^{-2}$.

Korousic and Osterc[28] also made a mineralogic analysis. They found that the phases crystallising out did not follow the phase diagram. The slag skin was stated to form under impeded metal ion exchange with consequent unbalanced fractional crystallisation. It is unfortunate that they failed to study vertical sections close to the metal meniscus.

Medovar et al,[1] mention three layers with no abrupt boundaries. The last layer is said to have a near eutectic composition. The first layer has an equilibrium composition and forms at very high cooling rates. The middle layer contains non equilibrium proportions of phases and multicomponent slags are more prone to this.

Bell and Mitchell[29] also observed the slag skin of slags in the calcium fluoride-alumina system. The slag skin was said to be a near equilibrium phase and they deduced the dissolution and melting of the skin, as the metal meniscus approached, from X-ray maps. Mitchell[30] has analysed the slag skins of various slags using X-ray diffraction. In a 70:30 slag skin CaF_2, Al_2O_3 and CA_6 were found. A 40:30:30 slag caused $C_{12}A_7$ and $C_{11}A_7F$ to crystallise and a 55:35:10 slag skin had CaF_2 and CA_2.

1.3.2 Slag Skin Effects On Surface Quality

. In the West, the suggestion of Mitchell and Etienne[26] has been generally accepted. The slag composition is important and if a high melting phase precipitates out during solidification then such a slag is conducive to the formation of a good surface. If the liquid head of metal is present, then it is held that some of the precipitated high melting phase is redissolved into the slag leaving a smooth surface for the liquid metal to solidify against.

The Russian workers[1] visualise a thin liquid film between the liquid metal and the solidified slag skin. They envisage some remelting and/or dissolution of the slag skin and rippled surfaces are attributed to meniscus solidification. Some Japanese researchers' opinions[31] tend to agree with the Russian view, others[9] favor the Mitchell viewpoint.

The surface of the ingot is said to be controlled by the freezing point of the alloy and the nature of the slag. A high melting phase precipitating out favors the formation of a smooth skin. Speculation in industry suggests that smooth skins may be encouraged by running the mould warmer. However, Mellberg[32] has pointed out that the heat flux in the molten head region of the ingot is very high and this may act to control the superheat in the liquid. This would mean that running a mould warmer may have no effect.

In industrial practice, the problem of a poor surface has been generally dealt with by increasing the power input, but this is limited due to adverse effects on solidification

structure. It is also known that a higher fill-ratio favors a better surface in fixed mould practice. An increase of slag depth is also favorable but this, it is stated, is unexpected.[33]

The mould, it appears, has no effect. Shevtsov et al,[34] suggest that a mould can have no effect on slag skin formation because no mould can be made that has a face temperature in excess of the slag melting point based on the premise that the slag skin thickness adjusts itself to match the heat flux from the bulk of the bath to the mould.

1.4 Objectives

The foregoing discussion suggests strongly that moulds to be used in electroslag casting will consist of channel-cooled sections made from aluminium. It is noted that electrodes to be used will normally be round bars. With this in mind, investigations were carried out to determine if such moulds could be designed to ensure smooth surfaces in electroslag casting.

It was of interest to design moulds to have a given limiting temperature at the mould surface. Besides the obvious necessity of keeping the mould cool enough to prevent disastrous melting, there were suggestions that temperature is the criterion for mould design. It was intended to determine if this criterion was correct or if there were other more important criteria in mould design.

II. EXPERIMENTAL

This chapter is divided into two sections. The first deals with experiments made on the 1 tonne electroslag furnace and the second is concerned with observations of the slag skin and the slag cap as obtained after melting.

2.1 Experiments On The Furnace

It was important to measure temperatures in the mould wall at different locations, since data was needed to compare with model predictions. A heat flux sensor also had to be developed since it was known that the heat flux varied with position in non-symmetrical geometries and values of heat flux were needed as input to mathematical models of heat transfer in the mould.

2.1.1 The Electroslag Furnace At UBC

A detailed description of the furnace has been presented earlier.[35,25] The furnace is capable of melting ingots and castings up to 1 tonne. There are two transformers, the first rated 250 KVA with voltage dropping from 12.5KV to 600V and the second delivering electrical power at between 25V to 60V in steps of 2.5V.

The electrode holder is water cooled and moves vertically up and down between aluminium rail guides. The holder carriage is suspended from a chain, the chain driven by a motor whose

speed is continuously variable up to 163mm/min.

The melting rate was controlled by varying the electrode descent velocity. The current was indirectly controlled by the electrode velocity and a saturable core reactor was not used.

Vertical channels were drilled in the mould and horizontal holes connected the channels to brass nipples at the ends of the mould. The open holes at the extremities of the channel were sealed by welding. The moulds were mechanically assembled and cooling water brought to the moulds through rubber hoses with thermometers monitoring the inlet and outlet temperature. Both aluminium and copper sections were used in the course of the work. A picture of the assembly is shown in fig. 3 and 4. Sketches of the mould sections in which the thermocouples were embedded are given in figs. 5(a,b,c) and 6.

2.1.2 Temperature Measurements

Thermocouples are the most convenient means of temperature measurement in moulds and have been used extensively by previous workers. The maximum temperature expected to be measured was about 300°C. Hence, copper-constantan thermocouples were chosen. These were available in thicknesses of 10 thou and sheathed in fibreglass, which also served as insulation with the diameter of the assembly being about 1mm.

Several holes of diameter 1.25 mm were drilled in a mould section as shown in figures 5(b,c) and 6. The type A thermocouples were expected to give an idea of the temperature
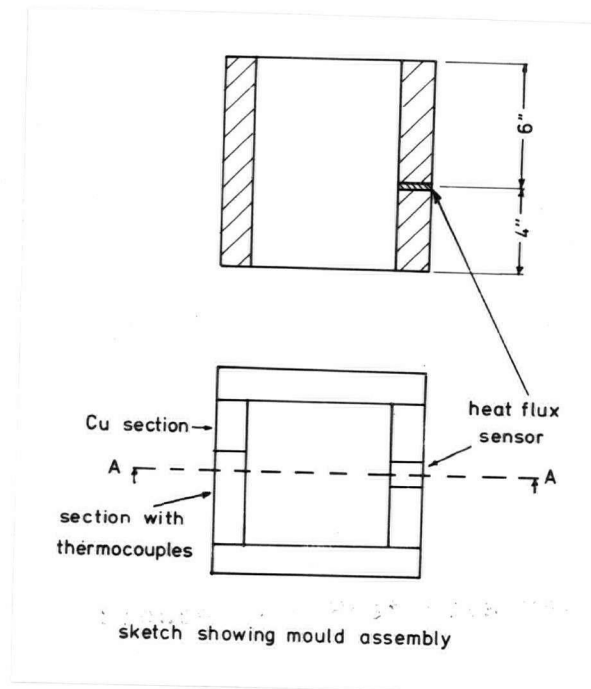
Figure 3 - Sketch of Mould Assembly
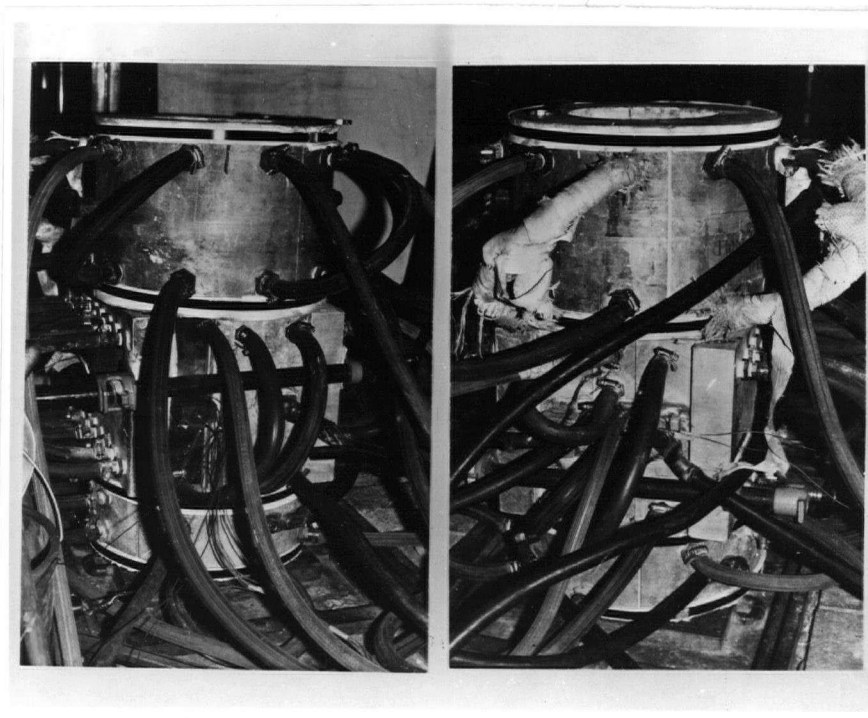
Figure 4 - Views of Mould Assembly

a
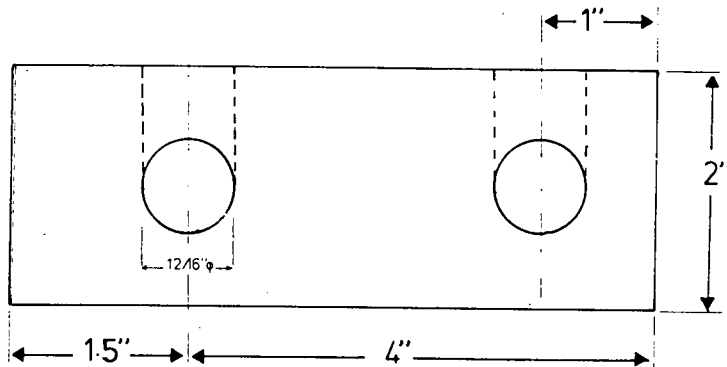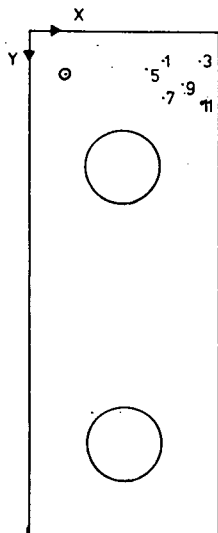
Type A Pos. No.	X (in cms.)	Y
1	3.57	.95
3	4.61	.95
5	3.11	1.43
7	3.58	1.91
9	4.60	1.51
11	4.66	2.05
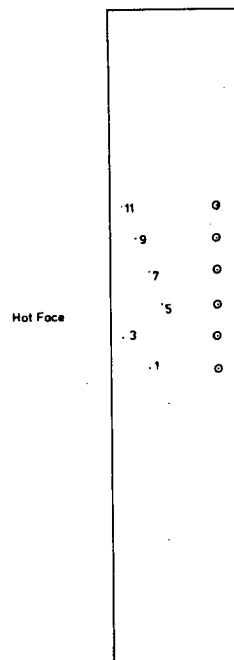
o ..... Type B

Type A Pos. No.	Z cm	X cm
1	11.46	3.57
3	12.67	4.61
5	13.97	3.11
7	15.22	3.58
9	16.52	4.10
11	17.78	4.66

○ ..... Type B

b   c

Figure 5 - Dimensions of Mould Section used
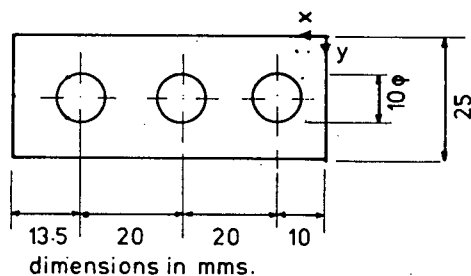
dimensions in mms.

section height = 254 mm

T/C No.	x	y	z
	(in mm)		
14	5.1	9.5	101.6
15	5.8	3.6	127
16	3.5	3.6	152.4

COPPER   SECTION   USED

Figure 6 - Dimensions of Copper Section

distribution in the mould, while type B thermocouples were to confirm the assumption of steady state heat flow, i.e. type B thermocouples were expected to give the same temperature history under steady state conditions.

The thermocouples were welded outside and soldered to the bottom of the holes using STRONGSET No. 509 solder. The cold junctions were encapsulated in insulation tape and placed in test-tubes which had some mercury in them to promote heat transfer and were kept at 0°C by partial immersion in an ice-water mixture.   The measuring junctions were connected to a Texas Instruments FM6WB multi-channel potentiometer-recorder.

2.1.3 The Heat Flow Sensor

Considerable difficulty was found in fitting published values of heat flux to the measured temperatures. It was evident that heat flow was definitely three dimensional and this created the need to develop a heat flow sensor. The heat flow sensor had to be thermally insulated from the rest of the mould and had to be as thin as practical to permit accurate heat flux measurement. Temperature measurement of water at the inlet and outlet was considered and rejected since it required too great a sensitivity in available measuring instruments.

The heat flux sensor was finally designed as shown in figure 7. The thermocouples were copper-constantan and the sensor was heavily water cooled so that no more than 0.5 degrees Celsius change in temperature was expected between the inlet water and the water at the outlet. The sensor was wrapped tightly in FIBREFRAX to thermally insulate it. Such sensors have been widely used by Russian researchers.[1] It is noted that the metal probably constitutes a negligible thermal resistance and so the choice of material for the sensor may not matter.

2.1.4 Verification Of Sensor Data

The temperature difference between the thermocouples was expected to be directly proportional to the heat flux. Published values of the heat transfer coefficient suggested that the Biot number was about .02 to .04. Here it is pointed out that the Biot number is normally used in cases where there is no

76.2 mm

8 mm

— 50 mm —
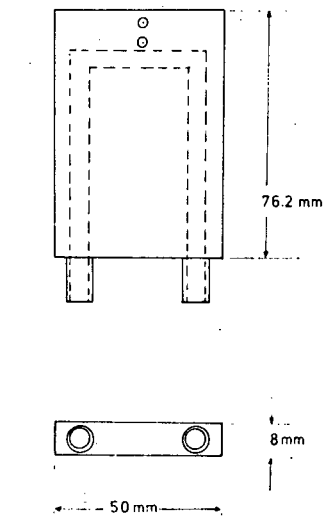
⊙ .... Thermocouples

Heat Flux Sensor

Figure 7 - Sketch of Heat Flux Sensor
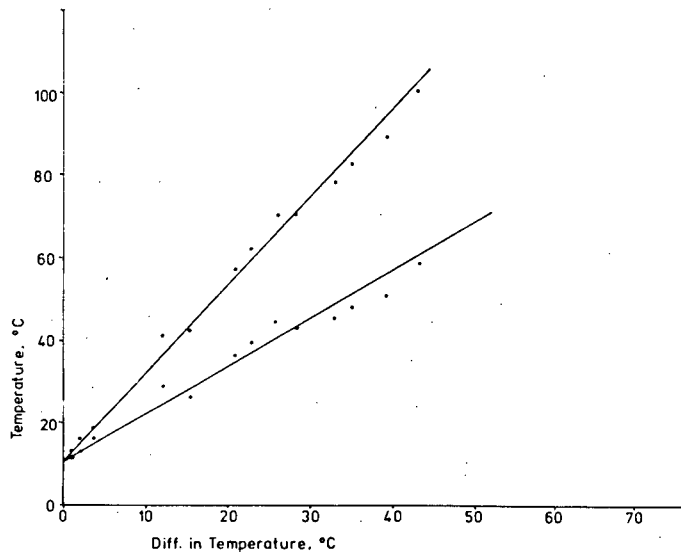
Figure 8 - For Verification of Sensor

sink as is present in the sensor, but an extension of the idea
may give an insight into the effectiveness of the sensor,
approximate as it may be. It is suggested that for a straight
line variation of temperature to exist in the sensor the Biot
number at the source should be small and that at the sink should
be large. Since the heat transfer coefficient at the coolant
interface is about 4 orders of magnitude higher than that at the
hot face, it appears likely that a straight line variation of
temperature will occur. The response time, L^2/A, where L is the
characteristic length and A the thermal diffusivity, was
calculated and found to be about 3 s. The rate of rise of ingot
is about .05 cm/s which suggests that the sensor will probably
respond quickly enough. To verify this estimate the difference
between the two temperatures (proportional to the heat flux) was
plotted against the temperatures. Provided that the sensor was
good the plot should be a straight line starting at the
temperature of the coolant at the inlet. This is shown in
figure 8. It was considered that the data was adequate to be
used after it had been normalised using figure 8.

2.1.5 Experimental Results

A summary of the 15 melts made is presented in table II.
Temperatures were measured at different positions in the mould.
Later, when it became apparent that the temperature could be
predicted reasonably well, only the temperature of position 3
and 11 were recorded. Run 8 had the mould section reversed so

TABLE II

Run #	Slag 8 kg.					Electrode Dia. (mm)	Special Features
	CaF_2 wt%	CaO wt%	Al_2O_3 wt %	SiO_2 wt %	MgO wt %		
1	70	–	30	–	–	75	Trial
2	70	–	30	–	–	75	Mould Temperatures and Heat Flux Measured
3	70	15	15	–	–	113	Thicker electrode, temp., heat flux measured
4	70	–	30	–	–	113	"
5	50	20	30			113	"
6	49	16	17	12	6	113	Slag leak, melt aborted
7	49	16	17	12	6	113	Thick electrode: temp., heat flux measured
8	70	–	30	–	–	113	Mould section reversed, power factor = 0.96
9	70	–	30	–	–	113	Melt aborted. Cable overheated
10	70	–	30	–	–	113	Copper section replaces aluminum
11	70	–	30	–	–	113	Run #10 repeated to avoid influence of power fluctuations
12	70	–	30	–	–	113	Grooved section used with T/Cs and flux sensor
13	70	–	30	–	–	113	Flux sensor at corner of box
14	70	–	30	–	–	113	Flux sensor at corner of box
15	70	–	30	–	–	113	Electrode as in Fig. 9
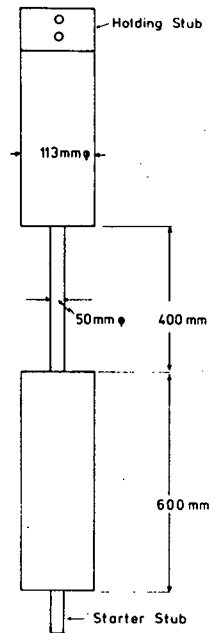
Figure 9 - Electrode used in Run 10
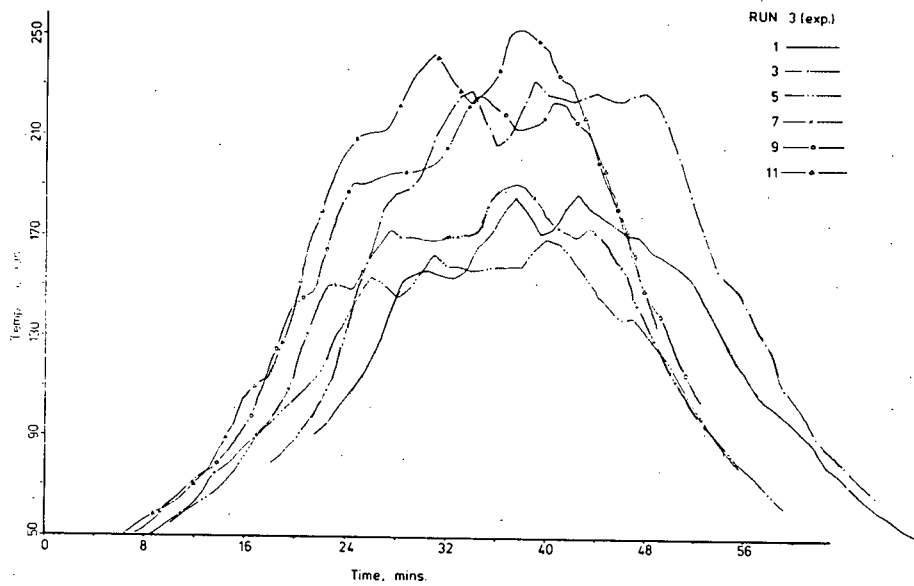
Figure 10 - Temp. History of RUN 3
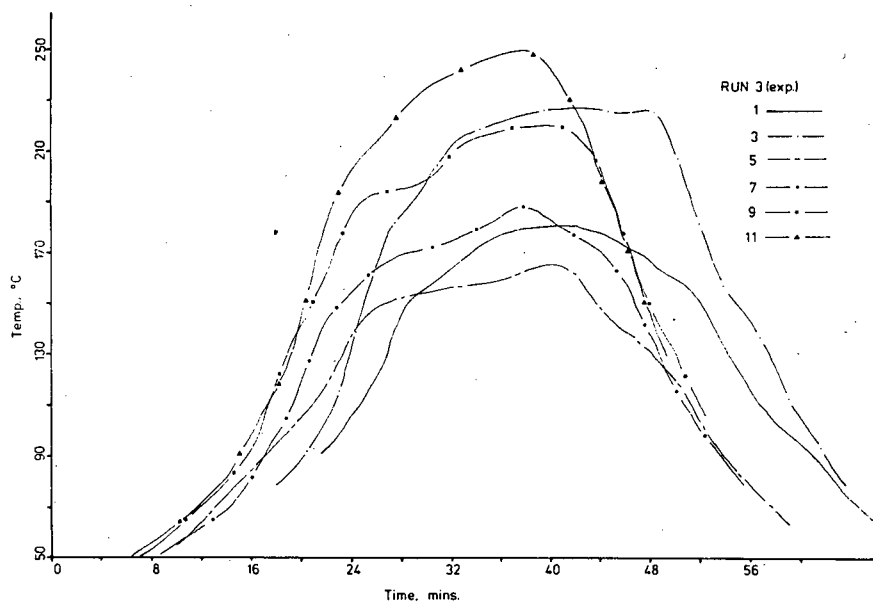
Figure 11 - Smoothened Temp. History of Run 3
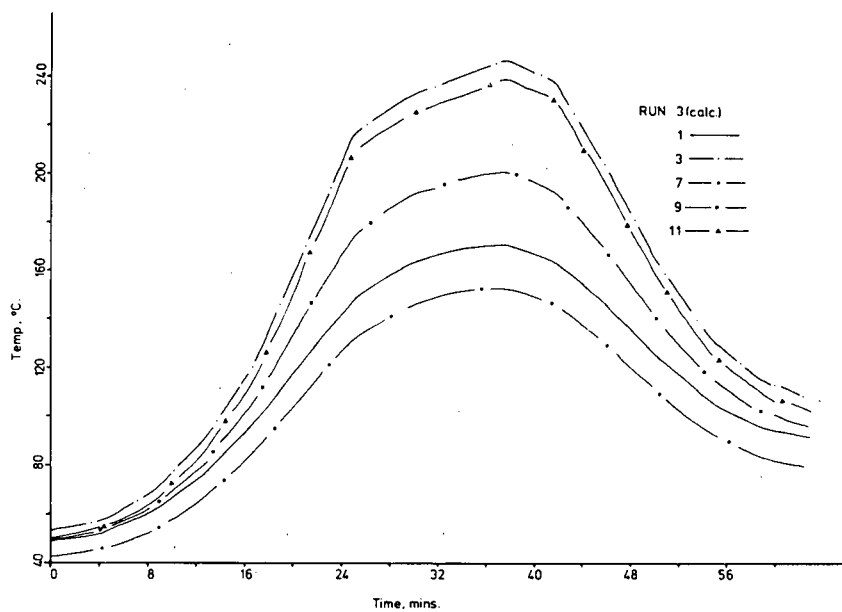
Figure 12 - Calculated Temp. for Run 3
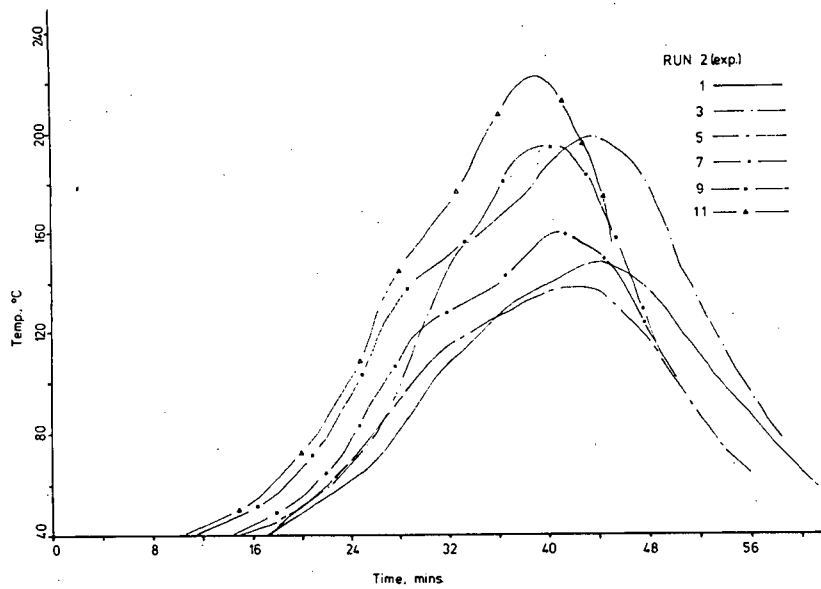
Figure 13 - Temp.History of Run 2
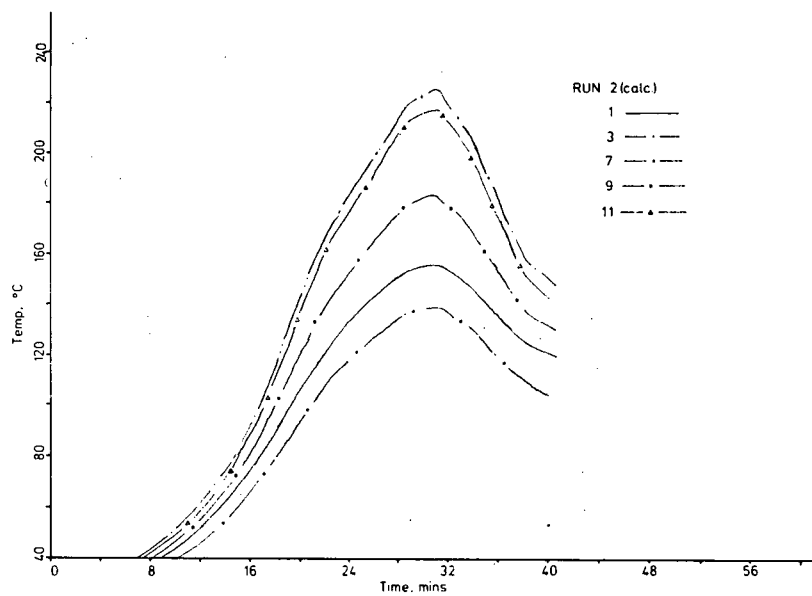
Figure 14 - Calculated Temp. for Run 2
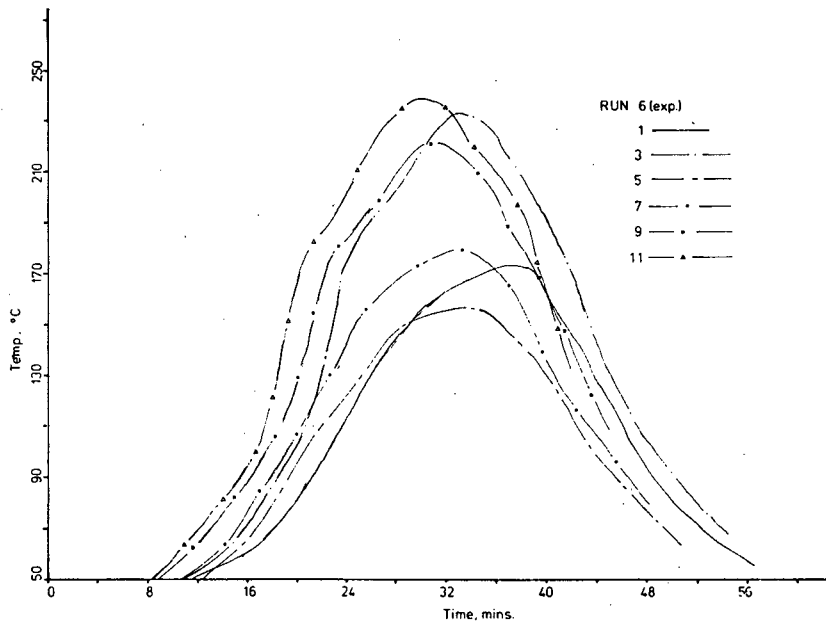
Figure 15 - Temp.History of Run 6
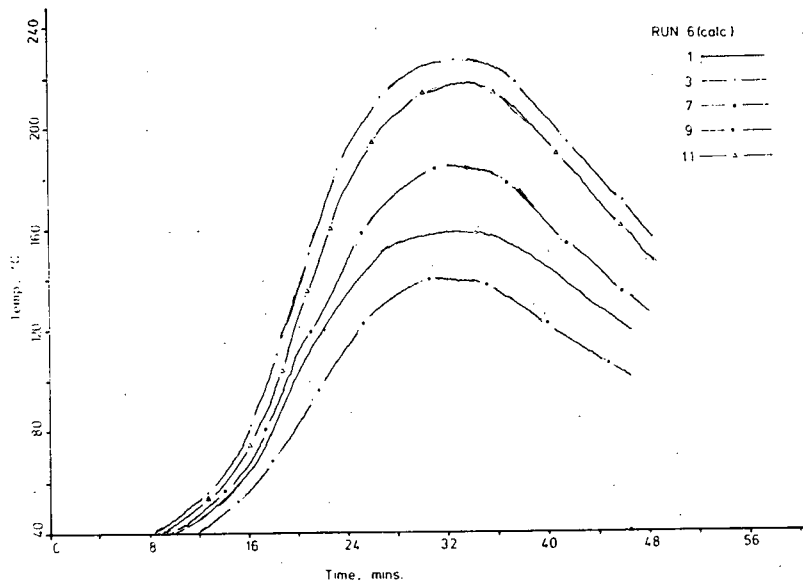
Figure 16 - Calculated Temp. for Run 6
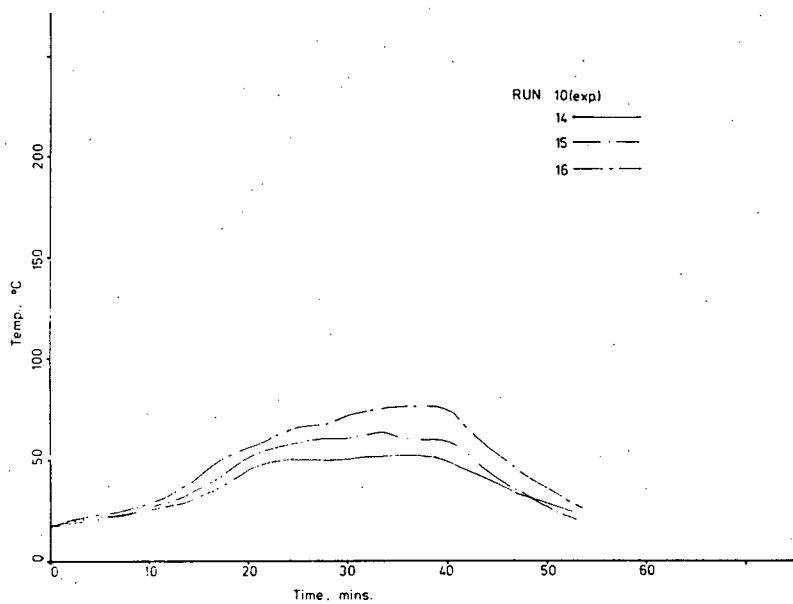
Figure 17 - Temp.History of Run 10
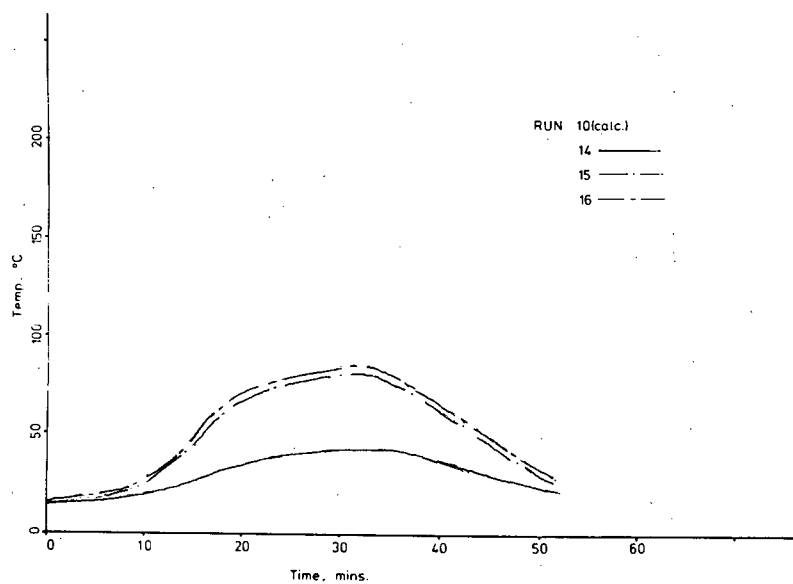
Figure 18 - Calculated Temp. for Run 10
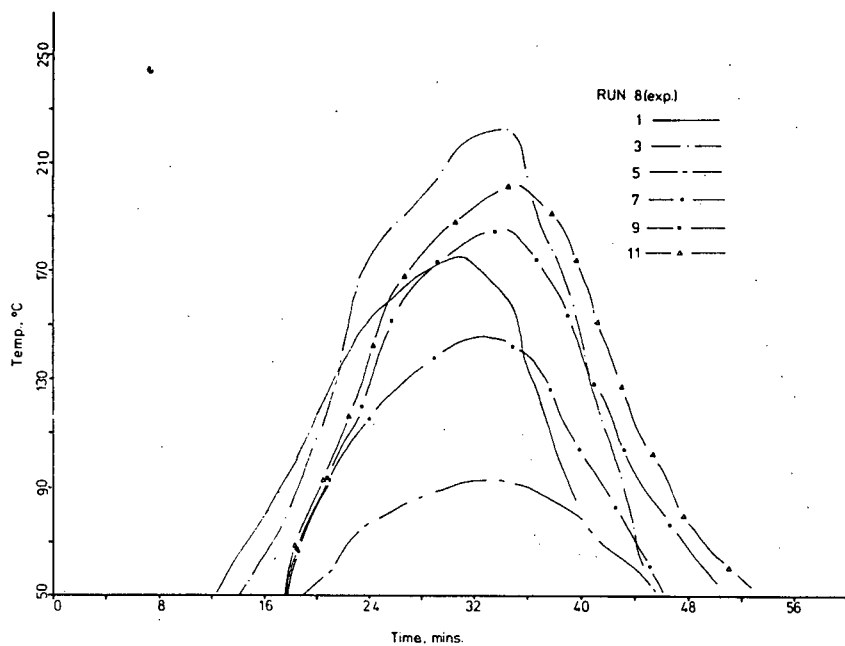
Figure 19 - Temp.History of Run 8
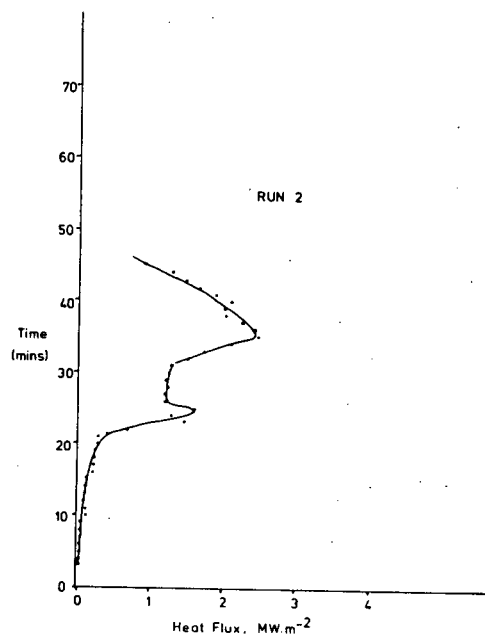
Figure 20 - Heat Flux Measurement-Run 2
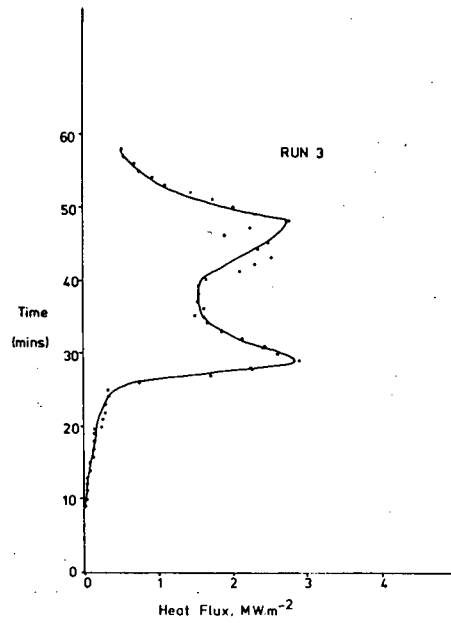
Figure 21 - Heat Flux Measurement-Run 3
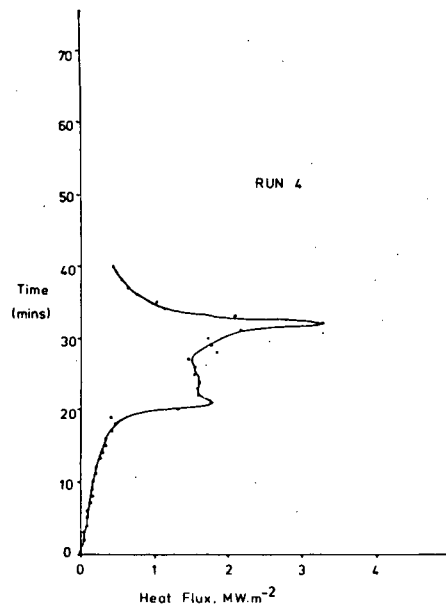
Figure 22 - Heat Flux Measurement-Run 4
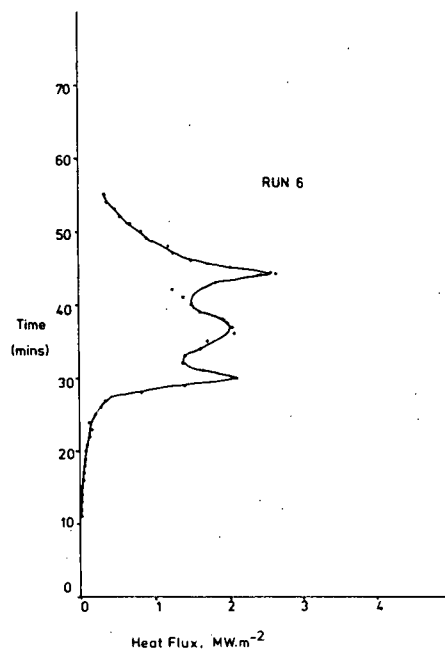
Figure 23 - Heat Flux Measurement-Run 6
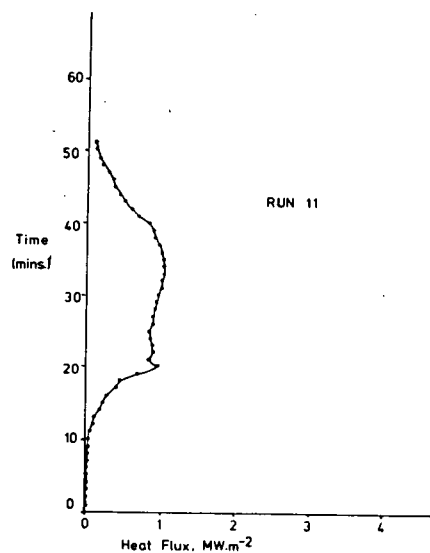
Figure 24 - Heat Flux Measurement-Run 11
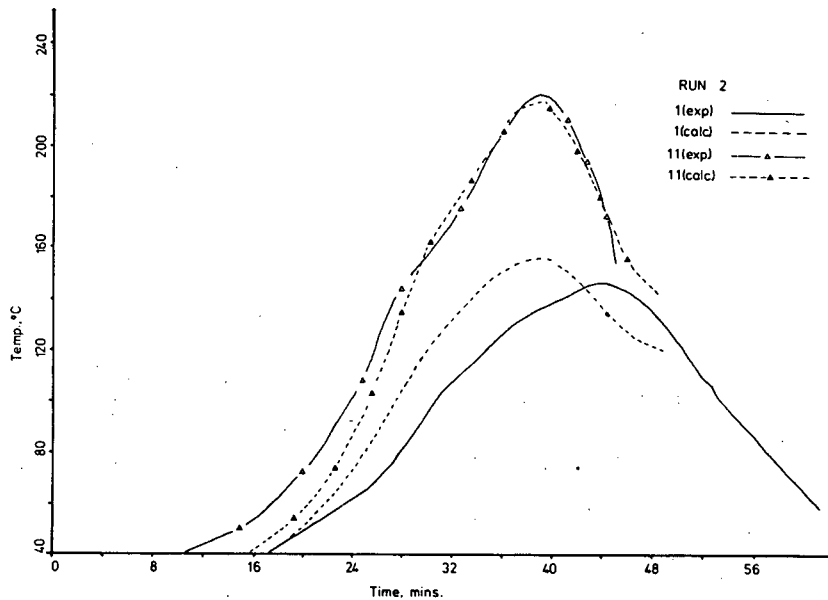
Figure 25 - Sample comparison between Calculated
temperature and measured

that thermocouples previously placed higher in the mould were
now at a lower position. In this run the power factor was
determined to be 0.96. Run 12 was made with a grooved face.
Runs 13 and 14 were made to measure the heat flux at the corner
of the box section. Run 15 had an electrode as shown in fig.
9.

Figures 10,11,13,15,17,19 detail the temperature history
obtained. The curves have been moved on the plots to simulate
the temperature fields on horizontal planes in the mould.
Fig.10 shows the variation obtained with heavy power
fluctuation. In the other runs the fluctuation was not so high,
but the curves have been smoothened to reduce the influence of
power fluctuation and facilitate better comparision with

computed results. It is clear from runs 2 and 4 that thinner electrodes have lower melting rates and cause lower heat fluxes to the mould than thicker electrodes. The temperature in the mould rose and fell smoothly as the slag passed across the measuring plane, except when there was a power instability. The heat flux curve showed two peaks, one at the slag-air interface and the other at the liquid metal head level with the peak flux level at the liquid metal head being much higher than previously reported. (see figs. 20 to 24)

The heat flux at the corner of the square section was determined with some difficulty. In the first attempt, the flux was found to be much higher than expected from mould temperature measurements. In the second attempt, special efforts were directed at ensuring that there was no slag penetration around the sensor. It was thought that such penetration would prevent contraction of the slag skin away from the sensor. Apparently, the air gap between the slag and the mould played a major role in controlling the heat flux. Therefore the values of heat flux determined at this position may not be very accurate. What is clear is that the average heat flux and the magnitude of the peak flux are both lower. Based on these results the total heat flux to the mould was calculated and compared to the power input and the match (shown in table III) was found to be satisfactory.

Run 8 was made to verify that there was some transient heat transfer. The maximum temperature reached by position 3 was found to be higher than that reached by position 11, whereas it was in the opposite sense in earlier runs thus demonstrating the

Table III - Comparison: Heat flow and Power input

Run#	Area	Rate of ingot rise	Heat flow (int.)	Power input	Mould ht. considered
	cm	cm/min.	kW	kW	cm
2	248.7	.37825	127.8	135.0	17.02
3	365	.22325	110.7	135.0	13.17
4	215	.38372	112.1	135.0	16.11
5	194	.40959	107.98	135.0	13.92
6	236.8	.28069	90.02	126.0	15.43

existence of transient heat transfer.

2.2 Observations On Slag Skins

The formation of the slag skin plays an important part in controlling heat transfer and in the formation of the metal surface. It was necessary to examine the process of skin formation in order to ascertain if it could be modified so that a smooth casting surface could be ensured. With this view, the slag skins formed with various slags were examined. The slag cap of 70:30 slag was also examined. This slag was chosen since its phase diagram is relatively well known.

2.2.1 Microstructure

Some micrographs of the slag skins are shown in figures 26 to 35 from which it is clear that the structure consists of three layers. The first seems to be a mixture being dark in some areas and light in others. There does not appear to be any particular regular structure or any predominant component in the
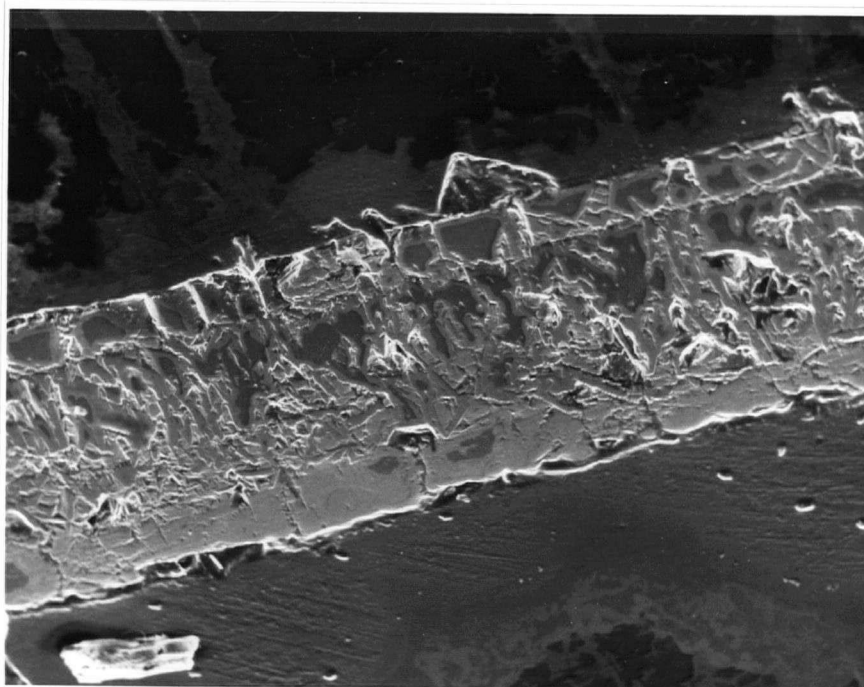
Figure 26 - SEM picture of 70:30 skin

Figure 27 - Spike on 70:30 skin
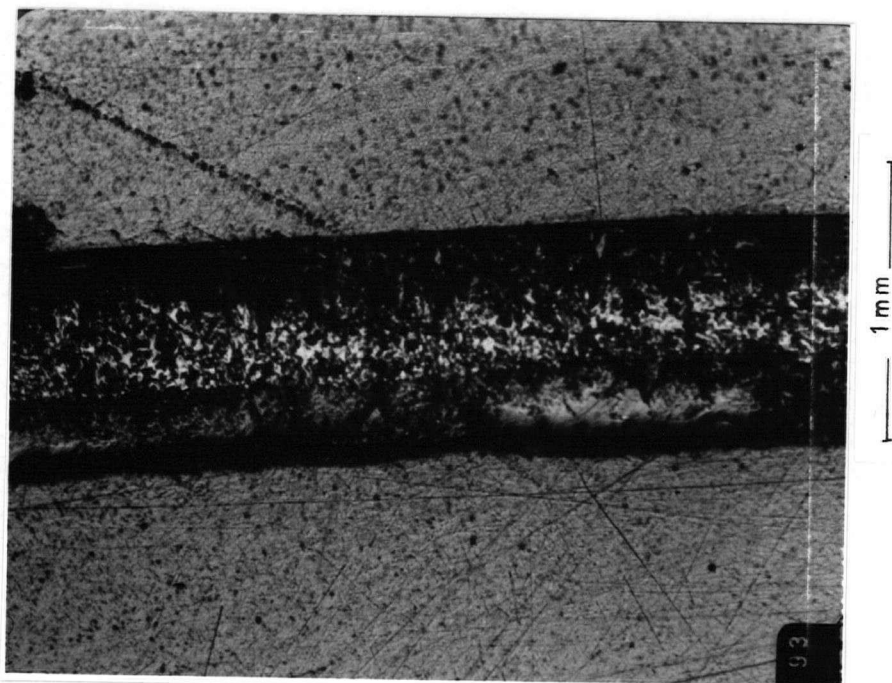
Figure 28 - 70:15:15 slag skin
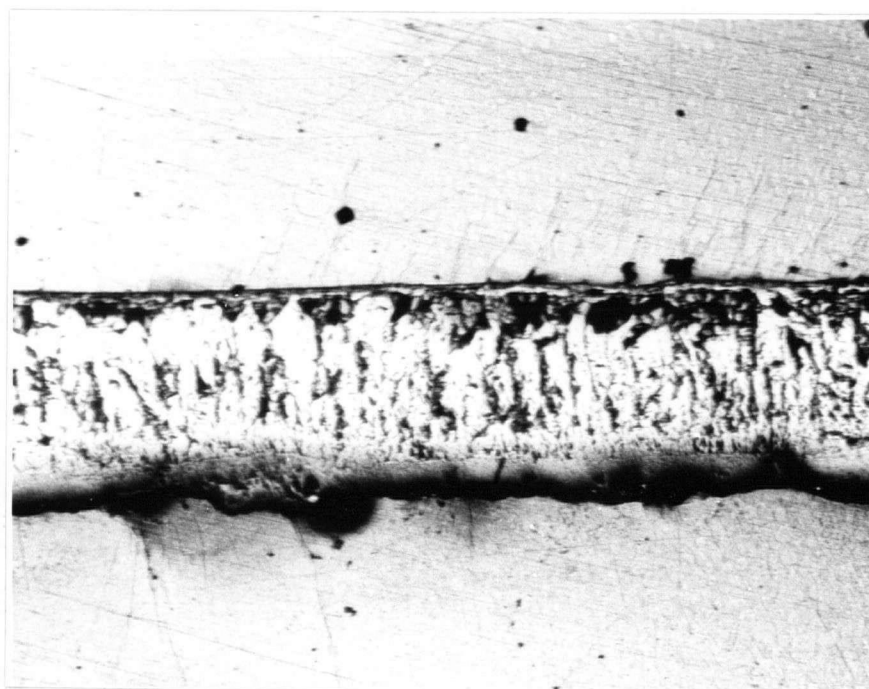
Figure 29 - 50:30:20 slag skin
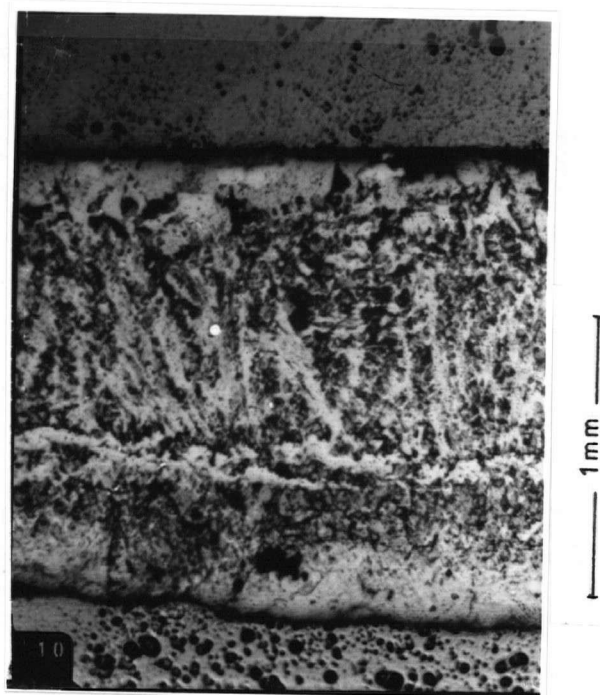
Figure 30 - Skin of Silica, Magnesia containing slag
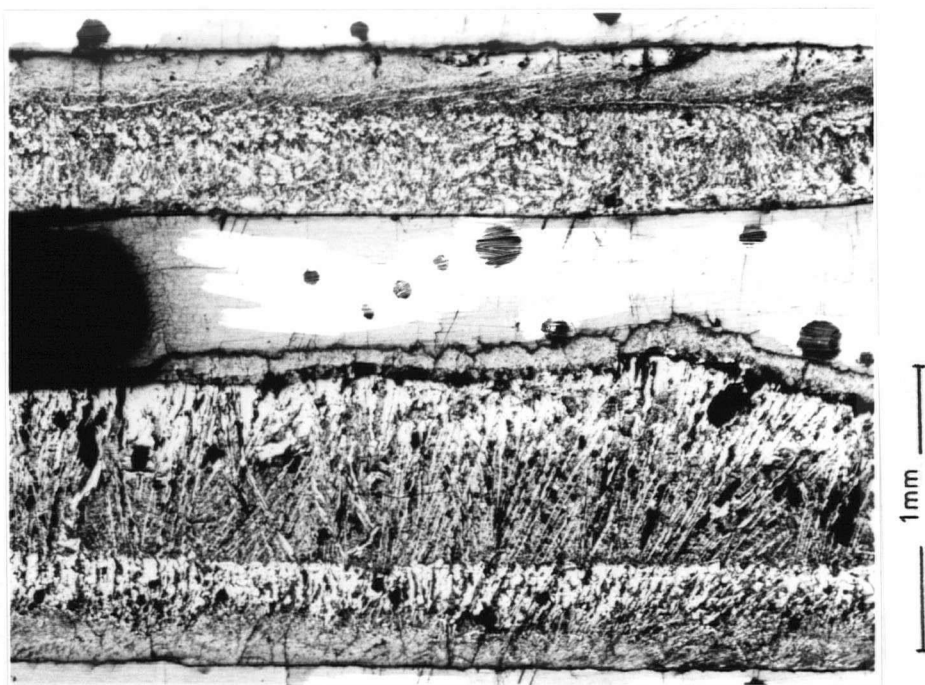
Figure 31 - Skins of complex slag
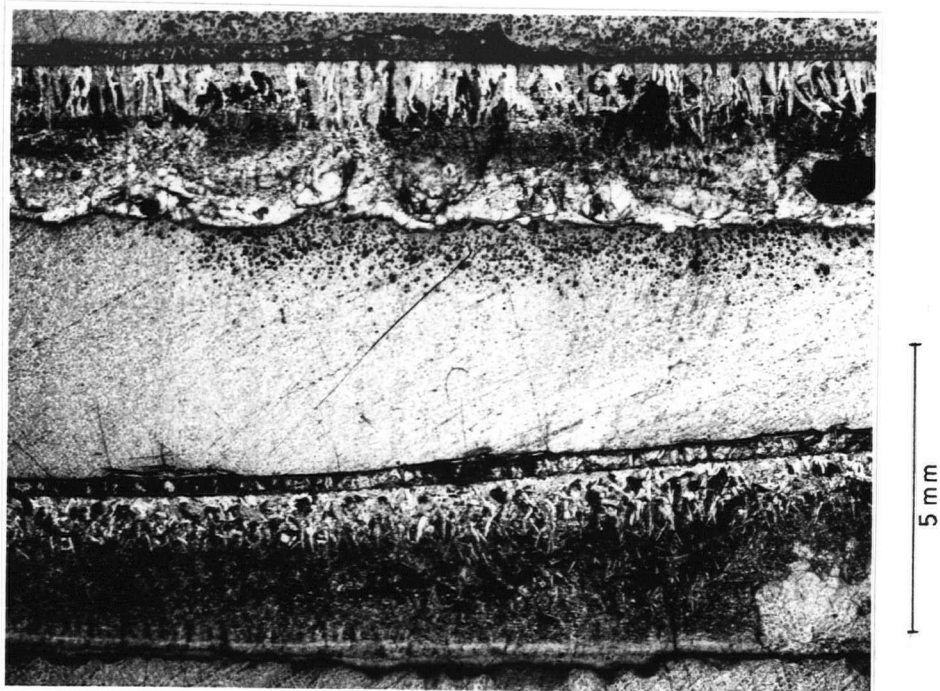
Figure 32 - Industrial 70:30 slag skin
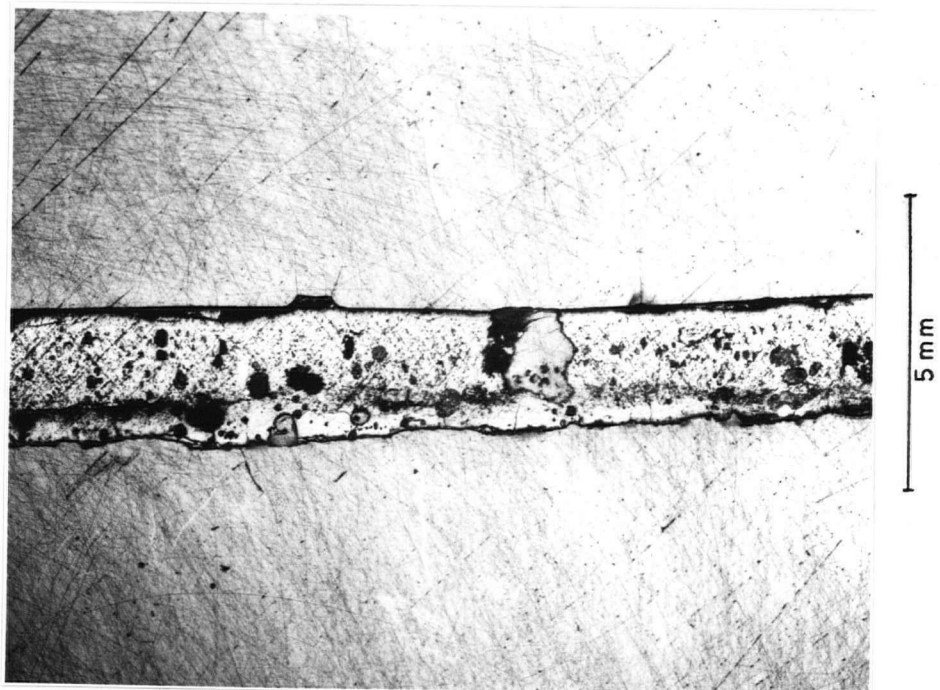
Figure 33 - Industrial 50:30:20 slag skin
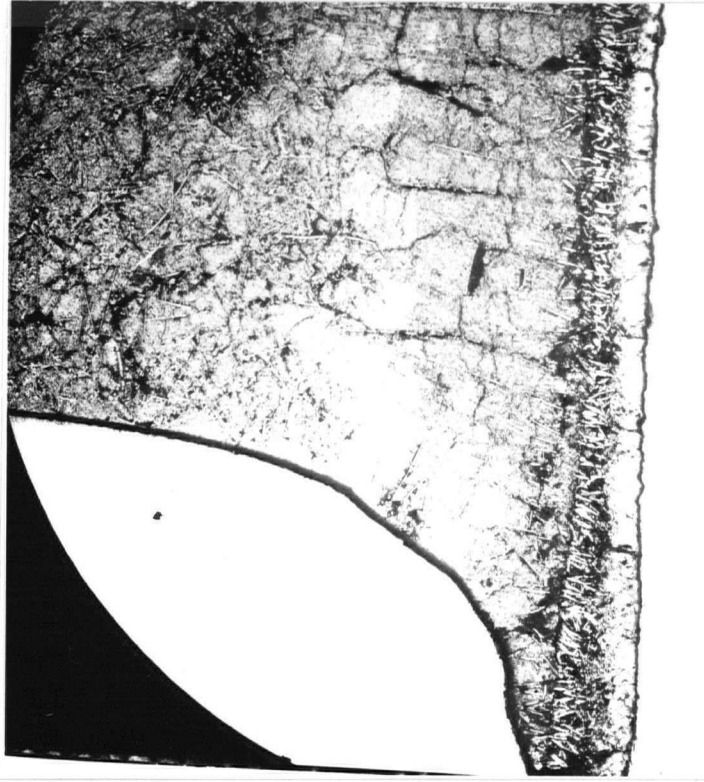
Figure 34 - 70:30 slag cap near metal meniscus
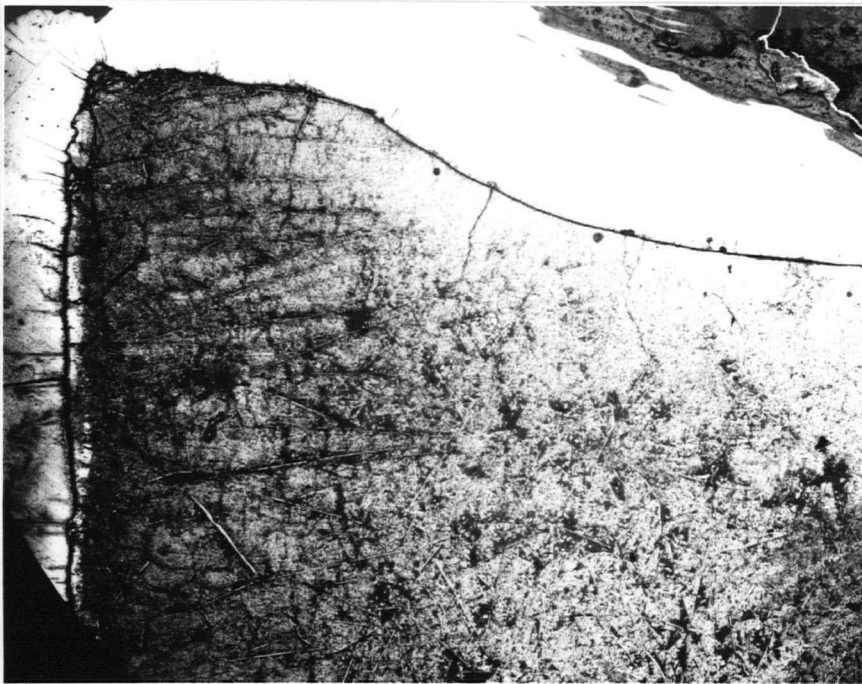
Figure 35 - 70:30 slag cap near top

layer.

The second, or the middle, layer displays relatively thick crystals oriented toward the ingot casting. There are several voids but most of the space in between the thick crystals is filled with a darker phase. The crystals appear to be the primary phase while the darker phase is probably the eutectic liquid which solidified later. Though the word 'crystal' has been used it is pertinent to note that in some of the complex slags the middle layer actually looks like a glassy porous mass.

The third layer, the one closest to the ingot casting does have some primary crystals, but surprisingly, has the physical appearance of the secondary phase. This layer was difficult to retain in the sample during polishing and caused considerable difficulty during that procedure. Apparently it is only lightly held against the skin. In the particular case of 70:30 slag, there were some spikes of glassy transparent material sticking to the slag skin at random intervals. In the other slags especially the 70:15:15 slag, the third layer was very thin and at some places not visible.

2.2.2 Observations On The SEM

Following the work under the light microscope, the EDX detector on the scanning electron microscope was used to identify the elements present in the three different layers. Quite obviously different slags would present different results, but the general pattern became clearer as seen in figs. 36 to

39.

In the case of 70:30 slag the outer layer was inconsistent; in some areas Al would be present and in other areas absent. This was not the case with Ca; it was always present and the Ca peak was higher than the Al peak. In the middle layer, there was a strong peak for Al, even larger than that for Ca. In the inner layer, close to the ingot, Al was noticeably absent except in the crystals that pierced their way through from the middle layer. The spikes of glassy material showed an even more surprising composition; apart from the presence of Al there was Si in significant content and noticeable quantities of S,Fe and Mn. This was surprising because neither the remelting theory nor the liquid film theory could explain the composition of the third layer or that of the spikes.

The structure of the 70:15:15 slag was different. The outer layer showed Al, Ca and Si. The middle layer had no Si and the peak due to Al had increased in height. The inner layer, closest to the ingot, showed an inconsistent presence of Al and Si especially at the very edge of the skin. There were no spikes on this slag skin.

The 50:30:20 slag skin had in its outer layer Al and Ca with the Ca peak stronger. The middle layer had two distinguishable phases, one darker than the other. Both Al and Ca were present with the Ca peak slightly larger in the dark phase but smaller in the light phase. The inner layer showed very little Al but Si, S and Mn were in evidence.

An industrial slag of 70:30 type used to melt stainless
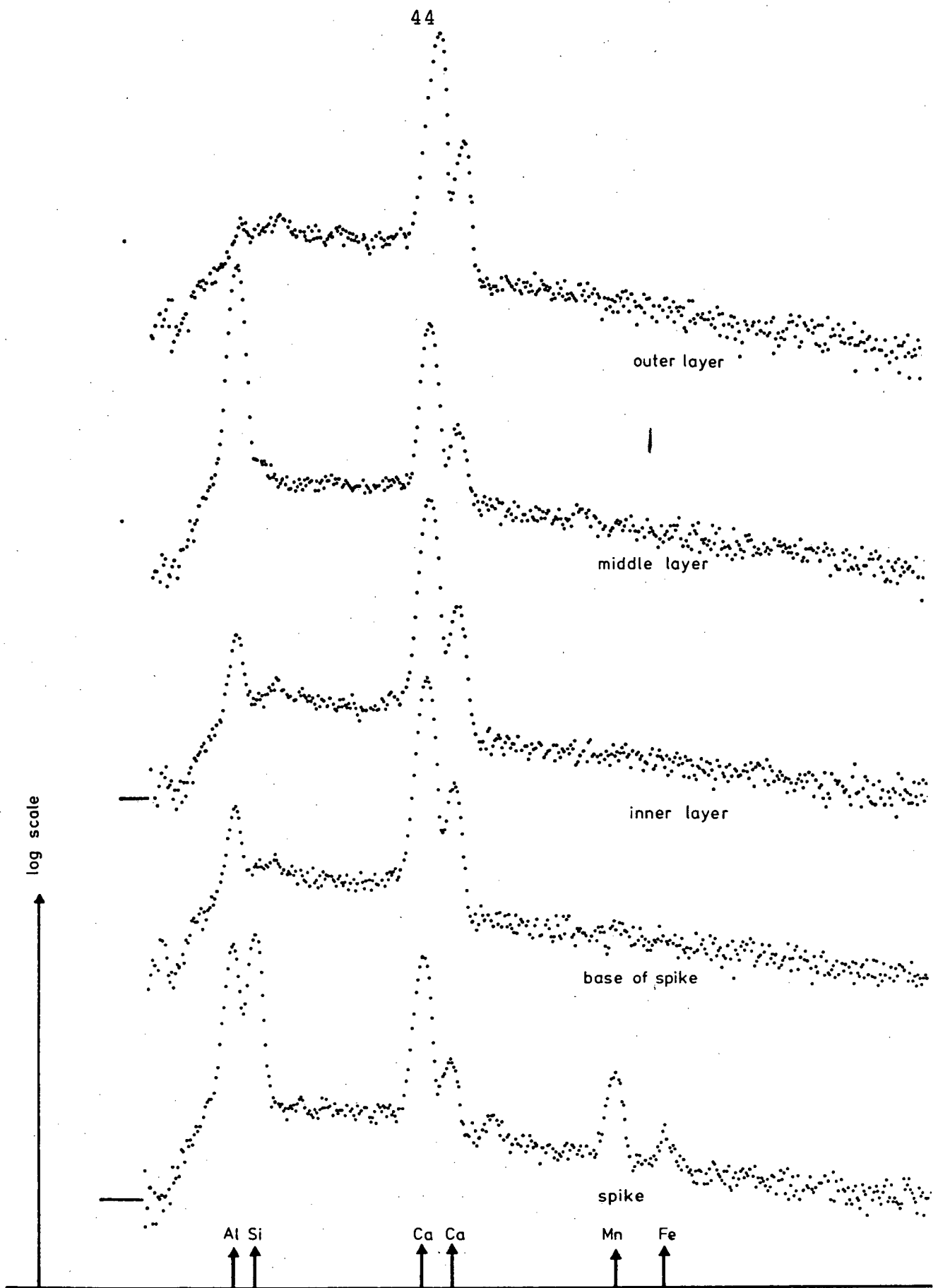
Figure 36 - EDX analysis of 70:30 skin
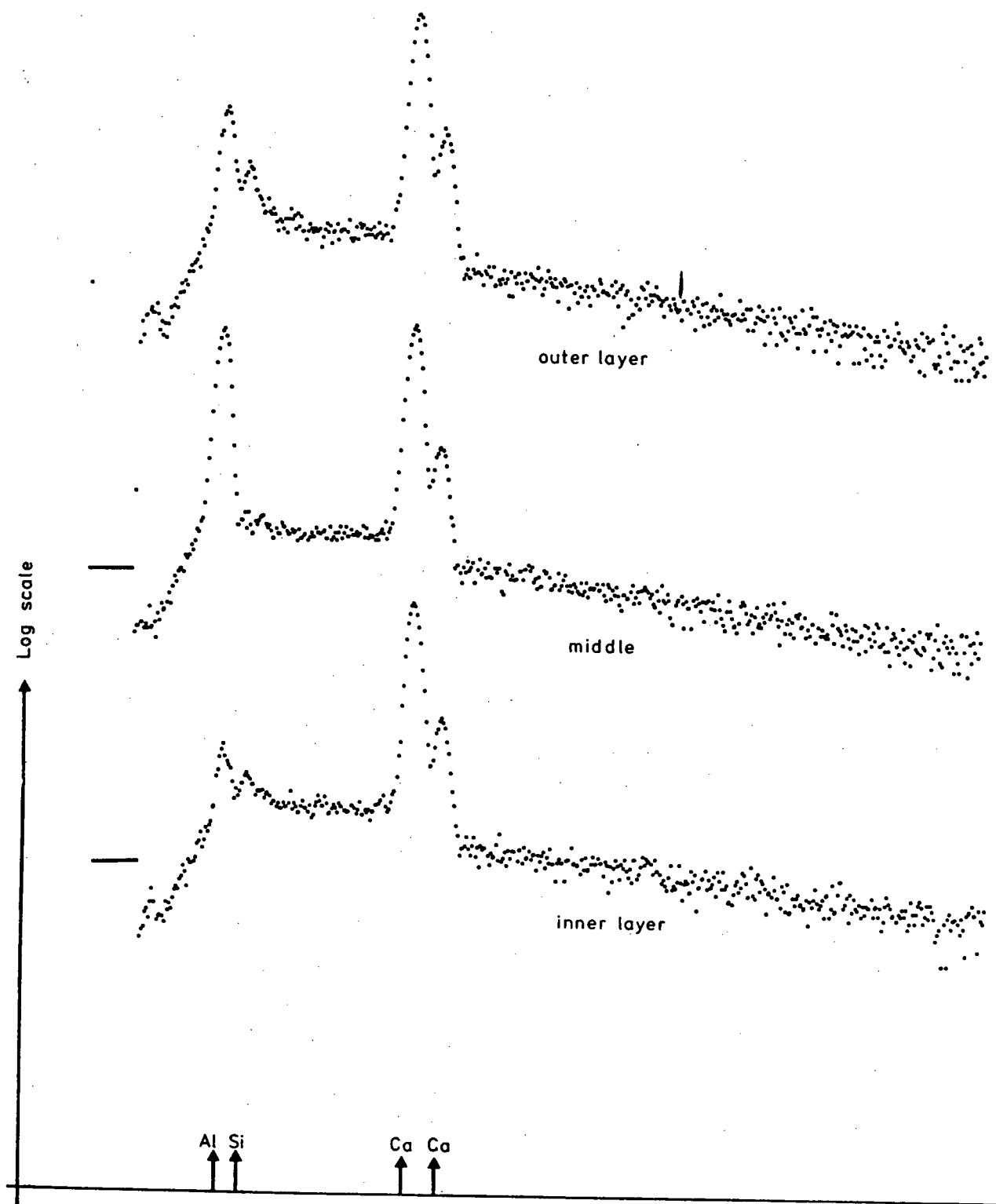
Figure 37 - EDX analysis of 70:15:15 skin
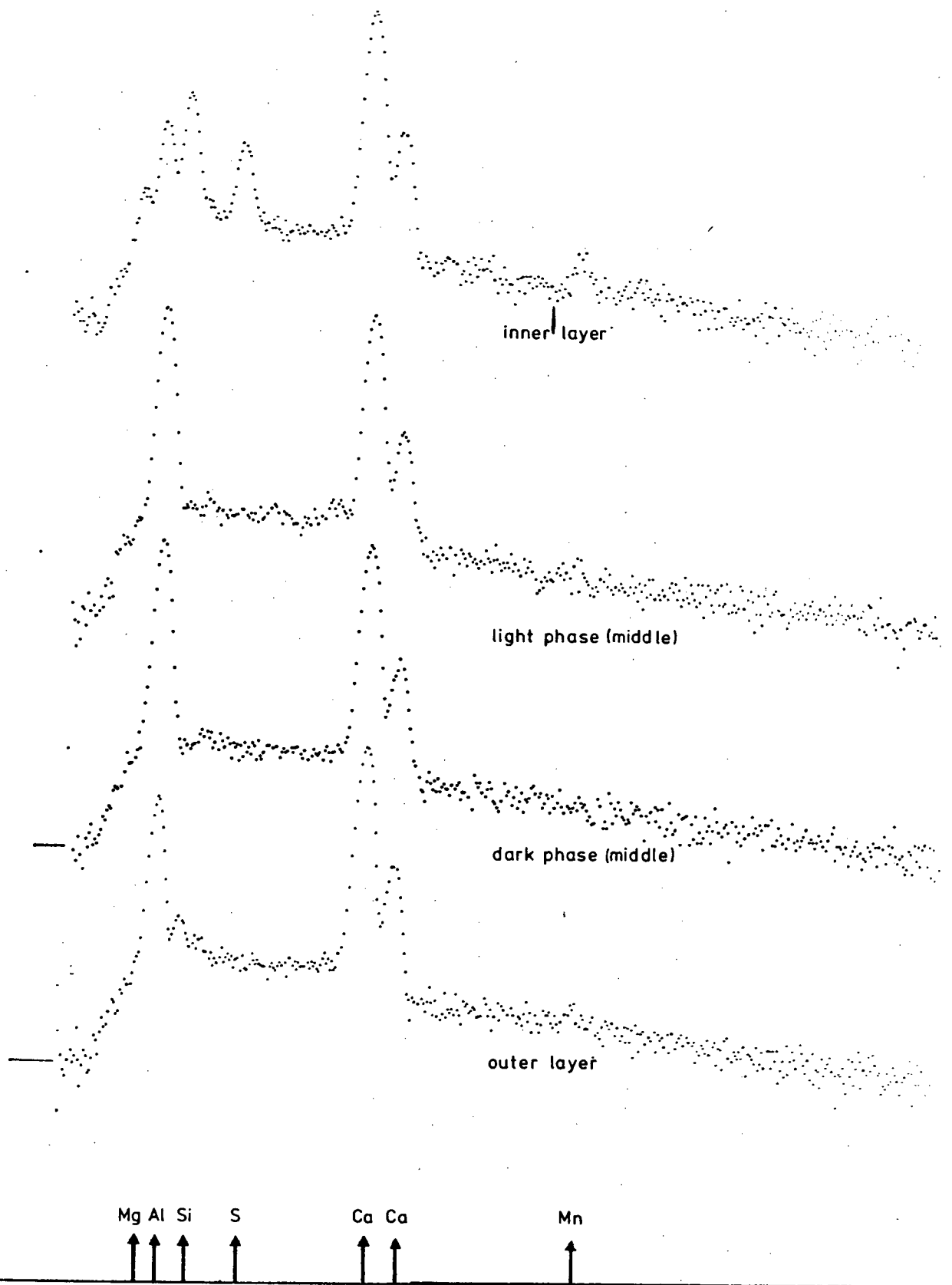
Figure 38 - EDX analysis of 50:30:20 skin
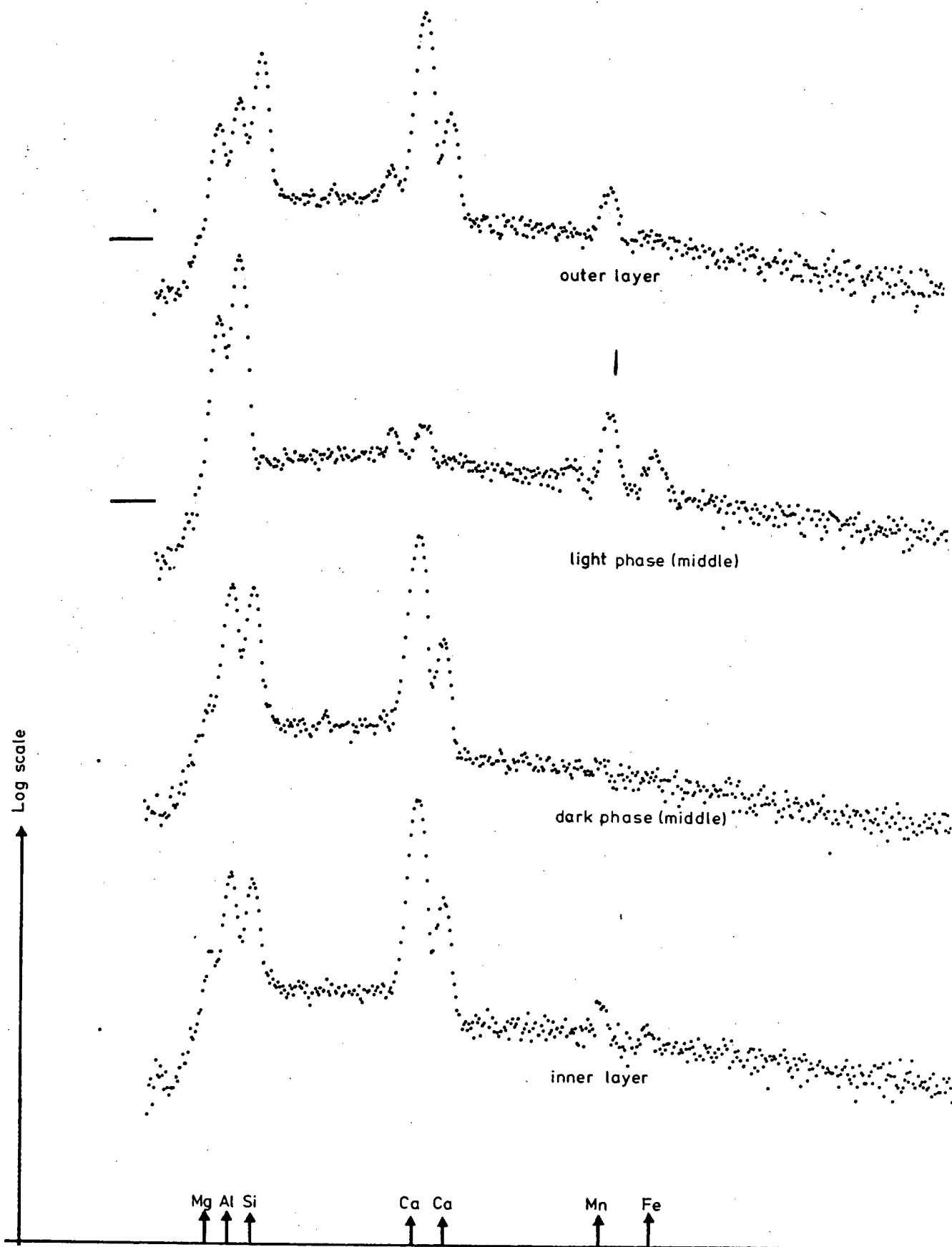
Figure 39 - EDX analysis of complex slag skin

steel was examined and displayed much the same pattern with Cr and Ti appearing on the inner layers reflecting the effect of the metal melted.

A slag having 12% SiO_2, 6% MgO, 16% Al_2O_3, 17% Cao, and the rest CaF_2 showed the presence of Mg, Si, Al, Ca and Mn, (the last a pickup from the metal) in the outer layer. The middle layer had two phases, the darker of which had Al, Si, and Ca ; the lighter had Mg, Al traces of Ca and small amounts of Mn and Fe. The inner layer had all the elements mentioned though the peak of Ca was dominant.

2.2.3 The 70:30 Slag Cap Near The Liquid Metal Meniscus

It was apparent that the middle layer consisted mainly of primary crystals. It was also clear that these crystals were

Table IV - Chemical analysis of some skins

Sample	CaF_2 wt%	Cao wt%	Al_2O_3 wt%
70:30(bulk)	80.7	--	15
70:30 skin	60 to 70	--	30 to 40
70:15:15 skin	38.4	17.9	17.5
50:30:20 skin	43.4	29.7	29.9

much thicker than the crystals that would have normally precipitated (those observed in the slag bulk) and definite macrosegregation was observed. Micrographs were taken and the proportion of primary phase in the skin and in the slag bulk determined. The proportion of primary phase was 4-5 times

higher in the skin than in the bulk. Further, there was a clean break at the skin and no evidence that remelting or dissolution took place at the meniscus. The middle layer started growing about 1cm below the slag top and increased in thickness till the metal meniscus in a nearly linear fashion.

An effort was made to quantitatively determine the proportion of elements present in the various phases using electron probe microanalysis. The presence of oxygen and fluorine meant that the use of a light element spectrometer was necessary. The fragile nature of the specimen coupled with the presence of voids in the specimen probably reduced the sensitivity so that reliable analysis became difficult. Analysis by atomic absorption was possible and the analysis is given in Table IV. Apparently much of the alumina did not dissolve in the slag and the composition of the 70:30 slag is actually close to 80:20, but the increase of alumina in the skin is evident. The latter analysis cannot, of course, indicate the individual composition of the three layers.

III. CALCULATIONS

Several simple models were formulated in an effort to explain the observations. The finite difference technique was used, with some success, to calculate mould temperatures. In a speculative calculation to determine the effect of grooves in the mould face on heat transfer to the mould, the finite element method was used.

3.1 Calculations In 2 Dimensions

The finite difference technique is now a standard method to solve the differential equation for steady state heat transfer. Good explanations are given in many textbooks, e.g. those by Kreith and Black,[38] by Patankar[36] and by Carnahan, Luther and Wilkes.[37]

Initially, a rough estimate of the temperature field was needed to determine the positioning of thermocouples in the mould. Therefore, a 2-D steady state heat flow situation in a horizontal slice of a flat mould section was examined. The finite difference discretisation was made, solved and the results are shown in figure 40 (for a heat flux of 25 cals/cm^{2}K). It is clear that the temperature gradients near the hot surface are very high and any error in placement of a thermocouple could lead to large errors in measurement, making them unreliable. It is also seen that the region marked B lies in a area of low temperature gradient which means that if one drills a hole from the rear face as shown there is little chance
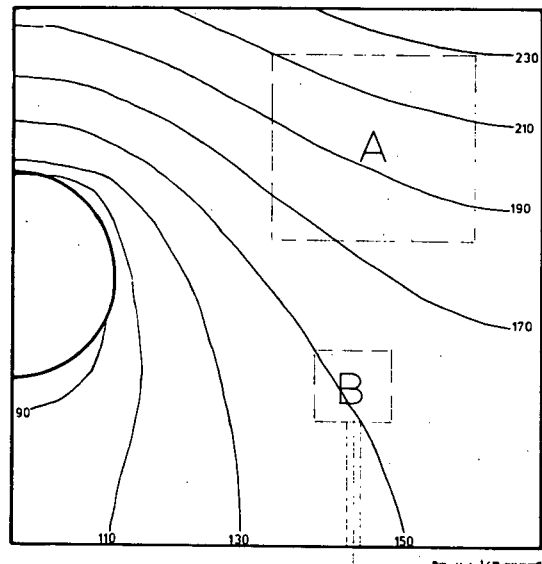
Figure 40 - Temp. field calc. with 2-D assumptions
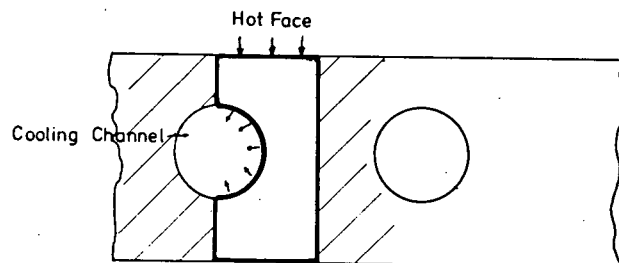
Using symmetry. only portion bounded by heavy lines
discretised. Arrows show heat flow.

Figure 41 - The slice which was discretised

of inaccuracy in temperature measurement in the region. Type B positions, it seems, may be used for verification.

Measured values of heat flux were used in the calculation and it was quickly discovered that a 2-D model was inadequate since it predicted extremely high temperatures at the hot face. It was evident that computation had to be extended to three dimensions.

3.2 Calculations In 3 Dimensions

The next step was to determine if a quasi steady state model could calculate temperatures in the mould that were reasonably representative. The results of the previous section suggests that an accuracy of no more than about 5 Celsius degrees in temperature measurement may be expected.

Following the type of assessment used for the heat flux sensor a similar line of reasoning indicated that a mould section such as considered was not very suitable for the assumption of quasi steady state heat transfer. Calculations of a "Biot" number indicated that the condition of quasi steady state may exist only in a body of size no greater than 4-5 cms. The thickness of the mould was 5cms and the height about 25 cms and so there is probably an inherent error in making quasi steady state assumptions. However, there is a relatively slow rise of the slag across the mould face. Further other workers have shown that the heat flux to the mould in the slag region is relatively constant[1] and it is possible that the maximum

temperatures computed on the mould face may not be inaccurate, i.e. a steady state calculation may predict maximum temperatures with acceptable accuracy. It is also to be noted that three dimensional unsteady state computing is potentially extremely costly and hence unsuitable in the field.

A three dimensional quasi steady state calculation was made. The technique used matrix solutions as well as iteration in an effort to balance computing costs against memory requirements. A single run took about 20 seconds CPU time on the AMDAHL computer at the University of British Columbia. A program listing in FORTRAN is given in Appendix C.

The results of the program written for 2-D approximation were used as the initial solution estimate for the program written assuming 3-D steady state heat flow.

The input required is the heat transfer coefficient to the coolant, the heat flux distribution, the thermal conductivity of the mould, the physical dimensions, the coolant flow rate, and the coolant temperature. In the calculation, the heat transfer coefficient to the cooling water was estimated by both the Sieder-Tate[55] correlation as well as the relation given by Petukhov.[56] (App.B) There was a small difference but it was seen later that the mould face temperatures were not significantly changed by these variations. The heat flux into the mould face was taken from the experimental data. Iteration to the nearest degree was deemed sufficient since the accuracy of measurement was no greater than that. The thermal conductivity was assumed constant and equal to the value at 200°C for aluminium but for

copper a linear variation with temperature was permitted. Since relatively good agreement with experimental data was observed, the program was not refined to allow a better estimate of the thermal conductivity.

The results are given in figures 12, 14, 16, 18 (p.27-30). The temperatures were calculated using 3 spatial dimensions but the vertical dimension (z) can be converted to time since the rate of rise of the ingot is relatively constant. The results have been given with respect to time to facilitate comparison. It is to be noted that points within the mould in the same position with reference to the slag have approximately the same temperature history. This is true except for the 2-3 cms at the base and at the top of the mould. The temperatures calculated are not quite the same as the measured temperatures (as expected) but are close enough to be considered reasonable and this comparison is visually available in figures 11 to 18 and 23. The temperature gradient with time is also reasonably correct. It is felt that such calculations may be used to predict maximum temperatures in mould sections though there is little doubt that transient heat transfer has a discernable effect on temperature fields. This is confirmed by the fact that steady state calculations under-predict temperatures at type B positions and also by the results of run 8.

Following the acceptable success of the model the effect of variation of mould material, channel positioning and channel spacing were made. As expected, the use of copper lowered hot face temperatures dramatically. This is seen in fig. 17 and 18

(p.30).

Moving the channels closer reduced the face temperature and made the temperature gradient more uniform (fig.43 a,b). If the channel is brought closer to the hot face, the face temperature is reduced but the gradient increases and becomes less uniform (fig.43 c,d). There is also a high temperature at the cooling channel and this may create boiling thus changing the cooling conditions. A small change (10%) of the heat transfer coefficient to the coolant brings only small changes in temperature distribution suggesting that the approximation used to estimate the coefficient is acceptable (fig.42 b,c). It is to be noted that the heat transfer coefficient depends on the mean temperature of the coolant film according to the method used and so should vary over the length of the channel. A calculation with an arbitrary variation was also performed and showed insignificant changes (fig.42 d). Variation of inlet water temperature also had only a small effect, but it is noted that if the temperature rises above 25-30°C at the same cooling velocities, then there is a strong possibility of boiling occurring (fig.44 a,b). The horizontal plane chosen is that where the hot face reaches its highest temperature.
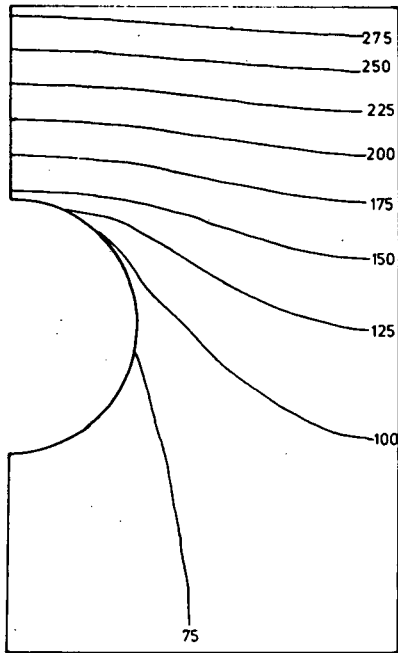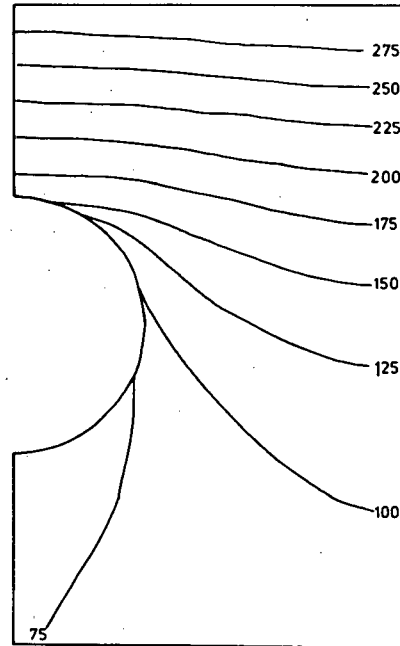
a) standard   b) h reduced 10%
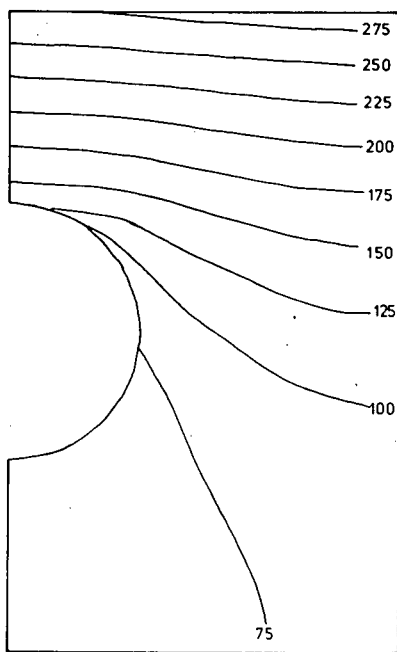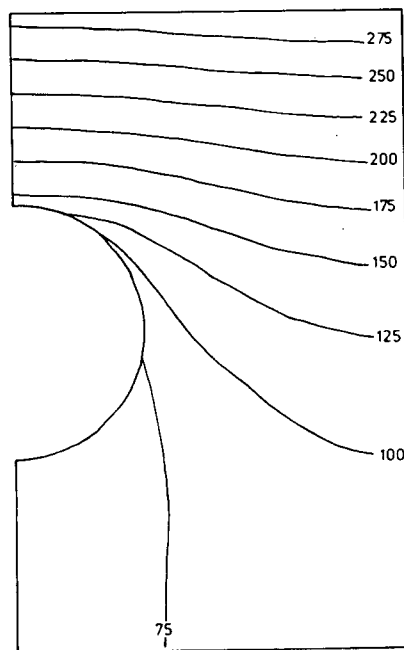
c) h raised 10%   d) arbitrary h

Figure 42 - Calculated Temp. fields
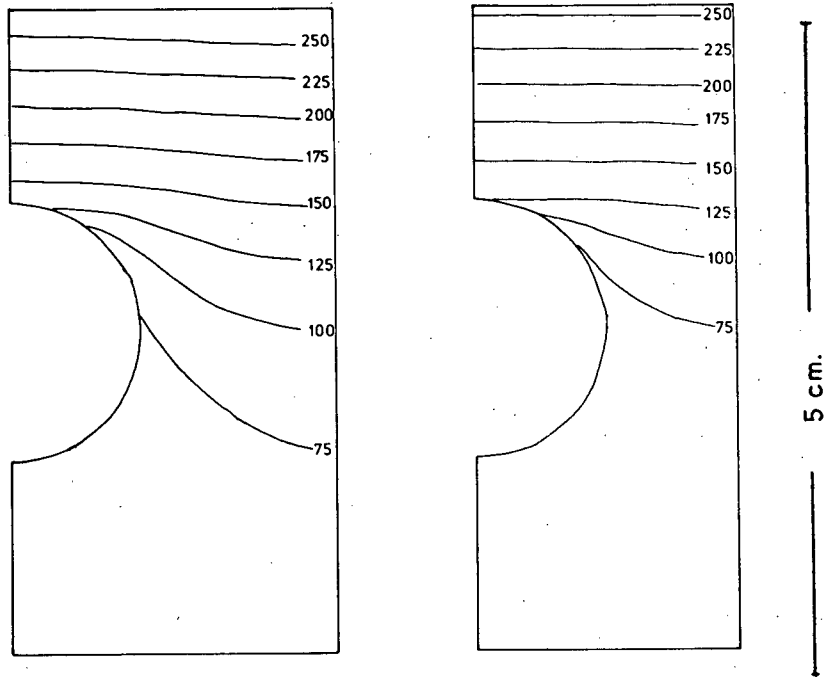
a,b) reduced inter-channel distance
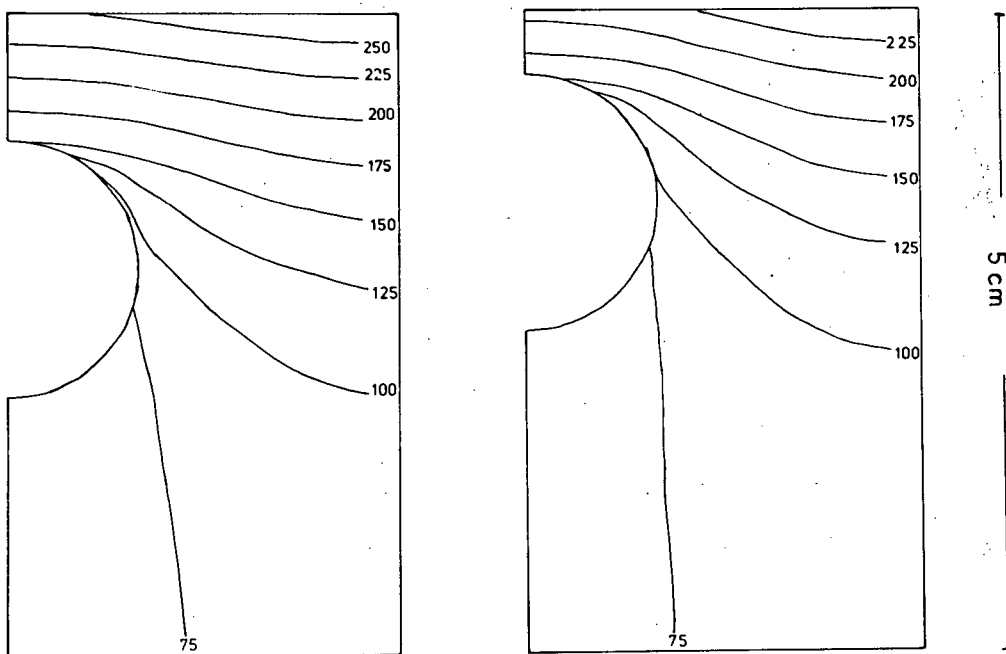
c,d) channel closer to hot face

Figure 43 - Calculated Temp. fields
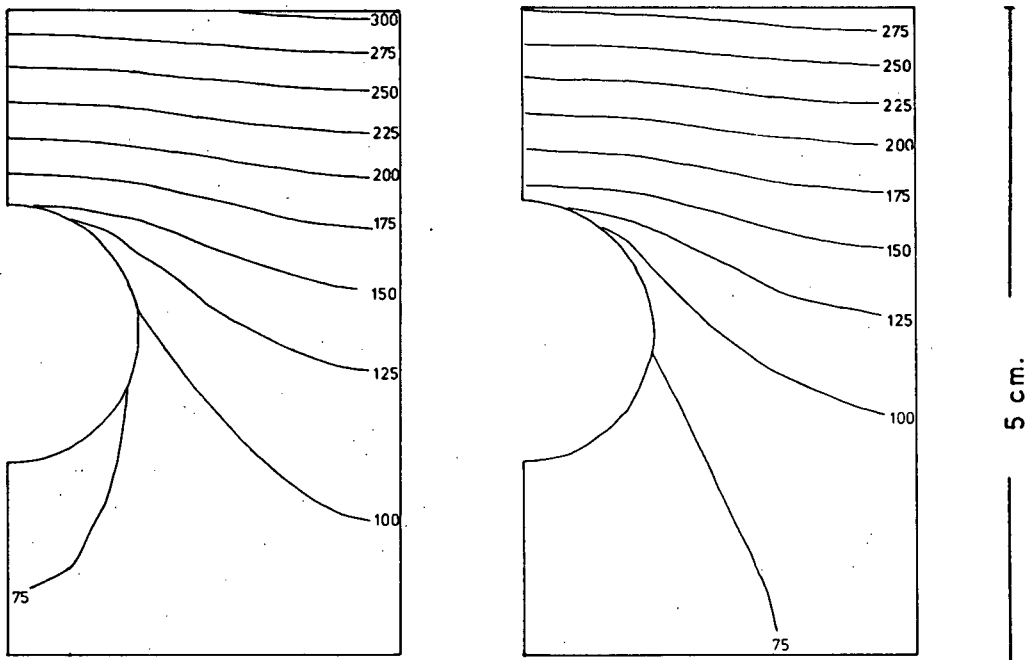
a) water at 25°C b) water at 10°C

Figure 44 - Calculated Temp. fields
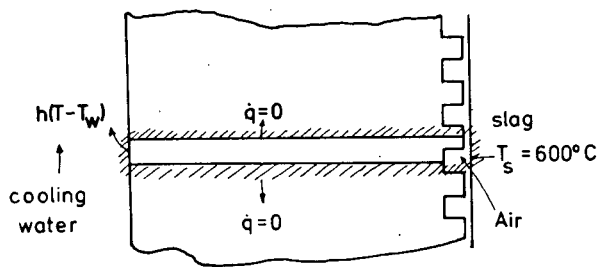
sketch of section taken for finite element
calculations

Figure 45 - Section taken for F.E. calculation
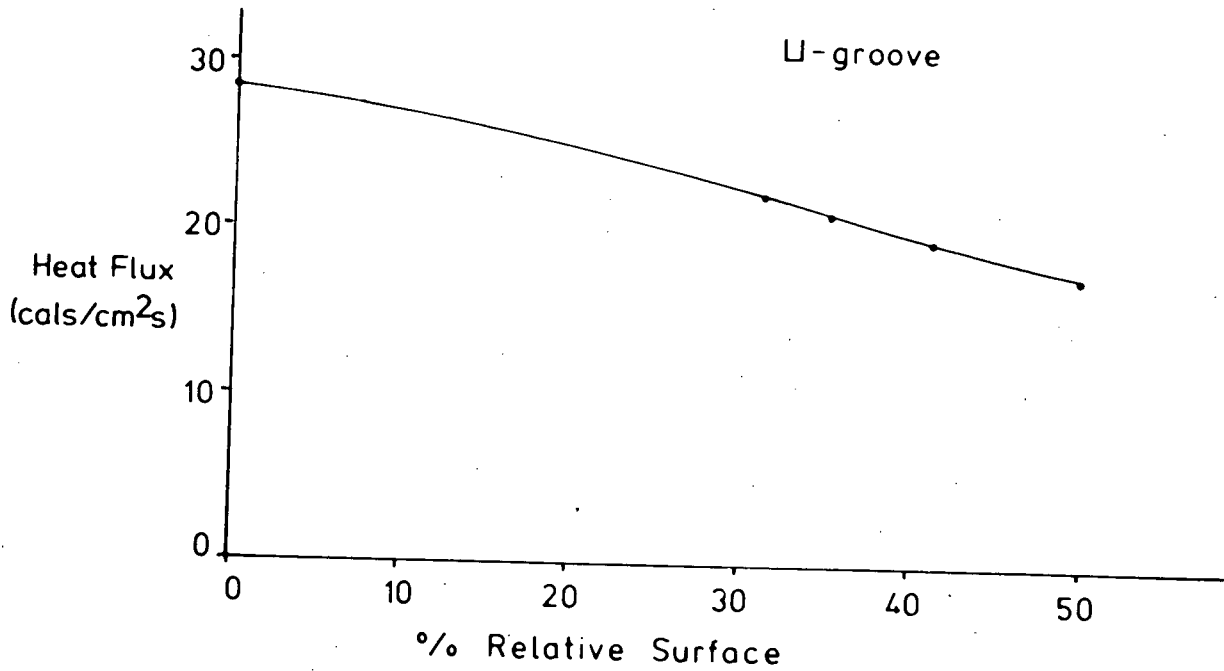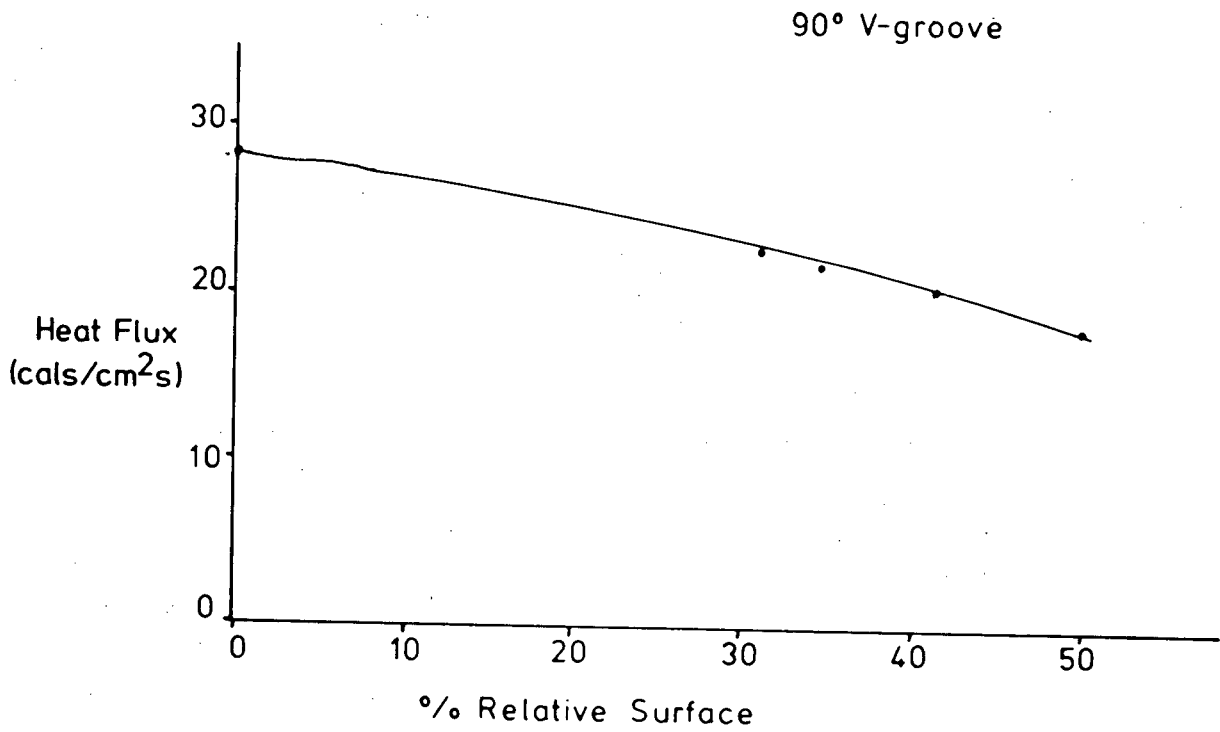
Figure 46 - Calculated results of speculation

3.3 Speculation On The Effect Of Grooves On Surface Quality

The assumption of steady state heat transfer coupled with knowledge of the slag skin thickness and its thermal conductivity indicated that the air gap had a smaller thermal resistance, though not insignificant, compared to that of the slag skin (see Table I, VI and VII the latter on p. 67-68). Thus, a slight increase of the air gap could reduce the heat flux significantly. It is known that rough mould surfaces in metal ingot casting lead to smoother surfaces, presumably due to lower heat fluxes. It was thought that machining grooves in the mould surface might have the same effect.

There were two assumptions made. The first was that the slag would not enter the grooves since it had been observed that slag did not enter the space between two mould sections, which could be as large as 2mms. The other was that the slag skin thickness would not change as the molten metal head approached.

To determine the effect of groove spacing on heat flux, a finite element model of a slice of mould was formulated, a sketch of which is shown in figure 45. The FORTRAN listing of the program is given in Appendix D. The results of the speculation are given in figure 46. It seemed that the heat flux could be effectively reduced by up to 25% if the grooves covered 50% of the hot face. Apparently, there was need to make experimental investigations since it seemed possible to design a mould to permit a molten head of metal to exist at lower power input than hitherto and this was the basis for run 12.

The experiment was unsuccessful since it was discovered

that to prevent slag from entering the grooves, it is necessary to quench the slag extremely rapidly. The general heating up of the mould with the rise of the slag makes this impossible. No experiments with a groove width smaller than 1 mm were attempted since it was thought that such fine grooves would be expensive to machine and so would be impractical.

IV. <u>DISCUSSION</u>

4.1 <u>Failure Of 2-D Model</u>

Russian workers[1] have calculated temperature fields using carbon conducting paper. This presupposes that heat flow can be adequately described as two dimensional. While this may be permissible for a vertical section exactly between two channels it is not sufficient for a horizontal section. This was realised and it was suggested by these workers that the heat flux be arbitrarily raised by 30%. No other predictions of temperature fields are available for channel cooled moulds.

Channel cooled moulds are used in continuous casting. For this case there are some literature studies. Chizhikov et al[40] and Simonov et al[39] accepted 2-D steady state approximations. Young, Sunaryo and Cross[41] used temperature measurements in a vertical section exactly between two channels as boundary conditions for the modelling of horizontal sections. This was probably done because of limited computing resources. Alberny et al[42] assumed negligible vertical heat flow in their measurements of heat flux.

Vertical heat flow has often been neglected in the past in measurements of heat flux in both the electroslag process and in continuous casting. This approach is flawed since appreciable heat flux gradients exist. The extent of error can be examined by considering a rectangle in the X-Y plane with boundary

conditions as shown in fig. 47. The error is negligible in the central region of the rectangle but varies from 0 to 10% in the extreme regions. A hypothetical heat flux variation was assumed (fig.48) and calculations performed to check the error. The results are shown in Table V. It is clear that if the thermocouples used to measure heat flux are placed close to the hot face the error is low (about 10%) and within experimental error. However, it is likely that the sharp peaks observed in this study would not have been uncovered since the type of error associated with the measurements would have obliterated them. It is also clear the heat flux in the X-direction reduces with increasing thickness falling about 15-20% from the hot face value. This indicates why temperature fields must be calculated in 2 dimensions even if heat flux measurements are made using 1-D approximation. In the case of channel cooled moulds, the reduction of symmetry necessitates an extension to three dimensions.

In the early stages of this work, it was seen that 2-D approximations of temperature fields were grossly inaccurate. The heat flux from the slag was an order of magnitude higher than that from the ingot or the region above the slag which caused appreciable vertical heat flow and meant that a 2-D approximation would not be satisfactory. 2-D models of vertical sections are acceptable for thin jacketed moulds or if the cooling channels are extremely closely spaced, i.e. where the isotherms are flat and parallel to the hot face. Such moulds will probably not be acceptable in electroslag casting from
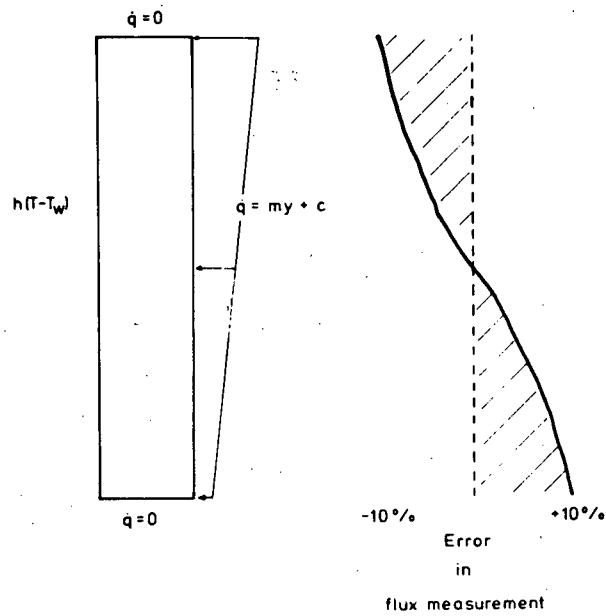
Figure 47 - Error in heat flux measurement
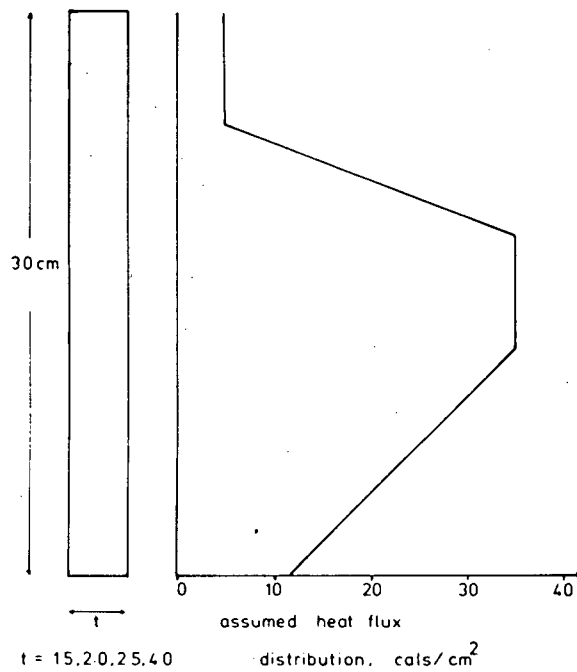
Figure 48 - Hypothetical heat flux variation

Table V - Possible Error in heat flow measurement

a. Measuring T/C's 3 and 11 mm from hot face

Position (cm)	Actual Flux Cals/cm²°C	'measured' heat flux in mould of thickness, cm.			
		1.5	2.0	2.5	4.0
0	5	5.46	5.62	5.74	6.02
6	10	11.5	11.51	11.54	11.61
12	35	32.01	31.99	31.93	31.81
17	35	33.63	33.55	33.46	33.26
24	21	21.08	21.11	21.13	21.18
30	9	11.47	11.51	11.58	11.74

b. 'Measurement' at cold face.

0	5	5.92	6.58	7.33	9.73
6	10	12.86	13.56	14.16	15.16
12	35	29.84	28.87	28.01	25.94
17	35	32.59	31.9	31.21	29.2
24	21	21.16	21.28	21.41	21.82
30	9	13.27	14.17	14.99	17.12

reasoning given in section 1.2.5 and thus the need to examine 3-D models arose.

4.2 Apparent Success Of 3-D Quasi Steady State Model

Three dimensional approximation is partially sucessful, as explained hereunder.

The correlations developed for estimating the heat transfer coefficient to the cooling channel are relatively accurate only for fully developed flow in the channel and they are restricted to conditions where the heat flux does not vary substantially along the channel. When the heat flux does vary the methods developed by Sleicher[43] and others[44,45,62] for the calculation of local heat transfer coefficients should be employed. In

theory, even this is not good enough since the heat flux varies with position even in a horizontal section and in any case the flow is not fully developed. It is fortunate that substantial axial conduction occurs, so that the temperatures in the mould near the hot face are not very sensitive to changes in the heat transfer coefficient. This means that correlations such the Petukhov relation[56] may be used. However, it is pointed out that boiling can cause drastic changes and in this case more complex calculations are necessary.

The other question regarding the utility of a 3-D calculation comes from the fact that the heat flow is actually time dependent. However, the experimental results show that the arguments brought forth earlier are justified, to some extent. In industrial conditions, it would seem unnecessary to go to the expense of making more complex calculations especially if the motive is to limit the maximum hot face temperature.

The impetus for 3-D unsteady state calculations may come from the the need to calculate thermal stresses. A knowledge of thermal stresses is necessary since the major cause for mould retirement is deformation by creep caused by such stresses. However, it is noted that the temperatures and temperature gradients may be predicted fairly well using quasi steady state calculations and so it may be worthwhile to make measurements and compare the results obtained. If the result is precise enough, no refinement of the assumptions may be necessary.

The most important variable, over which the designer has little control, is the heat flux to the mould. There have been

many measurements of the heat flux under various conditions, but as yet it does not seem possible to predict the heat flux for an arbitrary shape. There is need to develop a method of making reliable estimates using simple techniques before such an approach may be used in day to day work. It is suggested that the sharp flux peak observed may be neglected since the peak is very narrow and the heat flux approximated as a broad band of high heat flux.

4.3 Factors Affecting The Heat Flux To The Mould

Table VI - Temp. drop through slag skin

a. Heat Flux = 65 cals/cm²s

slag skin thickness(cm)	Drop in Temperature °C		
	.006*	.008*	.010*
0.15	1625	1218	975
0.12	1300	975	780
0.10	1083	812	650
0.08	866	650	520

b. Heat Flux = 35 cals/cm²s

0.5	2916	2187	1750
0.4	2333	1750	1400
0.3	1750	1312	1050
0.2	1166	875	700
0.1	583	437	350

* Thermal conductivity in cals./cm.s.°C

The thermal resistances to heat flow to the mould from the slag or the ingot are the slag skin and the air gap, presumed to exist between the slag skin and the mould. Simple fitting of

Table VII - Heat flow through air gap

Air Gap (cm)	Drop in Temperature, °C for heat flux(Cals/cm²s) of	
	65	35
0.1	65 000	35 000
0.05	32 500	17 500
0.001	650	350
0.0005	325	175
0.0001	65	35

All units in the CGS system. Thermal Conductivity of air taken to be 0.0001 cals./cm.s.°C

the known physical properties of air and the solid slag to the observed heat fluxes (as in Tables VI and VII) indicates that both the slag skin and the air gap are significant resistances. It appears that the air gap thickness is of the order of 10 microns and the temperature drop across it roughly 400°C the rest of the drop of roughly 700-800°C across the slag skin. It is pointed out that this is a very approximate analysis and that the "air gap" written about is only an average value and in fact probably varies dramatically from point to point. In any case one cannot neglect either resistance.

The examination of a 70:30 slag cap indicated that the slag skin is not a simple frozen layer and no remelting or dissolution as has been previously stated to occur was observed. The primary crystals (Al_2O_3 or CA_6) precipitated in the slag skin were physically much thicker than they were in the slag bulk. In fact, the average content of aluminium in the slag skin is much higher than in the nominal composition of the slag. It appears that the constant washing off of the secondary molten phase from the slag skin and the supply of fresh slag to the

region allows continuous precipitation of the primary phase till the passage between the crystals becomes so constricted that flow of liquid is no longer possible. In this scenario, the temperature of the slag skin-molten slag interface is the liquidus temperature and the temperature of the chilled layer-"equilibrium" layer interface is equal to the eutectic temperature (see fig. 49). Using the values of thermal
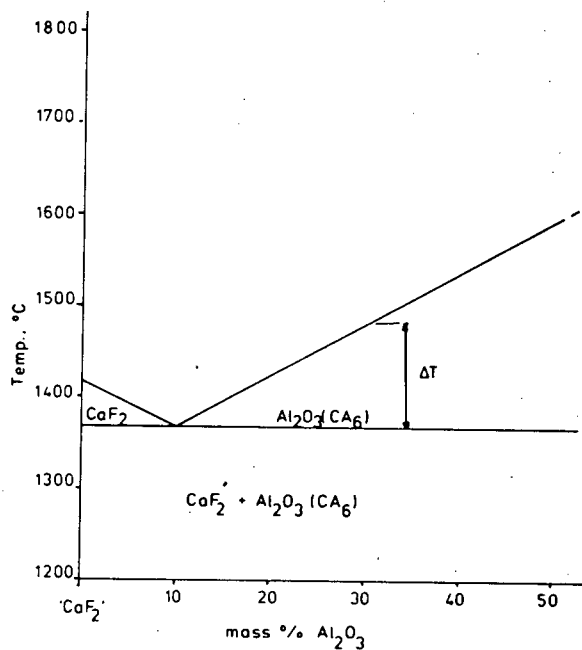
Figure 49 - Phase diagram for CaF_2-Al_2O_3

conductivity given by Taylor and Mills et al[61] a thickness of the "equilibrium" layer of 0.3 mm is obtained, which fits in well with observations.

The high heat flux (nearly double that in the slag region) from the molten head of metal to the mould must still be explained. From the measurements of other workers, the molten steel is generally at a temperature of 1600-1650°C at the ingot top surface periphery. For a 70:30 slag the liquidus is about 1500°C. If conduction is considered to be the major mode of heat transfer then the difference in temperature at the slag skin hot face caused by the rise of molten metal is not sufficient to explain the doubling of the heat flux. Radiation too is not a satisfactory answer since the structure of the slag skin ensures that substantial scattering takes place, i.e. only an increase in effective thermal conductivity may be expected. The only other reason could be a reduction of the air gap. On the face of it, even this appears doubtful since there is no reason why a couple of millimeters of molten metal head should do what 500 mm of slag head could not. However, if it is supposed that the higher metal temperature will melt the secondary phase and cause some dissolution of the primary crystals, then the slag skin will weaken structurally without apparent change on subsequent re-solidification. This then, will permit deformation of the slag skin and decrease the air gap. If the liquid metal head is excessively big, the skin may fracture and cause runout metal fins such as have been observed.[1,47]

As the ingot solidifies and withdraws from the slag skin on contraction, the reduced pressure created draws out the secondary phase and this solidifies on the solid ingot wall.

This explains why the third layer consisting of the secondary phase is found in the slag skin. The spikes observed on this surface mainly have easily oxidisable elements. It is possible that corrosion products collect near the metal meniscus since they are not readily soluble in the slag which may get trapped and stick to the slag skin thus creating the spikes.

In the other slags examined, for example the 70:15:15 composition, there is some melt back of the skin expected and this seems to be a reasonable explanation for the rise of the heat flux at the metal head level. Of course, some deformation of the slag skin is also possible but this does not change the situation qualitatively.

This explanation of the variation of the heat flux seems reasonable, but there is still no way of estimating the heat flux. The thickness of the slag skin will depend on the heat transfer coefficient to the slag skin from the molten slag depths, this in turn depending on the magneto-hydrodynamic flow field. The air gap will depend on the thermo-physical properties of slag skins. Work in this area, it seems, is necessary. Some work of this nature has been reported by Medovar et al[46] showing that 70:30 slags have a lower coefficient of thermal expansion than the complex slags having MgO and SiO_2. Al_2O_3 and CaO were found to increase the strength at the expense of reduced ductility while SiO_2 raised the ductility of CaF_2-CaO-Al_2O_3 system slags.

4.4 Crystallisation In Slag Skins

It is useful, at this juncture, to examine the crystallisation sequence according to the phase diagram. The diagram for the $CaO-Al_2O_3-CaF_2$ system is given by Mills and Keene[48] and is shown in fig.50. The compositions of four common slags are marked out. The works of Zhmoidin[49,50,51,52,53] and others show that there is little solid solubility and this is assumed in the following discussion.

A 70:30 slag, in practice, contains up to 5% CaO due to hydrolysis of CaF_2 by moisture and evaporation of AlF_3. At high temperatures this slag is in the 2-liquid region. The plait points are unknown but from a knowledge of the slag skins and the work of Zhmoidin[50] they may be placed at points A and B as shown. The two liquids will then have the composition C and D. If C has a higher liquidus the primary phase will possibly be CA_6 or Al_2O_3, both of which have been observed by Mitchell[30] in the slag skin. This is also supported by the work of Zhmoidin[50] who determined that CA_6 would be the primary phase in this system.

A 70:15:15 slag lies at the edge of the 2 liquid region though not in it. The primary phase should be C_3A_3F with CaF_2 and CaO crystallising later. However, small increases of CaO will change the crystallisation sequence significantly. Therefore, it is likely that $C_{11}A_7F$ will come out instead of C_3A_3F.

A 55:35:10 slag is in the 2 liquid region and following the arguments made earlier, the primary phase could be CA_2 or C_3A_3F
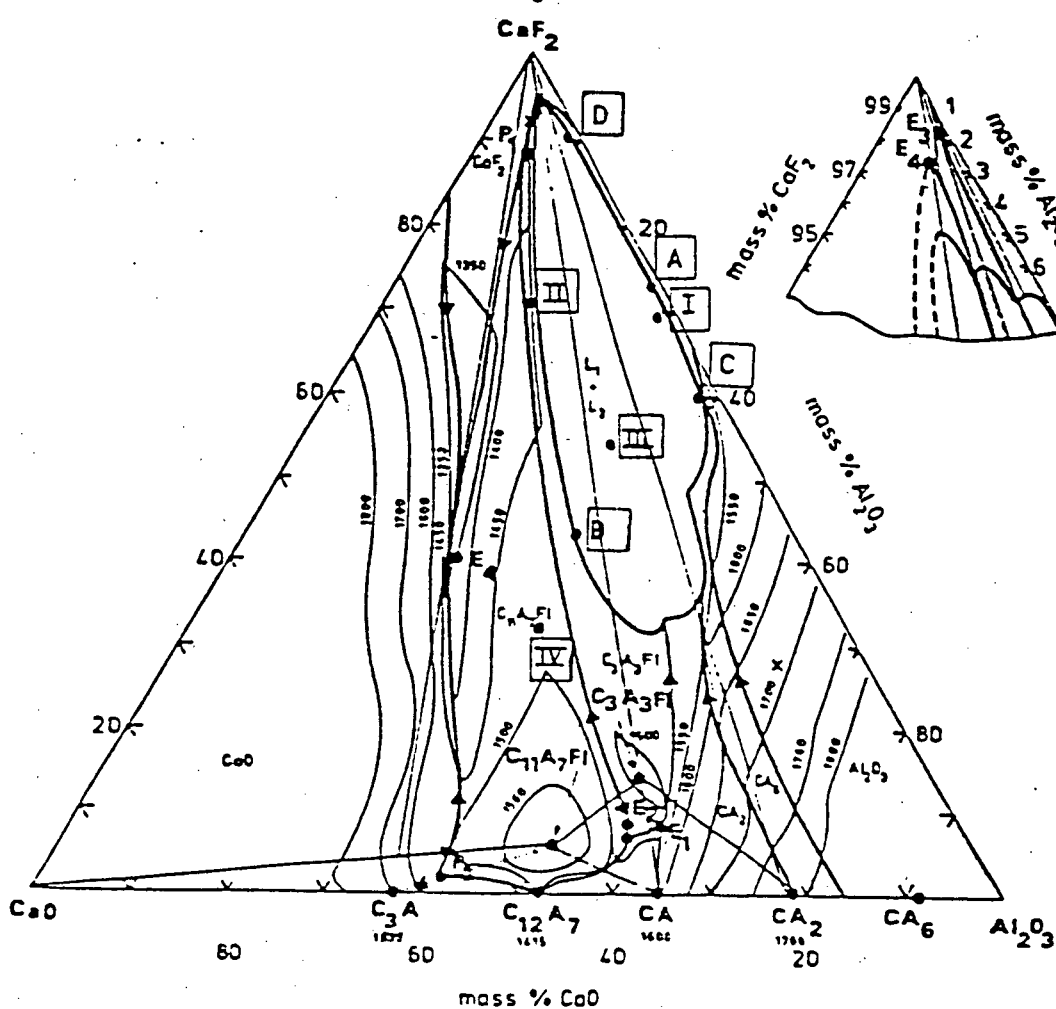
I	70:30
II	70:15:15
III	55:35:10
IV	33:33:33

Figure 50 - Phase diagram for CaF_2-Al_2O_3-CaO

depending on the tie-lines. Here, as for the 70:15:15 slag, small changes in the CaO content can change the precipitation sequence.

A 33:33:33 slag gave $C_{11}A_7F$ with CaF_2 and CaO constituting the eutectic. Mitchell[30] has found $C_{12}A_7$ and $C_{11}A_7F$ in the slag skin of this slag.

Apparently crystallisation of the slag skin follows the phase diagram. Fractional crystallisation as spoken of by Kamensky et al,[27] will take place owing to the slag motion in the electroslag process as described above. This means that the chances of finding the secondary phases in the slag skin are low and one expects to find, basically, only the primary phase in the bulk of the slag skin.

There is a great difference in the 70:30 slag owing to the characteristics of crystalline corundum (CA_6 has a closely similar structure to that of alpha Al_2O_3). This grows as a plate and so one finds CaF_2 in the skin in between the plates. As the plates thicken, one should find less of CaF_2 in the skin as may be seen in the slag skins of large ingots.

4.5 Slag Composition Effects On The Heat Flux

It was suggested earlier that the metal temperature at the metal ingot top periphery is between 1600-1650°C under normal melting circumstances. This temperature is above the melting point of the primary phases for all the slags mentioned in the preceding section with the exception of the 70:30 slag.

The implication is that the slag skin will be melted back in all cases except that of the 70:30 slag. The presence of light striations and the absence of "spikes" on the inside surface of a slag skin is indicative of this. The case for the 70:30 slag was dealt with in detail earlier. Continuing further, if the slag skin is thicker (as in large ingot manufacture), a peak of heat flux may be observed at the molten metal head level in cases where the slag skin melts back and where it does not melt, as for the 70:30 slag, the heat flux peak will be diffuse and may not even appear. This is seen in the the results of Kondo et al.[9]

In static mould conditions, the latter situation favors a smoother surface. In the moving mould case, the system is different. It has been observed that the skin of the 70:30 slag is prone to fracture and thus defects, such as fins, are produced. Paton[58] indicates that the slag skin should be plastic to reduce the chances of fracture and suggests the addition of MgO and SiO_2 to achieve this. This "plasticity" is probably due to the softening of glass present in the slag and the addition of SiO_2 probably favors this.

It is known that slags with low fluoride contents are operationally more efficient.[57] This is due to their higher electrical resistivity and higher viscosity which also means reduced slag flow velocities. Kusamichi et al,[8] report that there is a discernable radial temperature gradient in slags of low fluoride content which is absent in high fluoride slags. The net effects are thicker slag skins and lower heat flux to

the mould for low fluoride slags. Further, from the discussion
above, the slag skins of low fluoride (about 20-40%) slags have
a higher melting point and so remelting of the slag skin should
be less. These skins should be stronger and so give better
surfaces in moving mould operations. A 70:30 slag also will
give a thick skin but owing to the plate structure of corundum
this skin fractures easily.

The best skin, it appears, must have a high melting point,
must crystallise with no directional bias and should possess an
appropriate degree of "plasticity".

4.6 Factors Affecting Surface Quality

From the discussion, it appears that the mould cooling
regime has little to do with the surface quality. One thing is
clear; the slow rate of rise of the ingot means that meniscus
solidification is the only mechanism of formation of a bad
rippled surface. Therefore, a good surface is ensured by the
presence of a liquid metal head. Such a condition can be
improved by reducing the resistance to heat flow in the liquid
metal and by increasing the resistance to heat flow to the
mould.

The former is controlled by geometry and the power input to
the system. The latter is favoured by a thicker and/or stronger
slag skin. A thicker skin can be generated by lower power input
or by a thinner electrode, but this is counter productive in
that the thermal resistance in the liquid metal is adversely

affected.

The other method is to select the correct slag. The use of pure compounds or eutectic compositions is not recommended since in this case remelting of the slag skin is possible which causes a reduction of the thermal resistance. It is necessary for a high melting phase to precipitate out and it is preferable that the proportion of the primary phase be as high as possible. Thus the tendency of the slag skin to dissolve and weaken is combated. An increased slag depth at the same power input may also be beneficial but this is a limited option in that a large increase of slag depth has a substantial penalty in power losses.

V. SUMMARY

In conclusion,

1. Quasi steady-state three dimensional models may be used to calculate temperatures in mould sections to be used in electroslag casting. Temperature at the hot face may be changed by changing the spacing between channels but drastic changes can be made only by changing the mould material. For short production runs, temperature appears to be a valid criterion, but for long runs design to minimise stresses may be necessary.

2. It appears that temperature distributions generated in this way may be used to calculate thermal stresses, but verification is necessary.

3. A proposal to explain the variation of heat flux to the mould has been made. Work to determine if the properties of slag skins can be used to estimate heat fluxes for arbitrary shapes in a simple manner seems necessary.

4. The surface quality of a casting is not influenced by mould design but by the slag composition, the power input and the geometrical relationship between the electrode, the slag depth and the casting shape.

REFERENCES

1. B.I.Medovar, V.L.Shevtsov, G.S.Marinsky, V.F.Demchenko, V.E.Machenko, <u>Thermal Processes in Electroslag Flows</u> , Naukova Dumka, Kiev, 1978.

2. A.Mitchell, R.M.Smailer, Int. Met. Rev., (5&6), 1979, p.231.

3. W.Holzgruber, Stahl und Eisen, 88, (12), p.638 quoted in Ref. 4.

4. W.Duckworth, G.Hoyle, <u>Electroslag Refining</u> , Chapman and Hall, London, 1969.

5. S.Joshi, Ph.D. thesis, University of British Columbia, 1971.

6. D.N.Pocklington, B.Patrick, Met. Trans., 10B, 1979, p.359-366.

7. Staff, Albany Metallurgy Research Centre, <u>The Electroslag Process</u> , ed. R.H.Nafziger, U.S.Bureau of Mines, 1976, p.31-37.

8. T.Kusamichi, T.Ishii, T.Onoye, K.Narita, Tetsu-to-Hagane, 12, 1980, p.1640-1649.

9. Y.Kondo, H.Kodama, E.Niyama, S.Hanada, H.Ishikawa, 101 ISIJ meeting, April 1981, lecture S256.

10. R.C.Sun, J.W.Pridgeon, Proc. Second Int. Symp. on ESR Technology, Pittsburgh, 1969.

11. L.F.Carvajal, G.E.Geiger, Met. Trans., 2, 1971, p.2087-2092.

12. J.F.Elliott, M.Maulvault, Proc. Fourth Int. Symp. ESR Processes, Tokyo, 1973, p.69-80.

13. B.E.Paton, et al, Fifth Int. Symp. on ES and other Special Melting Technologies, Pittsburgh, 1974, p.323-344.

14. A.S.Ballantyne, Ph.D. thesis, University of British Columbia, 1978.

15. J.Kreyenberg, K.Schwerdtfeger, Arch. Eisen., 50, 1979, p. 1-6.

16. B.E.Paton, et al, <u>Special Electrometallurgy</u> , Naukova Dumka, Kiev, 1972.

17. A.H.Dilawari, J.Szekely, Met. Trans., 11B, 1980, p.77-87.

18. M.Choudhary, J.Szekely, Met. Trans., 11B, 1980, p.439-453.

19. M.Choudhary, J.Szekely, Ironmaking and Steelmaking, 5, 1981, p.225-232.

20. R.S.Cremisio, E.D.Zak, Proc. Fourth Int. Symp. ESR Processes, Tokyo, 1973, p.137-148.

21. E.D.Zak, Proc. Vac. Met. Conf., Pittsburgh, 1977, p.315-331.

22. S.S.Kutaladze, V.M.Borishansky, A Concise Encyclopaedia of Heat Transfer , Pergamon Press, Oxford, 1966.

23. I.V.Samarasekera, J.K.Brimacombe, Int. Met. Rev., (6), 1978, p.286-300.

24. I.V.Samarasekera, J.K.Brimacombe, Sec. Process Tech. Conf., Chicago, 1981, p.2-21.

25. A.Mitchell, S.Bala, A.S.Ballantyne, G.Sidla, Metals Tech., Aug. 1981, p306-312.

26. A.Mitchell, M.Etienne, Trans. AIME, 242, July 1968, p.1462-1463.

27. Y.M.Kamensky, Y.I.Afanasjev, B.N.Sakhotin, E.F.Vegoman, V.I.Yavoisky, L.A.Safronova, Reports of Int. Symp. on Special Electrometallurgy, Kiev, 1972.

28. B.Korousic, V.Osterc, Rad. Rundsch., 4, 1976, p.803-813.

29. M.Bell, A.Mitchell, JISI, 209, 1971, p.658-660.

30. A.Mitchell, unpublished.

31. K.Yamaguchi, M.Funazu, T.Ichihara, Proc. Fourth Int. Symp. ESR Processes, Tokyo, 1973, p.91-101.

32. P.O.Mellberg, Proc. Sixth Int. Vac. Met. Conf. on Special Melting, San Diego, 1979, p.535-542.

33. D.M.Longbottom, A.A.Greenfield, G.Hoyle, M.J.Rhydderch, Proc. Fourth Int. Symp. ESR Processes, Tokyo, 1973.

34. V.L.Shevtsov, B.I.Medovar, G.S.Marinski, V.P.Serdyukova, Henry Brutcher Trans. 9727, Refining Remelting , Naukova Dumka, Kiev, 1975, p.18-25.

35. A.Mitchell, G.Sidla, The Design, Construction and Operation of an ESC installation , Special Report to DREP/DSS, June 1980.

36. S.Patankar, <u>Numerical Heat Transfer and Fluid Flow</u> , Hemisphere(McGraw-Hill), 1980.

37. B.Carnahan, H.A.Luther, J.O.Wilkes, <u>Applied Numerical Methods</u> , J.Wiley and Sons, 1969.

38. F.Kreith, W.Z.Black, <u>Basic Heat Transfer</u> , Harper and Row, New York, 1980.

39. V.P.Simonov, et al, BISITS trans. 12266, Izv. Vuz. Chern. Met., 1, 1974, p.175-178.

40. A.I.Chizhikov, V.L.Iokhimovich, G.P.Rachuk, L.I.Morozenskii, I.A.Mikhailova, Stal' in English, 11, 1968, p.921-924.

41. R.W.Young, V.Sunaryo, M.Cross, British Steel Corp. Report NO. Tech/722/1/75/A, July 1975.

42. R.Alberny, A.Leclerq, D.Amainy, M.Lahousse, Rev. de Met., 74, July-Aug 1976.

43. C.A.Sleicher, M.Tribus, Trans. ASME, 79, 1957, p.789-797.

44. E.M.Sparrow, R.Siegel, Trans. ASME, 82, Aug 1960, p.170.

45. V.J.Berry, App. Sci. Res., 4A, 1953, p.61-75.

46. B.I.Medovar, V.S.Zhakhovsky, A.G.Bogachenko, V.M.Matryn, Proc. Seventh ICVM, Tokyo, 1982, p.1244-1251.

47. G.Hoyle, Proc. Sixth Int. Vac. Conf. on Special Melting, San Diego, 1979, p.624-640.

48. K.C.Mills, B.J.Keene, Int. Met. Rev., (1), 1981, p.21-69.

49. G.S.Smirnov, A.K.Chatterjee, G.I.Zhmoidin, J. of Mat. Sci., 8, 1973, p.1278-1282.

50. G.I.Zhmoidin, A.K.Chatterjee, Inorg. Mat., Proc. Akad. Nauk. USSR, 10, (10), 1974,p.1846-1851.

51. A.K.Chatterjee, G.I.Zhmoidin, INorg. Mat., Proc. Akad. Nauk. USSR, 8, (5), 1972, p.886-892.

52. G.I.Zhmoidin, G.S.Smirnov, V.N.Glotky, Inorg. Mat., Proc. Akad. Nauk. USSR, 13, (3), 1977, p.552-553.

53. G.I.Zhmoidin, Metals, Proc. Akad. Nauk. USSR, 6, 1969, p.9-15.

54. V.M.Borishansky, I.I.Paleev, A.A.Andreevsky, B.S.Fokin,

M.E.Lavzentiev, K.P.Malyus-Malitsky, V.N.Fromzel, G.P.Danilova, Int. J. Heat Mass Trans., (5), 1973, p.1073-1085.

55. E.N.Sieder, G.N.Tate, Ind. Eng. Chem., 28, (12), 1936, p.1429.

56. B.S.Petukhov, Adv. in Heat Transfer, 6, 1970, p.504-564.

57. J.D.W.Rawson, G.Jeszensky, A.W.Bryant, Proc. Sixth Int. Vac. Met. Conf. on Special Melting, San Diego, 1979, p.848-863.

58. B.E.Paton, B.I.Medovar, V.L.Artamonov, A.G.Bogachenko, Y.P.Shtanko, Henry Brutcher Trans. 9726, Refining Remelting , Naukova Dumka, Kiev, 1972, p.49-53.

59. K.C.Mills, J.S.Powell, J.W.Bryant, B.J.Keene, Can. Met. Quart., 20, (1), 1981, p.93-99.

60. A.A.Sharapov, C.E.Volkov, C.V.Lebedev, Teoriya Metal., 3, 1957, p.131-136.

61. R.Taylor, K.C.Mills, Arch. Eisen., 53, (2), 1982, p.55-63.

62. R.N.Noyes, Trans. ASME, 83, 1961, p.96-97.

APPENDIX A - SLAG NOTATION

i. 70:30 = 70% CaF_2 , 30% Al_2O_3

ii. 70:15:15 = 70% CaF_2, 15% Al_2O_3, 15% CaO.

iii. 50:30:20 = 50% CaF_2, 30% Al_2O_3, 20% CaO.

iv. 33:33:33 = 1/3 CaF_2, 1/3 Al_2O_3, 1/3 CaO.

APPENDIX B - MISC. DATA AND CORRELATIONS

i. Water flow measurements

through Al section 30 litres/min.

through Cu section 30 litres/min.

through heat flux sensor 14 litres/min.

These measurements were made by noting the time needed to fill a 100 litre drum.

ii. Some physical properties

Material	Thermal Conductivity (W/m.K)		
	at 273K	at 400K	at 600K
Aluminium	236	240	232
Copper	401	392	383

Water at sat. Pr. and at	Density	Absolute Viscosity	Prandtl No.
	kg/m^3	x10^6 m^2/s	
273 K	999.3	1794	13.7
313 K	999.2	658	4.3
353 K	971.8	352	2.25
373 K	958.4	278	1.75

iii. Sieder-Tate correlation

$$Nu = .027 \ Re^{.8} \ Pr^{.33} (\mu_b / \mu_s)^{.14}$$

where

Nu = Nusselt number

Re = Reynolds number

Pr = Prandtl number

μ_b = viscosity of fluid at bulk temperature

μ_s = viscosity of fluid at surface of tube

All properties except viscosity taken at average bulk temperature.

    iv.   <u>Petukhov correlation</u>

$$Nu = \frac{(\xi/8) \ Re \ Pr}{K_1(\xi) + K_2(Pr) \ (\xi/8)^{.5} \ (Pr^{.67} - 1)}$$

where $\xi = (1.82 \ Log \ Re - 1.64)^{-2}$

$$K_1 = 1 + 3.4 \ \xi$$

$$K_2 = 11.7 + 1.8 \ Pr^{-.33}$$

All properties taken at the mean film temperature

APPENDIX C - FORTRAN PROGRAM TO CALCULATE TEMPERATURES IN CHANNEL COOLED MOULDS

```
C
C
C  THIS IS A PROGRAMME TO CALCULATE TEMPERATURES IN
C  CHANNEL COOLED MOULDS USED IN ELECTROSLAG CASTING
C THE METHOD IS TO USE MATRIX METHODS TO CALCULATE
C THE TEMPERATURES FOR EACH SLICE AND ITERATE FROM
C SLICE TO SLICE TILL CONVERGENCE IS REACHED.
C  THE REQUIRED INPUT ON UNIT 5 IS AS GIVEN BELOW.
C  THE INITIAL TEMP. ESTIMATE MUST BE GIVEN ON UNIT 4
C AND THE OUTPUT IS GIVEN ON UNIT 7.
C *******************************************************
C  M = NUMBER OF 'X' DIVISIONS
C  N = NUMBER OF Y NODES
C  O = NUMBER OF Z NODES
C  L = MAX. NO. OF ITERATIONS ALLOWED
C  TOLER = TOLERANCE
C  TW = INLET TEMPERATURE OF COOLANT
C  H = HEAT TRANSFER COEFFICIENT TO THE COOLANT
C  DELX = DISTANCE BETWEEN 2 X NODES
C  DELZ = DISTANCE BETWEEN 2 Z NODES
C  RH = RADIUS OF ROUND CHANNEL IN TERMS OF DELX UNITS
C  CH = POSITION OF CHANNEL IN TERMS OF DELX UNITS
C  COTC = COEFFICIENT OF THERMAL CONDUCTIVITY AT 0 C
C  VELA = MASS FLOW VELOCITY OF COOLANT
C  CEE = GRADIENT OF THERMAL CONDUCTIVITY WITH TEMP.
C  QA(I) = HEAT FLUX INTO THE HOT FACE
C  INIT = 0 IF THERE IS NO GUESS SOLUTION, OTHERWISE ANY NO.
C  IT IS SUGGESTED THAT ALL UNITS BE FED IN IN CGS UNITS
C  TO AVERT FORMAT PROBLEMS.
C *******************************************************
C
C  [TE] {S} = {B} IS THE MATRIX EQUATION TO BE SOLVED
C  AT EACH SLICE. X,Y,Z ARE SPECIAL VARIABLES.
C  T -- TEMPERATURE
C  TT -- REFERENCE TEMPERATURE FIELD
C  IPERM, TS -- MEMORY REQUIRED BY SOLUTION ROUTINE
C *******************************************************
C THE ROUTINE FSLE IS A ROUTINE IN THE UBC LIBRARY AND
C  USES GAUSSIAN ELIMINATION TO SOLVE SIMULTANEOUS
C  EQUATIONS.
C *********************************************************
C THE ROUTINES MATDAT, BOTDAT AND TOPDAT SERVE TO CALCULATE
C THE MATRIX TERMS FOR THE MIDDLE SLICES, THE BOTTOM SLICE
C AND THE TOP SLICE RESPECTIVELY
C
C***********************************************************
        REAL*4 TT,B,T,DET
        DIMENSION TT(20,20,30),TS(400,400),IPERM(800),S(400),X(20)
```

```
      1,Y(20),HT(30)
       COMMON T(20,20,30),TE(400,400),B(400),QA(30),Z(20,20),
      1TH(30),DELT
C
C  READ IN MATRIX DATA
C
       INTEGER O
       READ(5,1) M,N,O,L,TOLER
     1 FORMAT(2X,3I3,I4,F3.1)
       READ(5,2) TW,H
     2 FORMAT(2X,F4.1,F7.3)
       READ(5,3) DELX,RH,CH,DELZ
     3 FORMAT(2X,F6.4,2F4.1,F6.4)
       READ(5,4) COTC,VELA,CEE
     4 FORMAT(2X,F5.4,F7.3,F8.6)
       READ(5,6) (QA(I),I=1,O)
     6 FORMAT(1X,10F6.2)
       READ(5,7) INIT
     7 FORMAT(1X,I2)
       IF (INIT .EQ. 0) GO TO 9
       CONTINUE
       READ(4,8) (((T(I,J,K),J=1,N),I=1,M),K=1,O)
     8 FORMAT(11F6.2)
C **********************************************************
C THE LINES BELOW TO BE USED TO VARY H ALONG THE HEIGHT OF
C THE MOULD.
C **********************************************************
C      HT(1) = H - 0.18
C      HT(2) = H - 0.16
C      HT(3) = H- 0.16
C      HT(4) = H-0.14
C      HT(5) = HT(4)
C      HT(6) = H - 0.10
C      HT(7) = H - 0.08
C      HT(8) = H
C      HT(9) = H+.02
C.     HT(10) = H+.04
C      HT(11) = H +.02
C      HT(12) = H- .06
C      HT(13) = H - 0.08
C      HT(14) = H-0.10
C      HT(15) = H-0.12
C      HT(16) = H - 0.14
C      HT(17) = H- 0.16
C      HT(18) = HT(17)
C **********************************************************
       MN=M*N
C
C  GIVE X, Y COORDINATES TO THE NODES
C
       DO 10 I=1,M
       DO 10 J=1,N
       DO 10 K=1,O
    10 T(I,J,K) = 0.0
```

```
      SUM = -1.0
      DO 11 I=1,M
      SUM=SUM+1.
   11 X(I) = SUM
      SCUM =-1.0
      DO 12 J=1,N
      SCUM=SCUM+1.
   12 Y(J) = SCUM
C
C       CODE DIFFERENT TYPES OF NODES
C
      DO 100 I=1,M
      DO 100 J=1,N
C
C THE FOLLOWING IS BASED ON COORDINATE GEOMETRY
C
      AB =ABS(Y(J)-CH)
      A = (X(I)**2 + (Y(J) - CH)**2)
      IF ((RH**2) .LE. A) GO TO 20
C
C THE NODE IS IN THE COOLING CHANNEL
C
      Z(I,J) = 1
      GO TO 100
   20 IF (X(I) .GE. (RH+1.)) GO TO 50
      IF (ABS(Y(J)-CH) .GE. (RH+1.)) GO TO 50
      D = ABS(SQRT(ABS(RH**2-X(I)**2))-AB)
      C = ABS(X(I) - SQRT(ABS(RH**2 - (AB)**2)))
      IF (D .GE. 1.) GO TO 28
      IF (X(I).GT. 0.) GO TO22
      IF (Y(J) .GT.CH) GO TO 21
C
C CODES 2 TO 9 REFER TO NODES BOUNDING THE COOLING CHANNEL
C
      Z(I,J) = 2
      GO TO 100
   21 Z(I,J) =3
      GO TO 100
   22 IF (C.GE.1.) GO TO 26
      IF (Y(J)-CH) 23,24,25
   23 Z(I,J) = 4
      GO TO 100
   24 Z(I,J) = 5
      GO TO 100
   25 Z(I,J) = 6
      GO TO 100
   26 IF (Y(J).GT.CH) GO TO 27
      Z(I,J) =7
      GO TO 100
   27 Z(I,J) = 8
      GO TO 100
   28 IF (C.GE.1.) GO TO 50
      Z(I,J) = 9
      GO TO 100
```

```
   50 IF (X(I).LT.(M-1)) GO TO 65
      IF (Y(J).GT.0.) GO TO 55
C
C CODES 10 TO 12 REFER TO THE LEFT SIDE OF THE SECTION
C INCLUDING THE CORNER NODES BUT EXCLUDING THE NODES
C INSIDE THE COOLING CHANNEL AND THOSE BOUNDING IT.
C
      Z(I,J) = 10
      GO TO 100
   55 IF (Y(J).LT.(N-1)) GO TO 60
      Z(I,J) = 11
      GO TO 100
   60 Z(I,J) = 12
      GO TO 100
   65 IF (X(I).GT.0.) GO TO 80
      IF (Y(J).GT.0.) GO TO 70
C
C CODES 13 TO 15 REFER TO THE NODES ON THE RIGHT SIDE OF
C THE SECTION INCLUDING THE CORNER NODES
C
      Z(I,J) = 13
      GO TO 100
   70 IF (Y(J).LT.(N-1)) GO TO 75
      Z(I,J) =14
      GO TO 100
   75 Z(I,J) =15
      GO TO 100
   80 IF (Y(J).GT.0.) GO TO 85
C
C CODE 16 REFERS TO THE BOUNDARY OPPOSITE THE HOT FACE
C
      Z(I,J) =16
      GO TO 100
   85 IF (Y(J).LT.(N-1)) GO TO 90
C
C CODE 17 REFERS TO THE HOT FACE BOUNDARY
C
      Z(I,J) =17
      GO TO 100
C
C CODE 18 REFERS TO INTERIOR NODES
C
   90 Z(I,J) =18
  100 CONTINUE
C
C SET THE TEMP. OF THE CHANNEL TO THAT OF THE COOLANT
C AT THE INLET
C
      DO 101 IC=1,O
  101 TH(IC) = TW
C
C    SET ASSUMED TEMP. FIELD = REFERENCE
C
      DO 105 K=1,O
```

```
      DO 105 J=1,N
      DO 105 I=1,M
  105 TT(I,J,K) = T(I,J,K)
C
C     ITERATE L TIMES
C
      DO 310 LL=1,L
C
C RESET INCREASE OF TEMP. OF THE COOLANT TO ZERO
C FOR THE NEXT SLICE
C
      DELT = 0.0
C *****************************************************
C TO BE USED ONLY IF H IS TO BE VARIED
C
C     DO 130 K=1,O
C     H = HT(K)
C***********************************************************
C
C
C     BOTTOM SLICE
C
      IF (K.EQ.1) GO TO 110
C
C     TOP SLICE
C
      IF (K.EQ.O) GO TO 120
      CALL MIDDAT(M,N,O,K,COTC,DELX,DELZ,VELA,H,CEE)
      CALL FSLE(MN,400,TE,1,400,B,S,IPERM,400,TS,DET,JEXP)
C
C RE-WRITE SOLUTION IN TERMS OF X,Y,Z COORDINATES
C
      DO 106 II=1,MN
      I = (II-1)/N+1
      J= II-N*(I-1)
  106 T(I,J,K) = S(II)
      GO TO 130
  110 CALL BOTDAT(M,N,O,K,COTC,DELX,DELZ,VELA,H,CEE)
      CALL FSLE(MN,400,TE,1,400,B,S,IPERM,400,TS,DET,JEXP)
      DO 115 II=1,MN
      I=(II-1)/N+1
      J= II-N*(I-1)
  115 T(I,J,K) = S(II)
      GO TO 130
  120 CALL TOPDAT(M,N,O,K,COTC,DELX,DELZ,VELA,H,CEE)
      CALL FSLE(MN,400,TE,1,400,B,S,IPERM,400,TS,DET,JEXP)
      DO 125 II=1,MN
      I = (II-1)/N+1
      J = II-N*(I-1)
  125 T(I,J,K) = S(II)
  130 CONTINUE
C
C     COMPARE REFERENCE AND CALCULATED FIELDS
C
```

```
      DO 200 I=1,M
      DO 200 J=1,N
      DO 200 K=1,O
      IF (ABS(TT(I,J,K)-T(I,J,K)) .GT. TOLER) GO TO 300
  200 CONTINUE
C
C WRITE OUT RESULTS. NOTE IF N > 20 THEN PRINTOUT WILL
C LOOK FUNNY
C
      DO 218 K=1,O
      DO 216 I=1,M
      WRITE(7,210) (T(I,J,K),J=1,N)
  210 FORMAT(20F7.2)
  216 CONTINUE
      WRITE(7,217)
  217 FORMAT(/,/)
  218 CONTINUE
      STOP
C
C        RESET REFERENCE FIELDS
C
  300 DO 310 K=1,O
      DO 310 J=1,N
      DO 310 I=1,M
  310 TT(I,J,K) = T(I,J,K)
C
C NO. OF ITERARIONS WERE INSUFFICIENT. WRITE OUT FAILURE
C AND TEMPERATURES.
C
      WRITE(7,320) TOLER,L
  320 FORMAT(1H ,'THE TEMPERATURES DO NOT CONVERGE TO WITHIN',F5.
     1' DEGREES IN',I4,' ITERATION STEPS.')
      DO 328 K=1,O
      DO 326 I=1,M
      WRITE(7,321) (T(I,J,K),J=1,N)
  321 FORMAT(20F7.2)
  326 CONTINUE
      WRITE(7,327)
  327 FORMAT(/,/)
  328 CONTINUE
      STOP
      END
      SUBROUTINE MIDDAT(M,N,O,K,COTC,DELX,DELZ,VELA,H,CEE)
C
C THIS ROUTINE CALCULATES MATRIX TERMS FOR THE MIDDLE SLICES
C
      COMMON T(20,20,30),TT(400,400),B(400),QA(30),Z(20,20),
     1TH(30),DELT
      INTEGER CODE,O
      MN=M*N
C
C THE FOLLOWING CALCULATIONS ARE EQUIVALENT TO THE VARIOUS
C COEFFICIENTS. THEY ARE MADE HERE TO AVOID REATING AGAIN
C
```

```
      H12 = H*DELX*DELZ*.5
      H1 = H12*2.
      H2 = H12*4.
      H12TH = H12*TH(K)
      H1TH= H12TH*2.
      H2TH = H12TH*4.
      QA12 = QA(K)*DELX*DELZ*.5
      QA1 = QA12*2.
C
C INITIALISE MATRICES TO ZERO
C
      CALL GSET(TT,400,400,400,0.)
      CALL GSET(B,400,1,400,0.)
      THEAT = 0.0
      DDH = DELZ * DELX*H
C
C DO FOR EACH NODE DEPENDING ON CODE
C
      DO 100 J=1,N
      DO 100 I=1,M
C
C SET THERMAL CONDUCTIVITY ACCORDING TO TEMP. OF NODE
C AS IN THE PREVIOUS ITERATION
C
      CT = CEE*T(I,J,K) + COTC
      COT12 = CT*.5*DELZ
      COT1 = COT12*2.
      COT2 = COT1*2.
      COT3 = COT1*3.
      COT4 =COT1*4.
      C14 = CT*(DELX**2)*.25/DELZ
      C12 = C14*2.
      C = C14*4.
      CODE = Z(I,J)
      KK = N*(I-1)+J
      GO TO (1,2,3,4,5,6,7,8,9,10,11,12,13,14,15,16,17,18),CODE
    1 TT(KK,KK) = 1.
      B(KK) = TH(K)
      GO TO 100
    2 TT(KK,KK-1) = COT12
      TT(KK,KK) = -(COT1+ H12 + C12)
      TT(KK,KK+N) = COT12
      B(KK) = -(H12TH+ C14*(T(I,J,K+1) + T(I,J,K-1)))
      HEAT = DDH*(T(I,J,K) - TH(K))
      THEAT = THEAT + HEAT*.5
      GO TO 100
    3 TT(KK,KK) = -(COT1+ H12+ C12)
      TT(KK,KK+1) = COT12
      TT(KK,KK+N) = COT12
      B(KK) = -(H12TH+ C14*(T(I,J,K+1) + T(I,J,K-1)))
      HEAT = DDH*( T(I,J,K) - TH(K))
      THEAT = THEAT + HEAT * .5
      GO TO 100
    4 TT(KK,KK-1) = COT1
```

```
      TT(KK,KK) = -(COT2+ H2+ C*2.)
      TT(KK,KK+N) = COT1
      B(KK) = -(H2TH+ C*(T(I,J,K+1) + T(I,J,K-1)))
      HEAT = DDH*(T(I,J,K) - TH(K))
      THEAT = THEAT+ HEAT *2.
      GO TO 100
    5 TT(KK,KK-1) = COT12
      TT(KK,KK) = -(COT2+ H1+ C)
      TT(KK,KK+1) = COT12
      TT(KK,KK+N) = COT1
      B(KK) = -(H1TH + C12*(T(I,J,K+1)+T(I,J,K-1)))
      HEAT = DDH*(T(I,J,K) - TH(K))
      THEAT = THEAT + HEAT *1.
      GO TO 100
    6 TT(KK,KK) = -(COT2+ H2+ C*2.)
      TT(KK,KK+1) = COT1
      TT(KK,KK+N) = COT1
      B(KK) = -(H2TH+ C*(T(I,J,K+1)+T(I,J,K-1)))
      HEAT = DDH*(T(I,J,K) - TH(K))
      THEAT = THEAT + HEAT*2.
      GO TO 100
    7 TT(KK,KK-1) = COT1
      TT(KK,KK) = -(COT2+ H1+ C)
      TT(KK,KK-N) = COT12
      TT(KK,KK+N) = COT12
      B(KK) = -(H1TH+C12*(T(I,J,K+1)+T(I,J,K-1)))
      HEAT = DDH*(T(I,J,K) - TH(K))
      THEAT = THEAT + HEAT*1.
      GO TO 100
    8 TT(KK,KK-N) = COT12
      TT(KK,KK) = -(COT2+ H1 + C)
      TT(KK,KK+1) = COT1
      TT(KK,KK+N) = COT12
      B(KK) = -(H1TH + C12*(T(I,J,K+1) + T(I,J,K-1)))
      HEAT = DDH*(T(I,J,K) - TH(K))
      THEAT = THEAT+ HEAT*1.
      GO TO 100
    9 TT(KK,KK-1) = COT12
      TT(KK,KK) = -(COT2+ H1+ C)
      TT(KK,KK+1) = COT12
      TT(KK,KK+N) = COT1
      B(KK) = -(H1TH+ C12*(T(I,J,K+1) + T(I,J,K-1)))
      HEAT = DDH*(T(I,J,K) - TH(K))
      THEAT = THEAT + HEAT *1.
      GO TO 100
   10 TT(KK,KK-N) = COT12
      TT(KK,KK) = -(COT1+ C12)
      TT(KK,KK+1) = COT12
      B(KK) = -(C14*(T(I,J,K+1) + T(I,J,K-1)))
      GO TO 100
   11 TT(KK,KK-N) = COT12
      TT(KK,KK) = -(COT1+ C12)
      TT(KK,KK-1) = COT12
      B(KK) = -(QA12+ C14*(T(I,J,K+1) + T(I,J,K-1)))
```

```
       GO TO 100
    12 TT(KK,KK-N) = COT1
       TT(KK,KK-1) = COT12
       TT(KK,KK) = -(COT2+ C)
       TT(KK,KK+1) = COT12
       B(KK) = -(C12*(T(I,J,K+1) + T(I,J,K-1)))
       GO TO 100
    13 TT(KK,KK) = -(COT1+ C12)
       TT(KK,KK+1) = COT12
       TT(KK,KK+N) = COT12
       B(KK) = -(C14*(T(I,J,K+1) + T(I,J,K-1)))
       GO TO 100
    14 TT(KK,KK-1) = COT12
       TT(KK,KK) = -(COT1+ C12)
       TT(KK,KK+N) = COT12
       B(KK) = -(QA12+ C14*(T(I,J,K+1) + T(I,J,K-1)))
       GO TO 100
    15 TT(KK,KK-1) = COT12
       TT(KK,KK) = -(COT2+ C)
       TT(KK,KK+1) = COT12
       TT(KK,KK+N) = COT1
       B(KK) = -(C12*(T(I,J,K+1) + T(I,J,K-1)))
       GO TO 100
    16 TT(KK,KK-N) = COT12
       TT(KK,KK) = -(COT2+ C)
       TT(KK,KK+1) = COT1
       TT(KK,KK+N) = COT12
       B(KK) = -(C12*(T(I,J,K+1) + T(I,J,K-1)))
       GO TO 100
    17 TT(KK,KK-N) = COT12
       TT(KK,KK-1) = COT1
       TT(KK,KK) = -(COT2+ C)
       TT(KK,KK+N) = COT12
       B(KK) = -(QA1+ C12*(T(I,J,K+1) + T(I,J,K-1)))
       GO TO 100
    18 TT(KK,KK-N) = COT1
       TT(KK,KK-1) = COT1
       TT(KK,KK) = -(COT4+ C*2.)
       TT(KK,KK+1) = COT1
       TT(KK,KK+N) = COT1
       B(KK) = -(C*(T(I,J,K+1) + T(I,J,K-1)))
   100 CONTINUE
C
C CALCULATE INCREASE OF TEMPERATURE AND ADD TO TEMP.
C OF COOLANT
C
       DELT = DELT + THEAT/VELA
       IF (DELT .LT. 0.001) GO TO 120
       KO1=K+1
       DO 110 KO=KO1,O
   110 TH(KO) = TH(1) + DELT
   120 CONTINUE
       RETURN
       END
```

```
      SUBROUTINE BOTDAT(M,N,O,K,COTC,DELX,DELZ,VELA,H,CEE)
C
C THIS ROUTINE SETS MATRIX TERMS FOR THE BOTTOM SLICE
C ALL COMMENTS GIVEN IN THE ROUTINE MIDDAT APPLY HERE TOO
C
      COMMON T(20,20,30),TT(400,400),B(400),QA(30),Z(20,20),
     1TH(30),DELT
      INTEGER CODE,O
      MN=M*N
      H12 = H*DELX*DELZ*.25
      H1 = H12*2.
      H2 = H12*4.
      H12TH = H12*TH(K)
      H1TH= H12TH*2.
      H2TH = H12TH*4.
      QA12 = QA(K)*DELX*DELZ*.25
      QA1 = QA12*2.
      CALL GSET(TT,400,400,400,0.)
      CALL GSET(B,400,1,400,0.)
      THEAT = 0.0
      DDH = DELZ*DELX*H
      DO 100 J=1,N
      DO 100 I=1,M
      CT= CEE * T(I,J,K) +COTC
      COT12 = CT*.25*DELZ
      COT1 = COT12*2.
      COT2 = COT1*2.
      COT3 = COT1*3.
      COT4 =COT1*4.
      C14 = CT*(DELX**2)*.25/DELZ
      C12 = C14*2.
      C = C14*4.
      CODE = Z(I,J)
      KK = N*(I-1)+J
      GO TO (1,2,3,4,5,6,7,8,9,10,11,12,13,14,15,16,17,18),CODE
    1 TT(KK,KK) = 1.
      B(KK) = TH(K)
      GO TO 100
    2 TT(KK,KK-1) = COT12
      TT(KK,KK) = -(COT1+ H12 + C14)
      TT(KK,KK+N) = COT12
      B(KK) = -(H12TH+ C14*(T(I,J,K+1) + 0.))
      HEAT = DDH*(T(I,J,K) - TH(K))
      THEAT = THEAT + HEAT *.25
      GO TO 100
    3 TT(KK,KK) = -(COT1+ H12+ C14)
      TT(KK,KK+1) = COT12
      TT(KK,KK+N) = COT12
      B(KK) = -(H12TH+ C14*(T(I,J,K+1) + 0.))
      HEAT = DDH*(T(I,J,K) - TH(K))
      THEAT = THEAT + HEAT * 0.25
      GO TO 100
    4 TT(KK,KK-1) = COT1
      TT(KK,KK) = -(COT2+ H2+ C)
```

```
      TT(KK,KK+N) = COT1
      B(KK) = -(H2TH+ C*(T(I,J,K+1) + 0.))
      HEAT = DDH*(T(I,J,K) - TH(K))
      THEAT = THEAT + HEAT *1.
      GO TO 100
    5 TT(KK,KK-1) = COT12
      TT(KK,KK) = -(COT2+ H1+ C12)
      TT(KK,KK+1) = COT12
      TT(KK,KK+N) = COT1
      B(KK) = -(H1TH + C12*(T(I,J,K+1)+0.))
      HEAT = DDH*(T(I,J,K) - TH(K))
      THEAT = THEAT + HEAT * 0.5
      GO TO 100
    6 TT(KK,KK) = -(COT2+ H2+ C)
      TT(KK,KK+1) = COT1
      TT(KK,KK+N) = COT1
      B(KK) = -(H2TH+ C*(T(I,J,K+1)+0.))
      HEAT = DDH*(T(I,J,K) - TH(K))
      THEAT = THEAT + HEAT * 1.
      GO TO 100
    7 TT(KK,KK-1) = COT1
      TT(KK,KK) = -(COT2+ H1+ C12)
      TT(KK,KK-N) = COT12
      TT(KK,KK+N) = COT12
      B(KK) = -(H1TH+C12*(T(I,J,K+1)+0.))
      HEAT = DDH*(T(I,J,K) - TH(K))
      THEAT = THEAT + HEAT *.5
      GO TO 100
    8 TT(KK,KK-N) = COT12
      TT(KK,KK) = -(COT2+ H1 + C12)
      TT(KK,KK+1) = COT1
      TT(KK,KK+N) = COT12
      B(KK) = -(H1TH + C12*(T(I,J,K+1) + 0.))
      HEAT = DDH*(T(I,J,K)-TH(K))
      THEAT = THEAT + HEAT * 0.5
      GO TO 100
    9 TT(KK,KK-1) = COT12
      TT(KK,KK) = -(COT2+ H1+ C12)
      TT(KK,KK+1) = COT12
      TT(KK,KK+N) = COT1
      B(KK) = -(H1TH+ C12*(T(I,J,K+1) + 0.))
      HEAT = DDH*(T(I,J,K) - TH(K))
      THEAT = THEAT + HEAT *0.5
      GO TO 100
   10 TT(KK,KK-N) = COT12
      TT(KK,KK) = -(COT1+ C14)
      TT(KK,KK+1) = COT12
      B(KK) = -(C14*(T(I,J,K+1) + 0.))
      GO TO 100
   11 TT(KK,KK-N) = COT12
      TT(KK,KK) = -(COT1+ C14)
      TT(KK,KK-1) = COT12
      B(KK) = -(QA12+ C14*(T(I,J,K+1) + 0.))
      GO TO 100
```

```
     12 TT(KK,KK-N) = COT1
        TT(KK,KK-1) = COT12
        TT(KK,KK) = -(COT2+ C12)
        TT(KK,KK+1) = COT12
        B(KK) = -(C12*(T(I,J,K+1) + 0.))
        GO TO 100
     13 TT(KK,KK) = -(COT1+ C14)
        TT(KK,KK+1) = COT12
        TT(KK,KK+N) = COT12
        B(KK) = -(C14*(T(I,J,K+1) + 0.))
        GO TO 100
     14 TT(KK,KK-1) = COT12
        TT(KK,KK) = -(COT1+ C14)
        TT(KK,KK+N) = COT12
        B(KK) = -(QA12+ C14*(T(I,J,K+1) + 0.))
        GO TO 100
     15 TT(KK,KK-1) = COT12
        TT(KK,KK) = -(COT2+ C12)
        TT(KK,KK+1) = COT12
        TT(KK,KK+N) = COT1
        B(KK) = -(C12*(T(I,J,K+1) + 0.))
        GO TO 100
     16 TT(KK,KK-N) = COT12
        TT(KK,KK) = -(COT2+ C12)
        TT(KK,KK+1) = COT1
        TT(KK,KK+N) = COT12
        B(KK) = -(C12*(T(I,J,K+1) + 0.))
        GO TO 100
     17 TT(KK,KK-N) = COT12
        TT(KK,KK-1) = COT1
        TT(KK,KK) = -(COT2+ C12)
        TT(KK,KK+N) = COT12
        B(KK) = -(QA1+ C12*(T(I,J,K+1) + 0.))
        GO TO 100
     18 TT(KK,KK-N) = COT1
        TT(KK,KK-1) = COT1
        TT(KK,KK) = -(COT4+ C)
        TT(KK,KK+1) = COT1
        TT(KK,KK+N) = COT1
        B(KK) = -(C*(T(I,J,K+1) + 0.))
    100 CONTINUE
        DELT = DELT + THEAT/VELA
        IF (DELT .LT. 0.001) GO TO 120
        KO1=K+1
        DO 110 KO=KO1,O
    110 TH(KO) = TH(1) + DELT
    120 CONTINUE
        RETURN
        END
        SUBROUTINE TOPDAT(M,N,O,K,COTC,DELX,DELZ,VELA,H,CEE)
C
C THIS ROUTINE CALCULATES MATRIX TERMS FOR THE TOP SLICE
C ALL OTHER COMMENTS GIVEN IN THE ROUTINE MIDDAT APPLY
C
```

```
      COMMON T(20,20,30),TT(400,400),B(400),QA(30),Z(20,20),
     1TH(30),DELT
      INTEGER CODE,O
      MN=M*N
      H12 = H*DELX*DELZ*.25
      H1 = H12*2.
      H2 = H12*4.
      H12TH = H12*TH(K)
      H1TH= H12TH*2.
      H2TH = H12TH*4.
      QA12 = QA(K)*DELX*DELZ*.25
      QA1 = QA12*2.
      CALL GSET(TT,400,400,400,0.)
      CALL GSET(B,400,1,400,0.)
      THEAT = 0.0
      DDH = 0.0
      DO 100 J=1,N
      DO 100 I=1,M
      CT = CEE * T(I,J,K) +COTC
      COT12 = CT*.25*DELZ
      COT1 = COT12*2.
      COT2 = COT1*2.
      COT3 = COT1*3.
      COT4 =COT1*4.
      C14 = CT*(DELX**2)*.25/DELZ
      C12 = C14*2.
      C = C14*4.
      CODE = Z(I,J)
      KK = N*(I-1)+J
      GO TO (1,2,3,4,5,6,7,8,9,10,11,12,13,14,15,16,17,18),CODE
    1 TT(KK,KK) = 1.
      B(KK) = TH(K)
      GO TO 100
    2 TT(KK,KK-1) = COT12
      TT(KK,KK) = -(COT1+ H12 + C14)
      TT(KK,KK+N) = COT12
      B(KK) = -(H12TH+ C14*(0. + T(I,J,K-1)))
      HEAT = DDH*(T(I,J,K) - TH(K))
      THEAT = THEAT + HEAT * 0.25
      GO TO 100
    3 TT(KK,KK) = -(COT1+ H12+ C14)
      TT(KK,KK+1) = COT12
      TT(KK,KK+N) = COT12
      B(KK) = -(H12TH+ C14*(0. + T(I,J,K-1)))
      HEAT = DDH*(T(I,J,K) - TH(K))
      THEAT = THEAT + HEAT *0.25
      GO TO 100
    4 TT(KK,KK-1) = COT1
      TT(KK,KK) = -(COT2+ H2+ C)
      TT(KK,KK+N) = COT1
      B(KK) = -(H2TH+ C*(0. + T(I,J,K-1)))
      HEAT = DDH*(T(I,J,K) -TH(K))
      THEAT =THEAT + HEAT * 1.
      GO TO 100
```

```
 5 TT(KK,KK-1) = COT12
   TT(KK,KK) = -(COT2+ H1+ C12)
   TT(KK,KK+1) = COT12
   TT(KK,KK+N) = COT1
   B(KK) = -(H1TH + C12*(0.+T(I,J,K-1)))
   HEAT = DDH*(T(I,J,K) - TH(K))
   THEAT = THEAT + HEAT * 0.5
   GO TO 100
 6 TT(KK,KK) = -(COT2+ H2+ C)
   TT(KK,KK+1) = COT1
   TT(KK,KK+N) = COT1
   B(KK) = -(H2TH+ C*(0.+T(I,J,K-1)))
   HEAT = DDH*(T(I,J,K) - TH(K))
   THEAT = THEAT + HEAT *1.
   GO TO 100
 7 TT(KK,KK-1) = COT1
   TT(KK,KK) = -(COT2+ H1+ C12)
   TT(KK,KK-N) = COT12
   TT(KK,KK+N) = COT12
   B(KK) = -(H1TH+C12*(0.+T(I,J,K-1)))
   HEAT = DDH*(T(I,J,K) - TH(K))
   THEAT = THEAT + HEAT * 0.5
   GO TO 100
 8 TT(KK,KK-N) = COT12
   TT(KK,KK) = -(COT2+ H1 + C12)
   TT(KK,KK+1) = COT1
   TT(KK,KK+N) = COT12
   B(KK) = -(H1TH + C12*(0. + T(I,J,K-1)))
   HEAT = DDH * (T(I,J,K) - TH(K))
   THEAT = THEAT + HEAT * 0.5
   GO TO 100
 9 TT(KK,KK-1) = COT12
   TT(KK,KK) = -(COT2+ H1+ C12)
   TT(KK,KK+1) = COT12
   TT(KK,KK+N) = COT1
   B(KK) = -(H1TH+ C12*(0. + T(I,J,K-1)))
   HEAT = DDH*(T(I,J,K) - TH(K))
   THEAT = THEAT + HEAT * 0.5
   GO TO 100
10 TT(KK,KK-N) = COT12
   TT(KK,KK) = -(COT1+ C14)
   TT(KK,KK+1) = COT12
   B(KK) = -(C14*(0. + T(I,J,K-1)))
   GO TO 100
11 TT(KK,KK-N) = COT12
   TT(KK,KK) = -(COT1+ C14)
   TT(KK,KK-1) = COT12
   B(KK) = -(QA12+ C14*(0. + T(I,J,K-1)))
   GO TO 100
12 TT(KK,KK-N) = COT1
   TT(KK,KK-1) = COT12
   TT(KK,KK) = -(COT2+ C12)
   TT(KK,KK+1) = COT12
   B(KK) = -(C12*(0. + T(I,J,K-1)))
```

```
      GO TO 100
 13 TT(KK,KK) = -(COT1+ C14)
    TT(KK,KK+1) = COT12
    TT(KK,KK+N) = COT12
    B(KK) = -(C14*(0. + T(I,J,K-1)))
      GO TO 100
 14 TT(KK,KK-1) = COT12
    TT(KK,KK) = -(COT1+ C14)
    TT(KK,KK+N) = COT12
    B(KK) = -(QA12+ C14*(0. + T(I,J,K-1)))
      GO TO 100
 15 TT(KK,KK-1) = COT12
    TT(KK,KK) = -(COT2+ C12)
    TT(KK,KK+1) = COT12
    TT(KK,KK+N) = COT1
    B(KK) = -(C12*(0. + T(I,J,K-1)))
      GO TO 100
 16 TT(KK,KK-N) = COT12
    TT(KK,KK) = -(COT2+ C12)
    TT(KK,KK+1) = COT1
    TT(KK,KK+N) = COT12
    B(KK) = -(C12*(0. + T(I,J,K-1)))
      GO TO 100
 17 TT(KK,KK-N) = COT12
    TT(KK,KK-1) = COT1
    TT(KK,KK) = -(COT2+ C12)
    TT(KK,KK+N) = COT12
    B(KK) = -(QA1+ C12*(0. + T(I,J,K-1)))
      GO TO 100
 18 TT(KK,KK-N) = COT1
    TT(KK,KK-1) = COT1
    TT(KK,KK) = -(COT4+ C)
    TT(KK,KK+1) = COT1
    TT(KK,KK+N) = COT1
    B(KK) = -(C*(0. + T(I,J,K-1)))
100 CONTINUE
    DELT = THEAT/VELA
    TH(K) = TH(K)
    RETURN
    END
```

APPENDIX D - FORTRAN PROGRAM REFERRED TO IN SECTION 3.3

```
C  ***************************************************************
       IMPLICIT REAL*8(A-H,O-Z)
       INTEGER BCC
C     THIS IS A PROGRAM USING TRIANGULAR OR RECTANGULAR FINITE
C   ELEMENTS TO SOLVE STEADY STATE HEAT TRANSFER PROBLEMS.
C  SPECIFICALLY IT IS BEING USED TO MODEL SECTIONS IN AN
C ELECTROSLAG CASTING MOULD. ALL VARIABLES BEGINNING WITH
C  THE LETTERS A-H AND O-Z ARE DECLARED DOUBLE PRECISION.
C
C   DEFINE VARIABLES
C       C = CONDUCTANCE MATRIX
C       T = TEMPERATURE MATRIX
C       B = [C]*[T]   MATRIX
C       ICO = ELEMENT CORNER NODE NUMBERS
C       X,Y = GLOBAL CO-ORDINATES
C       D = CONDUCTIVITY MATRIX
C       H = HEAT TRANSFER CO-EFFICIENT(
C       ITYPE = TYPE OF ELEMENT
C      IMAT = MATERIAL CODE
C     BCC = BOUNDARY CODE(CONVECTION)
C    BCT = BOUNDARY CODE (TEMPERATURE)
C    IHF = CODE TO CALCULATE HEAT FLUX
C    XX,YY,A,S ---ELEMENT CO-ORDINATES AND MATRICES
C
C
C
       DIMENSION C(200,200),T(200),B(200),X(200),Y(200),ITYPE(200)
      1BCT(200),IHF(200),IMAT(200),IPERM(400),TT(200,200),DA(2,2),
      2XX(8),BCC(200),YY(8),NO(8),ICO(200,8),S4(4,4),S3(3,3),A4(4)
      3S8(8,8),A8(8),A3(3),DC(2,2),RZ(200)
       COMMON /ZD/ DET,JEXP
       COMMON /DSLMP$/ NITER
C
C  CALL SUBROUTINE TO READ IN NECESSARY DATA FOR PROBLEM
C
       CALL LAYOUT(X,Y,ICO,200,ITYPE,NE,NNODES,BCT,BCC,H,TW,COTC,
      1IHF,COTA,IMAT)
C
C INITIALISE ARRAYS
C
       CALL DGSET(DC,2,2,2,0.D0)
       DC(1,1) = COTC
       DC(2,2) = DC(1,1)
       CALL DGSET(DA,2,2,2,0.D0)
       DA(1,1) = COTA
       DA(2,2) = DA(1,1)
       DO 3 I=1,200
       B(I) = 0.D0
       DO 3 J=1,200
```

```
    3 C(I,J) = 0.D0
C
C   BEGIN DO-LOOP TO GO THROUGH ÀLL ELEMENTS
C
      DO 8 IEL=1,NE
      NN = ITYPE(IEL)
      BC = BCC(IEL)
      DO 4 I=1,NN
      NO(I) = ICO(IEL,I)
      XX(I) = X(NO(I))
    4 YY(I) = Y(NO(I))
C
C    CALL SUBROUTINE TO CALCULATE I-TH CONDUCTANCE MATRIX
C
      IM = IMAT(IEL)
      IF (IM .EQ. 0) GO TO 20
      CALL COND(IEL,NN,XX,YY,S3,S4,S8,DC,A3,A4,A8,H,TW,BC)
      GO TO 21
   20 CALL COND(IEL,NN,XX,YY,S3,S4,S8,DA,A3,A4,A8,H,TW,BC)
   21 CONTINUE
C
C    CALL SUBROUTINE TO INSERT ELEMENT MATRIX INTO STRUCTURE
C MATRIX
C
      IF (NN .EQ. 3) GO TO 5
      IF (NN .EQ. 8) GO TO 6
      CALL SETUP(NO,NN,C,200,S4,NN,B,A4)
      GO TO 7
    5 CALL SETUP(NO,NN,C,200,S3,NN,B,A3)
      GO TO 7
    6 CALL SETUP(NO,NN,C,200,S8,NN,B,A8)
    7 CONTINUE
    8 CONTINUE
C
C   CALL SUBROUTINE TO ADJUST STRUCTURE MATRIX FOR BOUNDARY
C      CONDITIONS
C
      DO 50 I=1,NNODES
      IF (BCT(I)) 50,40,40
   40 CALL BOUND(I,BCT,C,B,200,NNODES)
   50 CONTINUE
      WRITE(7,55) ((C(I,J),I=1,NNODES),J=1,NNODES)
   55 FORMAT(1X,2D30.22)
      WRITE(7,56) (B(I),I=1,NNODES)
   56 FORMAT(/,/,/,1X,(2D30.12))
      DO 57 I=1,NNODES
      B(I) = B(I)*1.D45
      DO 57 J=1,NNODES
   57 C(I,J) = C(I,J) * 1.D45
C
C    CALL MATRIX SOLVER FROM UBC LIBRARY
C
      DEPS = 1.D-16
      CALL DSLIMP(C,TT,B,T,RZ,IPERM,NNODES,200,DEPS,1,14)
```

```
      WRITE(6,25) DET,JEXP
   25 FORMAT(1X,' DETERM. = ',G20.12,'*10**',I5,/)          '
      WRITE(6,26) ((IJK,T(IJK)),IJK=1,NNODES)
   26 FORMAT(1X,4('T(',I3,') = ',F6.2,3X))
   27 CONTINUE
C
C     CALCULATE HEAT FLUX   AT MOLD INSIDE SURFACE AND PRINT
C
      DO 100 IEL=1,NE
      IK = IHF(IEL)
      IF (IK .EQ. 0) GO TO 100
      NN = ITYPE(IEL)
      DO 90 I=1,NN
      NO(I) = ICO(IEL,I)
      XX(I) = X(NO(I))
      YY(I) = Y(NO(I))
      T(I) = T(NO(I))
   90 CONTINUE
      IM = IMAT(IEL)
      IF (IM .EQ. 0) GO TO 95
      CALL HFLUX(IEL,NN,XX,YY,T,DC,NO)
      GO TO 96
   95 CALL HFLUX(IEL,NN,XX,YY,T,DA,NO)
   96 CONTINUE
  100 CONTINUE
      STOP
      END
C ***************************************************************
      SUBROUTINE COND(I,NN,X,Y,S3,S4,S8,D,A3,A4,A8,H,TW,BC)
      IMPLICIT REAL*8(A-H,O-Z)
      DIMENSION X(1),Y(1),S3(3,3),S4(4,4),D(2,2)
     1,S8(8,8),A8(8),A3(3),A4(4)
      IF (NN.EQ. 4) GO TO 10
      IF (NN .EQ. 8) GO TO 15
      CALL TRICON(X,Y,S3,D,A3)
      GO TO 20
   10 CALL QUACON(X,Y,S4,D,A4,H,TW,BC)
      GO TO 20
   15 CALL LQCON(X,Y,S8,D,A8,H,TW,BC)
   20 CONTINUE
      RETURN
      END
C ***************************************************************
      SUBROUTINE QUACON(X,Y,S,D,A4,H,TW,BC)
C
C CALCULATES CONDUCTANCE MATRIX FOR RECTANGULAR ELEMENT
C
      IMPLICIT REAL*8(A-H,O-Z)
      DIMENSION S(4,4),X(4),Y(4),D(2,2),B(2,4),BT(4,2),BTD(4,2)
     1,AJ(2,2),XI(2),AI(2,2),ANU(4),ANV(4),ST(4,4)
     2,SP(4,4),A4(4),AN(1,4),ANT(4,1)
      DATA XI/-0.577350269189626D0,+0.577350269189626D0/
C
C   BEGIN DO-LOOPS FOR NUMERICAL INTEGRATION
```

```
C
      CALL DGSET(S,4,4,4,0.D0)
      DO 26 I=1,2
      DO 26 J=1,2
      CALL DGSET(AJ,2,2,2,0.D0)
      U = XI(I)
      V = XI(J)
C
C   CALCULATES DERIVATIVES OF SHAPE FUNCTIONS
C
      ANU(1) = -(1.D0-V)*0.25D0
      ANU(2) = -ANU(1)
      ANU(3) = (1.D0+V)*0.25D0
      ANU(4) = - ANU(3)
      ANV(1) = - (1.D0 - U) *0.25D0
      ANV(2) = - (1.D0 +U) * 0.25D0
      ANV(3) = -ANV(2)
      ANV(4) = -ANV(1)
C
C  CALCULATE JACOBIAN
C
      DO 6 K=1,4
      AJ(1,1) = AJ(1,1) + ANU(K)*X(K)
      AJ(1,2) = AJ(1,2) + ANU(K) * Y(K)
      AJ(2,1) = AJ(2,1) + ANV(K) * X(K)
      AJ(2,2) = AJ(2,2) + ANV(K) * Y(K)
    6 CONTINUE
C
C  CALCULATE DETERMINANT AND INVERT AJ
C
      DET = AJ(1,1)*AJ(2,2) - AJ(1,2)*AJ(2,1)
      AI(1,1) = AJ(2,2)/DET
      AI(1,2) = - AJ(1,2)/DET
      AI(2,1) = -AJ(2,1)/DET
      AI(2,2) = AJ(1,1)/DET
C
C  CALCULATE B
C
      DO 8 K=1,4
      B(1,K) = AI(1,1)*ANU(K) +AI(1,2)*ANV(K)
    8 B(2,K) = AI(2,1)*ANU(K) + AI(2,2)*ANV(K)
C
C  CALCULATE BT*D*B
C
      CALL DGTRAN(B,BT,2,4,2,4)
      CALL DGMULT(BT,D,BTD,4,2,2,4,2,4)
      CALL DGMULT(BTD,B,ST,4,2,4,4,2,4)
C
C  MULTIPLY BY DET AND WEIGHT
C
      DO 10 K=1,4
      DO 10 L=1,4
   10 S(K,L) = S(K,L) + ST(K,L)*DET
   26 CONTINUE
```

```
      ICODE= BC
      CALL DGSET(SP,4,4,4,0.D0)
      DO 30 K=1,4
 30 A4(K) = 0.D0
      DO 50 I=1,2
      CALL DGSET(AJ,2,2,2,0.D0)
      GO TO (34,33,32,31,50), ICODE
 31 U = -1.D0
      V = XI(I)
      ALINE = DABS(DSQRT((X(4)-X(1))**2 +(Y(4)-Y(1))**2))
      GO TO 35
 32 V = 1.D0
      U= XI(I)
      ALINE = DABS(DSQRT((X(3)-X(4))**2 + (Y(3)-Y(4))**2))
      GO TO 35
 33 U = 1.D0
      V = XI(I)
      ALINE = DABS(DSQRT((X(2)-X(3))**2 + (Y(2)-Y(3))**2))
      GO TO 35
 34 V = -1.D0
      U = XI(I)
      ALINE = DABS(DSQRT((X(1)-X(2))**2 + (Y(1)-Y(2))**2))
 35 AN(1,1) = (1.D0-U)*(1.D0-V)*.25D0
      AN(1,2) = (1.D0+U)*(1.D0-V) *.25D0
      AN(1,3) = (1.D0+U)*(1.D0+V)*.25D0
      AN(1,4) = (1.D0-U)*(1.D0+V)*.25D0
C
C   CALCULATE NT*N
C
      CALL DGTRAN(AN,ANT,1,4,1,4)
      CALL DGMULT(ANT,AN,SP,4,1,4,4,1,4)
      DO 40 K=1,4
      DO 40 L=1,4
 40 S(K,L) = S(K,L) + SP(K,L)*H*ALINE*.5D0
      DO 45 K=1,4
 45 A4(K) =A4(K) + AN(1,K)*H*TW*ALINE*.5D0
 50 CONTINUE
      RETURN
      END
C ***************************************************************
      SUBROUTINE TRICON(X,Y,S,D,A3)
C
C   CALCULATES CONDUCTANCE MATRIX FOR TRIANGULAR ELEMENT
C
      IMPLICIT REAL*8(A-H,O-Z)
      DIMENSION S(3,3),A3(3),X(3),Y(3),D(2,2),B(2,3),BT(3,2),
     1BTD(3,2)
      A= X(2)*Y(3) - Y(2)*X(3) + X(1)*(Y(2)-Y(3)) +
     1Y(1)*(X(3)-X(2))
      AINV = 1.D0/A
      B(1,1) = (Y(2) -Y(3)) *AINV
      B(1,2) = (Y(3)-Y(1)) * AINV
      B(1,3) = (Y(1)-Y(2)) * AINV
      B(2,1) = (X(3)-X(2)) * AINV
```

```
        B(2,2) = (X(1)-X(3)) * AINV
        B(2,3) = (X(2)-X(1)) * AINV
C
C CALCULATE BT*D*B
C
      CALL DGTRAN(B,BT,2,3,2,3)
      CALL DGMULT(BT,D,BTD,3,2,2,3,2,3)
      CALL DGMULT(BTD,B,S,3,2,3,3,2,3)
      DO 10 I=1,3
      DO 10 J=1,3
   10 S(I,J) = S(I,J)*0.5D0*A
      DO 20 I=1,3
   20 A3(I) = 0.D0
      RETURN
      END
C ****************************************************************
      SUBROUTINE LAYOUT(X,Y,ICO,NDIM,ITYPE,NE,NNODES,BCT,BCC,H,TW
     1,COTC,IHF,COTA,IMAT)
C
C   THIS ROUTINE READS IN DATA FOR FINITE ELEMENT HEAT CONDUCTION
C     PROBLEM
C
      IMPLICIT REAL*8(A-H,O-Z)
      INTEGER BCC
      DIMENSION X(NDIM),IHF(NDIM),Y(NDIM),ICO(NDIM,8),ITYPE(NDIM)
     1BCT(NDIM),BCC(NDIM),IMAT(NDIM)
      READ(5,28) COTC,COTA
   28 FORMAT(F5.3,F8.6)
      WRITE(6,29) COTC
   29 FORMAT(1X,'CO-EFF. OF THERMAL CONDUCTIVITY(AL) = ',F5.3,/)
      WRITE(6,60) COTA
   60 FORMAT(1X,'CO-EFF. OF THERMAL CONDUCTIVITY(AIR) = ',F8.6,/)
      READ(5,30) H,TW
   30 FORMAT(F7.3,F5.1)
      WRITE(6,32) H,TW
   32 FORMAT(1X,'HEAT TRAN. CO-EFF. = ',F7.3,3X,'WATER TEMP. = ',
     1 F5.1,/)
      READ(5,40) NE,NNODES
   40 FORMAT(2I5)
      WRITE(6,41) NE,NNODES
   41 FORMAT(1X,'NO. OF ELEMENTS= ',I5,2X,'NO. OF NODES= ',I5,/)
      WRITE(6,44)
   44 FORMAT(6X,' X CO-ORD ',2X,' Y CO-ORD ',2X,'BOUNDARY
     1CONDITIONS',/)
      DO 10 I=1,NNODES
C
C   IF BCT DOES NOT EXIST , IT SHOULD BE MADE NEGATIVE
C
      READ(5,43) X(I),Y(I),BCT(I)
   43 FORMAT(3F7.3)
      WRITE(6,45) I,X(I),Y(I),BCT(I)
   45 FORMAT(1X,I3,2X,F8.3,2X,F10.3,5X,F8.3)
   10 CONTINUE
C
```

```
C ITYPE IS 4 IF RECTANGULAR ; 3 IF TRIANGULAR
C
      READ(5,51) (ITYPE(I),I=1,NE)
   51 FORMAT(20I2)
      WRITE(6,52)
   52 FORMAT(/,/,1X,' ELEMENT ',3X,'BOUNDARY',3X,'MATERIAL'
     1,'   NODE   ')
      WRITE(6,53)
   53 FORMAT(1X,'  NO.  ',3X,' CODE ',3X,' CODE ',
     13X,' NUMBERS ',/)
      DO 11 I=1,NE
      IT = ITYPE(I)
C
C BCC ----> 1,2,3,4,5,: 1,2,3,4, REFER TO SIDES SUFFERING
C                              CONVECTION
C                    5 IF THE ELEMENT SUFFERS NO CONVECTION
C   IHF -----> 0 IF THERE IS NO NEED TO CALCULATE HEAT FLUX
C                  1   OTHERWISE
C
C   IMAT -----> 0 FOR AIR
C                  1 FOR COPPER
C
      READ(5,49) BCC(I),IHF(I),IMAT(I),(ICO(I,J),J=1,IT)
   49 FORMAT(15I5)
      WRITE(6,47) I,BCC(I),IMAT(I),(ICO(I,J),J=1,IT)
   47 FORMAT(1X,I6,6X,I6,5X,I6,3X,8(I5,','))
   11 CONTINUE
      RETURN
      END
C ***************************************************************
      SUBROUTINE SETUP(NODES,NNODEL,A,NDIMA,B,NDIMB,PMAST,PELEM)
C
C      PROGRAM TO SETUP MASTER STIFFNESS MATRIX FROM INDIVIDUAL
C FINITE ELEMENT STIFFNESS MATRICES.  ALSO SETS UP LOAD VECTOR.
C
C      NODES     = INTEGER VECTOR CONTAINING ELEMENT NODE NUMBERS
C                  IN ORDER.
C      NNODEL    = NUMBER OF NODES PER ELEMENT
C      NVAR      = NUMBER OF VARIABLES PER NODE
C      A         = MASTER STIFFNESS MATRIX WHICH MUST BE ZEROED
C                  BEFORE FIRST ENTRY TO SETUP
C      NDIMA     = FIRST DIMENSION OF A
C      B         = ELEMENT STIFFNESS MATRIX
C      NDIMB     = FIRST DIMENSION OF B
C      PMAST     = MASTER LOAD VECTOR WHICH MUST BE ZEROED BEFORE
C                  FIRST ENTRY.
C      PELEM     = ELEMENT LOAD VECTOR
C
C
      IMPLICIT REAL*8(A-H,O-Z)
      DIMENSION A(NDIMA,NDIMA),B(NDIMB,NDIMB),NODES(20),
     1PMAST(NDIMA),PELEM(20)
      DO 1 I=1,NNODEL
      MM = NODES(I)
```

```fortran
      PMAST(MM)=PMAST(MM)+PELEM(I)
      DO 1 J=1,NNODEL
      NN = NODES(J)
    1 A(MM,NN)=A(MM,NN)+B(I,J)
      RETURN
      END
C ****************************************************************
      SUBROUTINE BOUND(I,BCT,AK,B,NDIM,NN)
C
C  THIS SUBROUTINE MODIFIES MATRIX FOR FIXED TEMPERATURE
C     BOUNDARY CONDITIONS
C
      IMPLICIT REAL*8(A-H,O-Z)
      DIMENSION BCT(NDIM),AK(NDIM,NDIM),B(NDIM)
      PERM = AK(I,I)
      DO 10 J=1,NN
      B(J) = B(J) -AK(J,I)*BCT(I)
   10 AK(I,J) = 0.D0
      DO 11 J=1,NN
   11 AK(J,I) = 0.D0
      AK(I,I) = PERM
      B(I) = AK(I,I)*BCT(I)
      RETURN
      END
C ****************************************************************
      SUBROUTINE HFLUX(IEL,NN,X,Y,T,D,NO)
C
C   THIS ROUTINE CALCULATES HEAT FLUX
C
      IMPLICIT REAL*8(A-H,O-Z)
      DIMENSION X(NN),NO(8),HF(4),Y(NN),T(NN),HF4(4),D(2,2)
     1,HF8(8)
      IF (NN.EQ. 3) GO TO 5
      IF (NN .EQ. 8) GO TO 10
      CALL FLUX4(X,Y,T,HF4,D,HFI)
      WRITE(6,51)
   51 FORMAT(1X,' ELEMENT NO. ',5X,'         NODES        ','
     1 HEAT FLOW')
      WRITE(6,52) (NO(I),I=1,NN)
   52 FORMAT(1X,16X,4(I6,2X))
      WRITE(6,53) IEL,(HF4(I),I=1,NN),HFI
   53 FORMAT(1X,I6,10X,4(F6.2,2X),3X,F7.3)
      GO TO 20
    5 CALL FLUX3(X,Y,T,HF3,D)
      WRITE(6,54)
   54 FORMAT(1X,'  ELEMENT NO. ',5X,'  HRAT FLUX   ')
      WRITE(6,55) IEL,HF3
   55 FORMAT(1X,I6,12X,F7.3)
      GO TO 20
   10 CALL FLUX8(X,Y,T,HF8,D,HFI)
      WRITE(6,56)
   56 FORMAT(1X,' ELEMENT NO. ',5X,'         NODES        ',32X,'
     1HEAT FLOW')
      WRITE(6,57) (NO(I),I=1,NN)
```

```
   57 FORMAT(1X,16X,8(I6,2X))
      WRITE(6,58) IEL,(HF8(I),I=1,8),HFI
   58 FORMAT(1X,I6,10X,8(F6.2,2X),3X,F7.3)
   20 CONTINUE
      RETURN
      END
C ******************************************************************
      SUBROUTINE FLUX3(X,Y,T,HF,D)
      IMPLICIT REAL*8(A-H,O-Z)
      DIMENSION X(3),Y(3),B(2,3),BT(2),T(3),BTD(2)
      A = X(2)*Y(3) - Y(2)*X(3) + X(1)*(Y(2)-Y(3)) +Y(1)*
     1(X(3)-X(2))
      AINV= 1.D0/A
      B(1,1) = (Y(2) -Y(3))*AINV
      B(1,2) = (Y(3) - Y(1))*AINV
      B(1,3) = (Y(1) - Y(2))*AINV
      B(2,1) = (X(3) -X(2))*AINV
      B(2,2) = (X(1) - X(3))*AINV
      B(2,3) = (X(2) - X(1))*AINV
      CALL DGMATV(B,T,BT,2,3,2)
      CALL DGMATV(D,BT,BTD,2,2,2)
      HF = BTD(1)
      RETURN
      END
C ******************************************************************
      SUBROUTINE FLUX4(X,Y,T,HF,D,HFI)
C
C     CALCULATES HEAT FLUX IN RECTANGULAR ELEMENT
C
      IMPLICIT REAL*8(A-H,O-Z)
      DIMENSION X(4),Y(4),T(4),AJ(2,2),AI(2,2),ANU(4),ANV(4)
     1,XY(8),YX(8),YI(2),IC(4),B(2,4),XI(2),HF(4),BTD(2),BT(2),
     2D(2,2)
      DATA YI/-.577350269189626D0,+.577350269189626D0/
      DATA XI/-1.D0,+1.D0/
      DATA IC/1,2,4,3/
      IP = 0
      DO 200 I=1,2
      DO 200 J=1,2
      CALL DGSET(AJ,2,2,2,0.D0)
      U = XI(I)
      V = XI(J)
      ANU(1) = -(1.D0-V)*0.25D0
      ANU(2) = -ANU(1)
      ANU(3) = (1.D0+V)*0.25D0
      ANU(4) = - ANU(3)
      ANV(1) = - (1.D0 - U) *0.25D0
      ANV(2) = - (1.D0 +U) * 0.25D0
      ANV(3) = -ANV(2)
      ANV(4) = -ANV(1)
C
C  CALCULATE JACOBIAN
C
      DO 6 K=1,4
```

```
      IA = IC(K)
      XY(K) = X(IA)
      YX(K) = Y(IA)
      AJ(1,1) = AJ(1,1) + ANU(K)*X(K)
      AJ(1,2) = AJ(1,2) + ANU(K) * Y(K)
      AJ(2,1) = AJ(2,1) + ANV(K) * X(K)
      AJ(2,2) = AJ(2,2) + ANV(K) * Y(K)
    6 CONTINUE
C
C   CALCULATE DETERMINANT AND INVERT AJ
C
      DET = AJ(1,1)*AJ(2,2) - AJ(1,2)*AJ(2,1)
      AI(1,1) = AJ(2,2)/DET
      AI(1,2) = - AJ(1,2)/DET
      AI(2,1) = -AJ(2,1)/DET
      AI(2,2) = AJ(1,1)/DET
      DO 100 K=1,4
      B(1,K) = AI(1,1)*ANU(K) + AI(1,2)*ANV(K)
  100 B(2,K) = AI(2,1)*ANU(K) + AI(2,2)*ANV(K)
      CALL DGMATV(B,T,BT,2,4,2)
      CALL DGMATV(D,BT,BTD,2,2,2)
      IP = IP + 1
      IK = IC(IP)
      HF(IK) = BTD(1)
  200 CONTINUE
      HFI = 0.D0
      ALINE2 = DABS(DSQRT((X(2) - X(3))**2 + (Y(2) - Y(3))**2))
      DO 350 I=1,2
      CALL DGSET(AJ,2,2,2,0.D0)
      U = 1.D0
      V = YI(I)
      ANU(1) = -(1.D0-V)*0.25D0
      ANU(2) = -ANU(1)
      ANU(3) = (1.D0+V)*0.25D0
      ANU(4) = - ANU(3)
      ANV(1) = - (1.D0 - U) *0.25D0
      ANV(2) = - (1.D0 +U) * 0.25D0
      ANV(3) = -ANV(2)
      ANV(4) = -ANV(1)
C
C  CALCULATE JACOBIAN
C
      DO 250 K=1,4
      AJ(1,1) = AJ(1,1) + ANU(K)*X(K)
      AJ(1,2) = AJ(1,2) + ANU(K) * Y(K)
      AJ(2,1) = AJ(2,1) + ANV(K) * X(K)
      AJ(2,2) = AJ(2,2) + ANV(K) * Y(K)
  250 CONTINUE
C
C   CALCULATE DETERMINANT AND INVERT AJ
C
      DET = AJ(1,1)*AJ(2,2) - AJ(1,2)*AJ(2,1)
      AI(1,1) = AJ(2,2)/DET
      AI(1,2) = - AJ(1,2)/DET
```

```
      AI(2,1) = -AJ(2,1)/DET
      AI(2,2) = AJ(1,1)/DET
      DO 300 K=1,4
      B(1,K) = AI(1,1)*ANU(K) + AI(1,2)*ANV(K)
  300 B(2,K) = AI(2,1)*ANU(K) + AI(2,2)*ANV(K)
      CALL DGMATV(B,T,BT,2,4,2)
      CALL DGMATV(D,BT,BTD,2,2,2)
      HFI = HFI + BTD(1)*ALINE2*.5D0
  350 CONTINUE
      RETURN
      END
C **************************************************************
      SUBROUTINE LQCON(X,Y,S,D,A8,H,TW,BC)
C
C     CALCULATES CONDUCTANCE MATRIX FOR 8 NODE
C              ISOPARAMETRIC ELEMENT.
C
      IMPLICIT REAL*8(A-H,O-Z)
      DIMENSION X(8),Y(8),S(8,8),D(2,2),A8(8),W(3),XI(3),
     1AJ(2,2),AI(2,2),ANU(8),ANV(8),AN(1,8),ANT(8,1),ST(8,8),
     2SP(8,8),BT(8,2),BTD(8,2),B(2,8)
      DATA W/0.55555555555556D0,0.88888888888889D0,0.5555555555556
     1D0/
      DATA XI/-0.7745966692414830,0.D0,0.7745966692414830/
C
C  ZERO ARRAYS
C
      CALL DGSET(S,8,8,8,0.D0)
C
C  BEGIN DO-LOOPS FOR NUMERICAL INTEGRATION
C
      DO 26 I=1,3
      DO 26 J=1,3
      CALL DGSET(AJ,2,2,2,0.D0)
      U=XI(I)
      V= XI(J)
C
C  CALCULATE DERIVATIVES FOR SHAPE FUNCTIONS
C
      ANU(1) = (1.D0-V)*(2.D0*U+V)*.25D0
      ANU(2) = (1.D0-V)*(2.D0*U-V)*.25D0
      ANU(3) = (1.D0+V)*(2.D0*U+V)*.25D0
      ANU(4) = (1.D0+V)*(2.D0*U-V)*.25D0
      ANU(5) = -U*(1.D0-V)
      ANU(6) = (1.D0-V*V)*.5D0
      ANU(7) = -U*(1.D0+V)
      ANU(8) = -(1.D0-V*V)*.5D0
      ANV(1) = (1.D0-U)*(U+2.D0*V)*.25D0
      ANV(2) = (1.D0+U)*(2.D0*V-U)*.25D0
      ANV(3) = (1.D0+U)*(2.D0*V+U)*.25D0
      ANV(4) = (1.D0-U)*(2.D0*V-U)*.25D0
      ANV(5) = -(1.D0-U*U)*.5D0
      ANV(6) = -V*(1.D0+U)
      ANV(7) = (1.D0-U*U)*.5D0
```

```
      ANV(8) = -V*(1.D0-U)
C
C   CALCULATE JACOBIAN
C
      DO 6 K=1,8
      AJ(1,1) =AJ(1,1) +ANU(K)*X(K)
      AJ(1,2) = AJ(1,2) + ANU(K)*Y(K)
      AJ(2,1) = AJ(2,1) + ANV(K) * X(K)
    6 AJ(2,2) = AJ(2,2) + ANV(K)*Y(K)
C
C  CALCULATE DET AND INVERT AJ
C
      DET = AJ(1,1)*AJ(2,2) - AJ(1,2)*AJ(2,1)
      AI(1,1) = AJ(2,2)/DET
      AI(1,2) = -AJ(1,2)/DET
      AI(2,1) = -AJ(2,1)/DET
      AI(2,2) =AJ(1,1)/DET
C
C  CASLCULATE CONDUCTANCE MATRIX
C
      DO 8 K=1,8
      B(1,K) = AI(1,1)* ANU(K) +AI(1,2)* ANV(K)
    8 B(2,K) = AI(2,1) *ANU(K) + AI(2,2) * ANV(K)
C
C  MULTIPLY BT*D*B
C
      CALL DGTRAN(B,BT,2,8,2,8)
      CALL DGMULT(BT,D,BTD,8,2,2,8,2,8)
      CALL DGMULT(BTD,B,ST,8,2,8,8,2,8)
C
C  MULTIPLY RESULT BY WEIGTHS AND DET. OF J AND
C  ADD INTO CONDUCTANCE MATRIX
C
      DO 11 K=1,8
      DO 11 L=1,8
   11 S(K,L) = S(K,L) +W(I)*W(J)*ST(K,L)*DET
   26 CONTINUE
      ICODE = BC
      CALL DGSET(SP,8,8,8,0.D0)
      DO 30 K=1,8
   30 A8(K) = 0.D0
      DO 50 I=1,3
      CALL DGSET(AJ,2,2,2,0.D0)
      GO TO (34,33,32,31,50), ICODE
   31 U= -1.D0
      V= XI(I)
      GO TO 35
   32 V= 1.D0
      U= XI(I)
      GO TO 35
   33 U = 1.D0
      V= XI(I)
      GO TO 35
   34 V= -1.D0
```

```
      U= XI(I)
   35 AN(1,1) = -(1.D0-U)*(1.D0-V)*(1.D0+U+V)*.25D0
      AN(1,2) = -(1.D0+U)*(1.D0-V)*(1.D0-U+V)*.25D0
      AN(1,3) = -(1.D0+U)*(1.D0+V)*(1.D0-U-V)*.25D0
      AN(1,4) = -(1.D0-U)*(1.D0+V)*(1.D0+U-V)*.25D0
      AN(1,5) = (1.D0-U**2)*(1.D0-V)*.5D0
      AN(1,6) = (1.D0-V**2)*(1.D0+U)*.5D0
      AN(1,7) = (1.D0-U**2)*(1.D0+V)*.5D0
      AN(1,8) = (1.D0-V**2)*(1.D0-U)*.5D0
C
C  CALCULATE DERIVATIVES FOR SHAPE FUNCTIONS
C
      ANU(1) = (1.D0-V)*(2.D0*U+V)*.25D0
      ANU(2) = (1.D0-V)*(2.D0*U-V)*.25D0
      ANU(3) = (1.D0+V)*(2.D0*U+V)*.25D0
      ANU(4) = (1.D0+V)*(2.D0*U-V)*.25D0
      ANU(5) = -U*(1.D0-V)
      ANU(6) = (1.D0-V*V)*.5D0
      ANU(7) = -U*(1.D0+V)
      ANU(8) = -(1.D0-V*V)*.5D0
      ANV(1) = (1.D0-U)*(U+2.D0*V)*.25D0
      ANV(2) = (1.D0+U)*(2.D0*V-U)*.25D0
      ANV(3) = (1.D0+U)*(2.D0*V+U)*.25D0
      ANV(4) = (1.D0-U)*(2.D0*V-U)*.25D0
      ANV(5) = -(1.D0-U*U)*.5D0
      ANV(6) = -V*(1.D0+U)
      ANV(7) = (1.D0-U*U)*.5D0
      ANV(8) = -V*(1.D0-U)
C
C   CALCULATE JACOBIAN
C
      DO 37 K=1,8
      AJ(1,1) =AJ(1,1) +ANU(K)*X(K)
      AJ(1,2) = AJ(1,2) + ANU(K)*Y(K)
      AJ(2,1) = AJ(2,1) + ANV(K) * X(K)
   37 AJ(2,2) = AJ(2,2) + ANV(K)*Y(K)
      IF (ICODE .EQ. 1) GO TO 38
      IF (ICODE .EQ. 3) GO TO 38
      ALINE = AJ(2,1) + AJ(2,2)
      GO TO 39
   38 ALINE = AJ(1,1) +AJ(1,2)
   39 CONTINUE
C
C  CALCULATE NT*N
C
      CALL DGTRAN(AN,ANT,1,8,1,8)
      CALL DGMULT(ANT,AN,SP,8,1,8,8,1,8)
      DO 40 K=1,8
      DO 40 L=1,8
   40 S(K,L) = S(K,L) +SP(K,L)*H*W(I)*ALINE
      DO 45 K=1,8
   45 A8(K) = A8(K) + AN(1,K)*H*TW*W(I)*ALINE
   50 CONTINUE
      RETURN
```

```
      END
C***************************************************************
      SUBROUTINE FLUX8(X,Y,T,HF,D,HFI)
      IMPLICIT REAL*8(A-H,O-Z)
      DIMENSION X(8),Y(8),T(8),AJ(2,2),AI(2,2),ANU(8),ANV(8)
     1,XY(8),YX(8),YI(3),IC(8),B(2,8),XI(3),HF(8),BTD(2),BT(2)
     2,D(2,2),W(3)
      DATA YI/-0.774596669241483D0,0.D0,0.774596669241483D0/
      DATA W/0.55555555555556D0,0.8888888888889D0,0.5555555555556
     1D0/
      DATA XI/-1.D0,0.D0,+1.D0/
      DATA IC/1,5,3,8,6,4,7,3/
      IP=0
      DO 200 I=1,3
      DO 200 J=1,3
      CALL DGSET(AJ,2,2,2,0.D0)
      U= XI(I)
      V = XI(J)
      IF (U .EQ. 0) GO TO 2
      GO TO 3
    2 IF (V .EQ. 0) GO TO 200
    3 CONTINUE
C
C   CALCULATE DERIVATIVES FOR SHAPE FUNCTIONS
C
      ANU(1) = (1.D0-V)*(2.D0*U+V)*.25D0
      ANU(2) = (1.D0-V)*(2.D0*U-V)*.25D0
      ANU(3) = (1.D0+V)*(2.D0*U+V)*.25D0
      ANU(4) = (1.D0+V)*(2.D0*U-V)*.25D0
      ANU(5) = -U*(1.D0-V)
      ANU(6) = (1.D0-V*V)*.5D0
      ANU(7) = -U*(1.D0+V)
      ANU(8) = -(1.D0-V*V)*.5D0
      ANV(1) = (1.D0-U)*(U+2.D0*V)*.25D0
      ANV(2) = (1.D0+U)*(2.D0*V-U)*.25D0
      ANV(3) = (1.D0+U)*(2.D0*V+U)*.25D0
      ANV(4) = (1.D0-U)*(2.D0*V-U)*.25D0
      ANV(5) = -(1.D0-U*U)*.5D0
      ANV(6) = -V*(1.D0+U)
      ANV(7) = (1.D0-U*U)*.5D0
      ANV(8) = -V*(1.D0-U)
C
C    CALCULATE JACOBIAN
C
      DO 6 K=1,8
      IA = IC(K)
      XY(K) = X(IA)
      YX(K) = Y(IA)
      AJ(1,1) =AJ(1,1) +ANU(K)*X(K)
      AJ(1,2) = AJ(1,2) + ANU(K)*Y(K)
      AJ(2,1) = AJ(2,1) + ANV(K) * X(K)
    6 AJ(2,2) = AJ(2,2) + ANV(K)*Y(K)
C
C   CALCULATE DET AND INVERT AJ
```

```
C
      DET = AJ(1,1)*AJ(2,2) - AJ(1,2)*AJ(2,1)
      AI(1,1) = AJ(2,2)/DET
      AI(1,2) = -AJ(1,2)/DET
      AI(2,1) = -AJ(2,1)/DET
      AI(2,2) =AJ(1,1)/DET
      DO 8 K=1,8
      B(1,K) = AI(1,1)* ANU(K) +AI(1,2)* ANV(K)
    8 B(2,K) = AI(2,1) *ANU(K) + AI(2,2) * ANV(K)
      CALL DGMATV(B,T,BT,2,8,2)
      CALL DGMATV(D,BT,BTD,2,2,2)
      IP = IP + 1
      IK = IC(IP)
      HF(IK) = BTD(1)
  200 CONTINUE
      HFI = 0.D0
      DO 350 I=1,3
      CALL DGSET(AJ,2,2,2,0.D0)
      U = 1.D0
      V= YI(I)
C
C  CALCULATE DERIVATIVES FOR SHAPE FUNCTIONS
C
      ANU(1) = (1.D0-V)*(2.D0*U+V)*.25D0
      ANU(2) = (1.D0-V)*(2.D0*U-V)*.25D0
      ANU(3) = (1.D0+V)*(2.D0*U+V)*.25D0
      ANU(4) = (1.D0+V)*(2.D0*U-V)*.25D0
      ANU(5) = -U*(1.D0-V)
      ANU(6) = (1.D0-V*V)*.5D0
      ANU(7) = -U*(1.D0+V)
      ANU(8) = -(1.D0-V*V)*.5D0
      ANV(1) = (1.D0-U)*(U+2.D0*V)*.25D0
      ANV(2) = (1.D0+U)*(2.D0*V-U)*.25D0
      ANV(3) = (1.D0+U)*(2.D0*V+U)*.25D0
      ANV(4) = (1.D0-U)*(2.D0*V-U)*.25D0
      ANV(5) = -(1.D0-U*U)*.5D0
      ANV(6) = -V*(1.D0+U)
      ANV(7) = (1.D0-U*U)*.5D0
      ANV(8) = -V*(1.D0-U)
C
C   CALCULATE JACOBIAN
C
      DO 250 K=1,8
      AJ(1,1) =AJ(1,1) +ANU(K)*X(K)
      AJ(1,2) = AJ(1,2) + ANU(K)*Y(K)
      AJ(2,1) = AJ(2,1) + ANV(K) * X(K)
  250 AJ(2,2) = AJ(2,2) + ANV(K)*Y(K)
C
C  CALCULATE DET AND INVERT AJ
C
      DET = AJ(1,1)*AJ(2,2) - AJ(1,2)*AJ(2,1)
      AI(1,1) = AJ(2,2)/DET
      AI(1,2) = -AJ(1,2)/DET
      AI(2,1) = -AJ(2,1)/DET
```

```
      AI(2,2) =AJ(1,1)/DET
      DO 300 K=1,8
      B(1,K) = AI(1,1)* ANU(K) +AI(1,2)* ANV(K)
  300 B(2,K) = AI(2,1) *ANU(K) + AI(2,2) * ANV(K)
      CALL DGMATV(B,T,BT,2,8,2)
      CALL DGMATV(D,BT,BTD,2,2,2)
      HFI = HFI + BTD(1)*W(I)*(AJ(1,1)+AJ(1,2))
  350 CONTINUE
      RETURN
      END
```

APPENDIX E - F.E. FORMULATION FOR STEADY HEAT TRANSFER IN A PLANE

a.   The Fourier heat conduction equation for steady heat transfer in a plane may be written as

$$[q_x \ q_y]^T = -[k] \ [\partial T/\partial x \ \partial T/\partial y]^T$$

where $[k] = \begin{bmatrix} k_x & k_{xy} \\ k_{xy} & k_y \end{bmatrix}$

For homogeneous isotropic materials $k_{xy} = 0$ and $k_x = k_y$.

Then $k(\partial^2 T/\partial x^2) + k(\partial^2 T/\partial y^2) = 0$.

A functional for this problem is

$$\Pi = 0.5 \ \iint (\{\partial T/\partial x \ \partial T/\partial y\} \ [k] \ \{\partial T/\partial x \ \partial T/\partial y\}^T \ dA$$
$$+ \int_{S_N} q^* \ T \ dS + \int_{S_c} (h/2)(T^2 - 2TT\infty) dS$$

where q^* - prescribed heat flux on boundary S_N .

  h - heat transfer coefficient on boundary S_c .

  and $T\infty$ - the attendant bulk temperature of the surrounding medium.
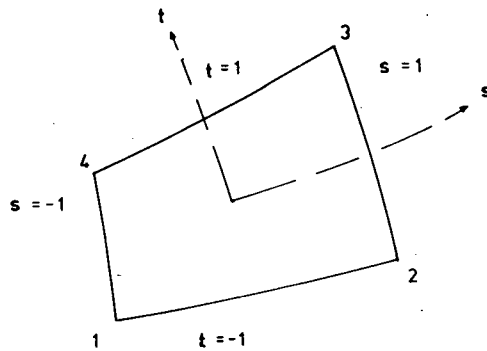
On minimisation, the matrix equation

$$[K \ ] \ \{T\} = \{P_q\} + \{P_r\}$$

is obtained where $\{T\}$ is the solution for the temperature distribution and $[K \ ]$ is the conductance matrix given by $\int [B \ ]^T \ [k] \ [B] \ dA$ (The spatial field for temperature in an element is $[N \ ] \ \{T \}$ where $[N]$ is the shape function matrix. Then $\{\partial T/\partial x \ \partial T/\partial y\} = [B \ ] \ \{T \}$ where $[B \ ] = \{\partial \ /\partial x \ \partial \ /\partial y\} \ [N \ ])$

$$\{P_q\} = \int_{S_N} [N \ ]^T \ q^* \ dS$$

$$N = [\,N_1 \quad N_2 \quad N_3 \quad N_4\,]$$
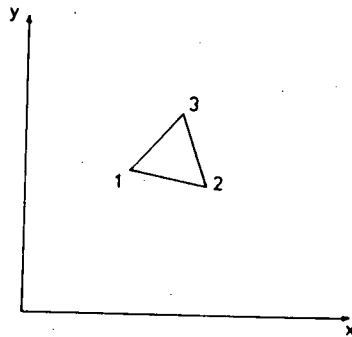
where
$$N_1 = 1/4 \ (1-s)(1-t)$$
$$N_2 = 1/4 \ (1+s)(1-t)$$
$$N_3 = 1/4 \ (1+s)(1+t)$$
$$N_4 = 1/4 \ (1-s)(1+t)$$

Figure 51 - Shape functions-Rect.   isoparametric element

$$N = \frac{1}{2(area)}[\,N_1 \quad N_2 \quad N_3\,]$$

where
$$\begin{Bmatrix} N_1 \\ N_2 \\ N_3 \end{Bmatrix} = \begin{bmatrix} X_2 Y_3 - Y_2 X_3 & Y_2 - Y_3 & X_3 - X_2 \\ X_3 Y_1 - Y_3 X_1 & Y_3 - Y_1 & X_1 - X_3 \\ X_1 Y_2 - Y_1 X_2 & Y_1 - Y_2 & X_2 - X_1 \end{bmatrix} \begin{Bmatrix} 1 \\ x \\ y \end{Bmatrix}$$

Figure 52 - Shape functions-Triangular element

$$\{P_r\} = \int_{S_c} [N \ ]^T \ h \ T_\infty \ dS$$

the last two equations representing the boundary conditions.

b.   The shape functions for a rectangular isoparametric
element and those for a triangular element are given
in fig. 51 and 52.

Ref. R.D.Cook, <u>Concepts and Applications of Finite Element Analysis</u> , J.Wiley and Sons, 1981.